AN INVESTIGATION OF THE UNDERLYING MECHANISMS OF ARTERIAL VASOMOTION

Thesis submitted for the degree of

Doctor of Philosophy

in the

University of Oxford

Joshua F Smith

Magdalen College

Supervisor:

Professor Christopher J Garland

Hilary Term 2020

Abstract

The role of the endothelium in regulating resistance arterial tone is well established, both through endogenous nitric oxide production and endothelium-dependent hyperpolarization or EDH. Also well reported is the link between endothelial cell dysfunction and cardiovascular diseases, resulting in increased vascular smooth muscle sensitivity to constrictor inputs, and compromising endothelium-dependent vasodilatation. A consequence is loss of small artery vasomotion and myogenic tone, disrupting the autoregulation of tissue blood flow. Vasomotion is an important physiological mechanism for optimising blood perfusion of tissues, and myogenic tone ensures constant flow. The loss of this capacity is thought to contribute to elevated blood pressure and associated adverse effects concurrent with cardiovascular disease. This thesis examines the role of the endothelium in the regulation and maintenance of vasomotion, and the effect of dysfunction, particularly loss of nitric oxide. Initially this involved probing the possible downstream actions of nitric oxide, including direct nitrosylation and mediation via soluble guanylyl cyclase (sGC). Upon establishing the route of the dysfunction was sGC-facilitated, electrophysiology studies were performed to investigate the electrical basis for the aforementioned observations. Of particular novelty were the appearance of smooth muscle action potentials in cells that are usually electrically quiescent. This effect could be reversed by introducing exogenous nitric oxide and depression of electrical activity seemed to reflect a direct action of cGMP, independent of PKG. EDH appeared responsible for intermittent repolarization, causing partial vasorelaxation and leading to a chaotic form of vasomotion. Further removal of EDH abolished the intermittent repolarization and led to sustained vasospasm.

Action potentials had an absolute requirement for T-type voltage-dependent calcium channels, and channel block abolished these events and the associated vasoconstriction. The relationship between T-type and L-type voltage-dependent calcium channels indicated the latter could sustain but not initiate action potentials. Interestingly, action potentials could be initiated by direct, pharmacological opening of L-type VGCCs once eNOS was blocked, although this did not occur during vasomotion, in which L-type VGCCs are responsible for, and therefore open. The association between BK_{Ca} channels and ryanodine receptors was also investigated and indicated a limiting influence but not a link to initiation of action potentials. Activation of T-type channels via oxidative stress also appeared not to play a role in action potential generation. Finally, an endogenous inhibitor of eNOS, ADMA was studied and found also to switch on an ability to generate action potentials, and longer term may represent a new therapeutic target as levels of this endogenous inhibitor rise in disease.

Acknowledgements

I am incredibly grateful for the constant support and close guidance of my supervisors Professor Christopher Garland and Professor Kim Dora. It is hard to overstate the assistance and direction they have given me, and it is certain that I would not have made it this far, or enjoyed such an interesting project, without their help.

I also thank my colleague Dr Lyudmyla Borysova, and former colleague Dr Xi Ye, for their help and unfailing optimism, which contributed immensely with making the lab an enjoyable environment to work in. Additionally, I would like to thank my fellow DPhil student Hamish Lemmey, as my academic and recreational experience simply would not have been the same without him. I genuinely could not have asked for a better team to be a part of.

I must say a special thank you to my parents, Stephen and Karen, who, in between telling me I needed to finish university and get a job, never failed to support me. I must thank my sister, Megan, for this fantastic backing also.

I am grateful to Magdalen College, which as well as being my home for almost four years, has provided me with my scholarship to enable me to complete the research outlined below. It has also given me some of my closest friends, of which there are too many to mention individually by name, but a special thank you has to go to my girlfriend Charlotte Franssen, who has endured me and given nothing but support.

Table of contents

Abstract ..... *II*

Acknowledgements ..... *IV*

Table of contents *1*

Table of figures *5*

Abbreviations *7*

Chapter 1 ..... *9*

Introduction *9*

1.1 The cardiovascular system **10**

1.2 Structure of resistance arteries and arterioles **10**

1.3 The control of vascular smooth muscle contraction **11**

1.3.I Voltage-gated calcium channels in vascular smooth muscle 14

1.4 Endothelial control of vascular function **18**

1.4.I Endothelium-derived relaxing factor(s) 19

1.4.II Endothelium-derived hyperpolarization 20

1.5 Nitric oxide and its role in the resistance vasculature **22**

1.6 The physiological significance and basis of vasomotion **25**

Chapter 2 ..... *29*

Methods & Materials *29*

2.1 Tissue isolation 30

2.2 Wire myography 32

2.2.I Mounting arteries for wire myography 32

2.2.II Analysis of wire myography data 33

2.3 Sharp microelectrode intracellular recording 35

2.3.I Preparation of arteries 35

2.3.II Preparation of microelectrodes 35

2.3.III Determination of successful intracellular recordings 36

2.4 Calcium imaging 37

2.4.I Preparation of arteries for calcium imaging 37

2.4.II Measurement of smooth muscle intracellular calcium 37

2.5 Solutions and drugs 38

2.6 Statistical analysis 40

Chapter 3 41

Assessing nitrosylation and sGC-mediated mechanisms of vasomotion 41

3.1 Introduction 42

3.2 Methods & Materials 47

3.2.I Wire myography 47

3.2.II MATLAB analysis and Fourier transforms 47

3.3 Results 48

3.4 Discussion 58

3.5 Conclusion 64

Chapter 4 65

T-type calcium channel involvement in endothelial dysfunction 65

4.1 Introduction 66

4.1.I T-type calcium channels and their connection to the vasculature 67

4.2 Materials & Methods 70

4.2.I Wire myography 70

4.2.II Sharp microelectrode studies of membrane potential 70

4.3 Results 72

4.4 Discussion 87

4.5 Conclusion 93

Chapter 5 94

Investigating alternative pathways for the initiation of action potentials in vascular smooth muscle 94

5.1 Introduction 95

5.1.I Alternative regulators of the T-type channels 96

5.1.II An endogenous inhibitor of eNOS 97

5.2 Methods & Materials 98

5.2.I Wire myography 98

5.2.II Sharp microelectrode studies of membrane potential 98

5.3 Results 100

5.4 Discussion 111

5.5 Conclusion 116

Chapter 6 117

Summary and future directions 117

References *124*

Appendix *156*

Appendix 1: MATLAB vasomotion script **156**

Table of figures

Figure 1.3.1: Mechanism of vasoconstriction of vascular smooth muscle cells.....17

Figure 1.5.1: Endothelium-mediated relaxation of vascular smooth muscle.....24

Figure 2.1.1: Dissection of rat mesenteric arteries 31

Figure 2.2.1: Wire myograph preparation setup with two wires through the arterial lumen 34

Table 2.5.1: Origin and stock details of drugs and chemicals used in this thesis 39

Figure 3.3.1: Comparison between control vasomotion and L-NAME treated vessels, with SNOG mediated reversal.....49

Figure 3.3.1: Comparison between control vasomotion and L-NAME treated vessels, with SNOG mediated reversal.....49

Figure 3.3.2: Comparison between ODQ treatment and the subsequent addition of SNOG.....51

Figure 3.3.3: The signal to noise ratios of various treatments against control vasomotion. 52

Figure 3.3.4: Effect on vasomotion of Bay 41-2272 on L-NAME treated vessels. 54

Figure 3.3.5 Effect of eNOS blocking treatment on tone levels in rat intra-septal coronary arteries.....56

Figure 3.3.6 Comparison of control vasomotion with the addition of nickel chloride...57

Figure 3.4.1.: Algebraic representation of Fast Fourier transform. 61

Figure 4.3.1: Representative membrane potential and tension traces for control vasomotion, L-NAME treatment, and physical denudation.....73

Figure 4.3.2 Quantification of the different levels of endothelial function with regards to membrane potential and tension. 74
Figure 4.3.3 The effect of T-type calcium channel inhibitors on L-NAME-treated arteries. 76
Figure 4.3.4: Examination into whether EDH blockade could induce action potentials. 79
Figure 4.3.5: Representative traces of two different stages of EDH inhibition. 80
Figure 4.3.6 Dose-response curves showing the impact of NNC 55-0396 on various disruptions of the endothelial function. 82
Figure 4.3.7 Electrical activity of eNOS blockade on intra-septal coronary arteries, and recovery with NNC 55-0396. 84
Figure 4.3.8 Effect of the L-type calcium channel opener Bay K8644 on denuded mesenteric arteries. 86
Figure 5.3.1: Quantification of calcium imaging of spike generation 101
Figure 5.3.2: Representative calcium imaging trace and time lapse recording of spike generation 102
Figure 5.3.3: Effect of PKG and sGC blockade on tension and membrane potential ... 104
Figure 5.3.4: The effect of paxilline and ryanodine on membrane potential 106
Figure 5.3.5: The effect of NADPH oxidase and superoxide inhibition. 108
Figure 5.3.6: The effect of ADMA and L-arginine on tension and membrane potential. 110
Figure 5.4.1: The potential NADPH oxidase facilitated pathway of $Ca_v3.x$ activation .. 115
Figure 6.1.1: The proposed pathway for action potential generation 123

Abbreviations

AC	adenylyl cyclase
ACh	acetylcholine
ATP	adenosine 5'-triphosphate
BH_4	(6R)-5,6,7,8-tetrahydrobiopterin
BK_{Ca}	large conductance calcium-activated potassium channel
CaM	calmodulin
cAMP	cyclic adenosine monophosphate
cGMP	cyclic guanosine monophosphate
COX	cyclooxygenase
Cx	connexin
EC	endothelial cell
EDH	endothelium-derived hyperpolarization
EDHF	endothelium-derived hyperpolarizing factor
EDRF	endothelium-derived relaxing factor
Em	membrane potential
eNOS	endothelial nitric oxide synthase
ER	endoplasmic reticulum
GPCR	G-protein coupled receptor
GTP	guanosine triphosphate
IEL	internal elastic lamina
IK_{Ca}	intermediate conductance calcium-activated potassium channel

IP_3	inositol trisphosphate
IP_3R	inositol triphosphate receptor
K_{ATP}	ATP-sensitive potassium channels
K_{Ca}	calcium-activated potassium channel
K_v	voltage gated potassium channels
MEJ	myoendothelial junction
NA	noradrenaline
NO	nitric oxide
NOS	nitric oxide synthase
PE	phenylephrine
PKA	cAMP-dependent protein kinase
PKG	cGMP-dependent protein kinase
PLC	phospholipase C
sGC	soluble guanylyl cyclase
SK_{Ca}	small conductance calcium-activated potassium channel
SOD	superoxide dismutase
SR	sarcoplasmic reticulum
TRP	transient receptor potential

Chapter 1

Introduction

1.1 The cardiovascular system

The cardiovascular system is a highly complex network primarily consisting of the heart and blood vessels, which facilitates the delivery of fundamental nutrients and oxygen combined with the removal of waste products from our organs and tissues. The focus of this investigation mainly concerns the small mesenteric resistance arteries, with some experimentation utilising intra-septal coronary arteries.

1.2 Structure of resistance arteries and arterioles

In common with all blood vessels resistance arteries consist of three layers: the tunica intima, tunica media and tunica adventitia. The tunica intima is comprised of a single layer of endothelial cells (ECs) arranged perpendicular to the smooth muscle cells (SMCs), part of the tunica media, which wrap around the continuous cylindrical structure of the endothelium (Haas & Duling, 1997). Both of these layers are separated by an elastin sheet, the internal elastic lamina (IEL), which is peppered with perforations allowing for intercellular signalling between adjacent ECs and SMCs, where myoendothelial junctions (MEJ) occur (Heberlein et al., 2009). Outwards beyond the SMCs is the tunica adventitia, which consists of many different cell types including fibroblasts, connective tissue and perivascular nerves. The adventitial layer has been implicated in varying mechanisms of vascular function, including neuronal regulation of vascular tone levels (Gutterman, 1999). Resistance arteries as a term describes small arteries and arterioles that together offer the greatest resistance to blood flow, and are thus the vessels accounting for the greatest drop in pressure.

1.3 The control of vascular smooth muscle contraction

Regulation of resistance artery tone is complex and relies upon several separate intracellular signalling pathways that incorporate inputs from sources surrounding the vascular smooth muscle including the endothelium, perivascular nerves, changes in blood flow and the tissue bed that the arteries are perfusing. Vasoconstriction is primarily determined by a rise in intracellular calcium in the smooth muscle, following influx into the cell or release from intracellular stores, principally the sarcoplasmic reticulum (SR), in response to a depolarization in membrane potentials (as discussed below). Calcium binds with calmodulin to activate myosin light chain kinase (MLCK), leading to the phosphorylation of serine residues on the myosin light chain, facilitating crossbridge formation between myosin and actin filaments, producing contraction or vasoconstriction.

Upon repolarization or hyperpolarization intracellular calcium levels are reduced, prompting the closure of L-type voltage-gated calcium channels ($Ca_v1.2$) which represent the chief conduits for extracellular calcium entry. Intracellular calcium is sequestered by various pumps, such as the sarcoplasmic reticular Ca^{2+}-ATPase (SERCA) or mitochondria or extruded from the cell via plasma membrane Ca^{2+}-ATPase or Na^{+}/Ca^{2+} exchanger (NCX) (Amberg & Navedo, 2013). With a lack of calcium within the cell, myosin light chain phosphatase (MLCP) will activate and detach the myosin-actin crossbridges to effect vasodilation (Brozovich et al., 2016). Additionally, a pathway exists in which GPCRs linked to G_{12} α-subunits will activate RhoA, additionally leading to the activation of Rho-associated protein kinase (ROCK). This drives the inhibition of MLCP,

hence preventing the contractile machinery from promoting relaxation. Protein kinase C (PKC) also inhibits MLCP, and is activated by DAG and an increase in intracellular Ca^{2+}.

Stimulation of G protein-coupled receptors (GPCR) containing the G_q α-subunit, such as α_1-adrenergic receptors, causes the production of diacylglycerol (DAG) and inositol trisphosphate (IP_3). DAG opens various receptor-operated channels (ROCs) which subsequently allow an inward cation current, therefore depolarizing the SMC (Large, 2003; Brozovich et al., 2016). Included in this category of receptors are purinergic receptors, such as the ATP-gated P2X receptors, an ionotropic class of receptors that are known to mediate a rapid cation influx (Lamont et al., 2003; Nausch et al., 2012). Also included are the TRPM4 channels, which have been observed to be upregulated by PKC to aid vasoconstriction in cerebral arteries by facilitating cation influx and subsequent depolarization (Crnich et al., 2010). Additionally, TRPC3/6 channels are also known to be directly activated by DAG and contribute to cation influx driven depolarization in VSMCs (Liu et al., 2009; Inoue et al., 2009). This decrease in membrane potential reaches the activation threshold of the VGCCs, activating them and promoting calcium entry (Brozovich et al., 2016). VSM membrane potential is also modulated by calcium-activated chloride channels, such as TMEM16A, which allow an efflux of chloride ions, hence contributing a positive inward current (Hartzell et al., 2005; LeBlanc et al., 2011). Other ion channels are also active in controlling membrane potentials, such as various store-operated channels (SOCs), including some transient receptor potential (TRP) channels (Albert & Large, 2003; Beech, 2005; Earley & Brayden, 2015; Ghosh et al., 2017). For example, blockade of TRPC1 channels has been observed to prevent contraction in response to endothelin-1 in certain arteries (Xu & Beech, 2001; Bergdahl

et al., 2013), with evidence existing of interaction with STIM1 to induce activation of the TRPC1 channels (Shi et al., 2016).

Certain resistance arteries and arterioles also exhibit a level of depolarization in response to an increase in intraluminal pressure, which causes VGCC-dependent vasoconstriction. This occurrence, called myogenic tone, was first reported at the beginning of the 20th Century and was thought to enable the maintenance of blood flow over a range of perfusion pressures (Bayliss, 1902). Later investigations demonstrated pressure-induced contraction is controlled by a number of various mechanisms such as: luminal flow, perivascular nerve stimulation, and endothelial input (Brozovich et al., 2016; Garland et al., 2017). The underlying cause of the Bayliss effect has not yet been fully determined in terms of the link between stretch and Ca^{2+} influx, however, there are observations to suggest that TRP channels may play a role (Gonzales et al., 2010; Ghosh et al., 2016).

As will be discussed below (**Chapter 1.4**), the main mechanisms for vasodilation are mediated by, and originate from, the endothelium. However, there are also processes within the SMCs that enable vasorelaxation. As mentioned above noradrenaline (NA) stimulates α_1-adrenergic receptors to cause vasoconstriction, in some vessels it will also bind β-adrenergic receptors on the membrane of SMCs to produce vasodilation. It was historically supposed that β_2 receptors were the main driver of β-mediated responses within the vasculature (Lands et al., 1967), but it is now known that β_1 is the main initiator instead (Briones et al., 2005; Garland et al., 2011). These β-adrenergic receptors are also GPCRs, but, are G_s, as opposed to G_q coupled, stimulation of which

will initiate adenylyl cyclase to start producing cyclic adenosine monophosphate (cAMP). cAMP in turn activates protein kinase A (PKA) which acts to phosphorylate several targets, decreasing the myosin-actin crossbridge formation responsible for contraction. PKA supports calcium sequestration into the SR and increases the open-state probability of K^+ channels, hyperpolarizing the VSM, and closing VGCCs (Garland et al., 2011). Additionally, it phosphorylates MLCK, inhibiting the enzymes and reducing the sensitivity of the contractile machinery to calcium (Brozovich et al., 2016). A feedback relationship between ryanodine receptors (RyRs) in the SR membrane and large-conductance calcium-activated K^+ channels (BK_{Ca}) in the plasma membrane also acts to produce vasodilation. In VSMCs, activation of RyRs causes a localised calcium event, a Ca^{2+} spark, which can stimulate the opening of neighbouring BK_{Ca} channels, leading to an efflux of K^+ and subsequent hyperpolarization (Nelson et al., 1995; Perez et al., 2001).

1.3.I Voltage-gated calcium channels in vascular smooth muscle

Within vascular smooth muscle voltage-gated calcium channels are the principal regulators of extracellular Ca^{2+} influx of which the most characterised with respect to vascular smooth muscle are the L-type channels, followed by the T-type channels.

The critical role of L-type channels within vascular smooth muscle has been established both *in vivo* and *in vitro*. For example, the blockade of these channels with dihydropyridines leads to the prevention of pressure-induced myogenic tone (Nelson et al., 1990; Knot & Nelson, 1998). Opposed to this, if an opener of the same dihydropyridine class is used *in vitro* it precipitates a large increase in the myogenic tone

observed in isolated arteries (Hwa & Bevan, 1986). Knockout models are also well established, and reports from their usage in mice indicates that, as would be predicted, a decrease in mean arterial pressure and the myogenic response is observed (Moosmang et al., 2003). In addition to the documented pharmacology, L-type channels are an established target of secondary messenger signalling pathways, and as such are an important determinant of cell function. An example of this is the effect of PKC on these channels, as a response to G_q-coupled receptor activation (e.g α_1, endothelin-1, angiotensin-2). When PKG is upregulated as a result of stimulation of these receptors it leads to an increased opening probability of the L-type channels, increasing extracellular Ca^{2+} influx, and raising intracellular Ca^{2+} levels. In contrast to this, the role of PKA in regulation of vascular smooth muscle L-type channels is more equivocal (Keef et al., 2001). Sparklets, or transient Ca^{2+} influx events, mediated by L-type channels are thought to be critical for the maintenance of myogenic tone, and that PKC-mediated increases in this sparklet activity leads to increased tone levels in certain animal models of hypertension (Amberg et al., 2007; Takeda et al., 2011; Navedo & Amberg, 2013).

The T-type channels are less well charaterised within vascular smooth muscle, but significant research has still been undertaken into their role and some compounds exist with which to probe them pharmacologically. Within vascular smooth muscle two out of three of the sub-types have been reported: $Ca_v3.1$ and $Ca_v3.2$, with the $Ca_v3.2$ sub-type being the most frequently observed and considered (Perez-Reyes, 2006). The α_1H subunit forms the main constituent of the channel machinery and is responsible for the transmembrane pore, through which Ca^{2+} flows (Iftinca, 2011). Further sub-units such as α_2 and β, that would be found on L-type channels, are not present. As these sub-units

are responsible for regulating the ion conductance and kinetics, as well as the voltage sensitivity, in other types of voltage-gated calcium channels, the channels may solely be composed of the α_1H subunit (Perez-Reyes, 2003). There appears to be a suggestion that L-type channel auxiliary sub-units can regulate some neuronal T-type channel functions (Perez-Reyes, 2006).

Prior reports have observed arterial tone being directly modulated by T-type channels (Navarro-Gonzalez et al., 2009; McNeish et al., 2010; Abd El-Rahman et al., 2013; Harraz et al., 2014). The bulk of previous vascular studies into the function of the channels has been performed in myogenically active arteries, and it is indeed into their role in the governance of myogenic tone that they have been most characterised (Lam et al., 1998; VanBavel et al., 2002; Navarro-Gonzales et al., 2009; McNeish et al., 2010). This has included their role in cerebral arteries in aiding spontaneously transient outward currents (STOCS), where they appear to allow a small influx of Ca^{2+} which then activates the RyRs to further release Ca^{2+}, leading to BK_{Ca} activation and a reduction in membrane potential (Harraz et al., 2014; Hashad et al., 2018). This slightly differed in cremasteric arterioles, where the channels appeared to aid myogenic tone (VanBavel et al., 2002).

Regarding the activation profile of these channels, in vascular smooth muscle $Ca_v3.2$ channels have been observed to activate at -60 to -50 mV, or 10 to 15 mV more negative than $Ca_v1.2$ channels (Perez-Reyes, 2003). Several structurally different classes of inhibitors of the $Ca_v3.2$ channels have been described: Ni^{2+} (Lee et al., 1999; Harraz et al., 2013; Harraz et al., 2014), NNC 55-0396 (Huang et al., 2004; Li et al., 2005), TTA-A2 (Kraus et al., 2010), and Efonidipine (Harada et al., 2003).

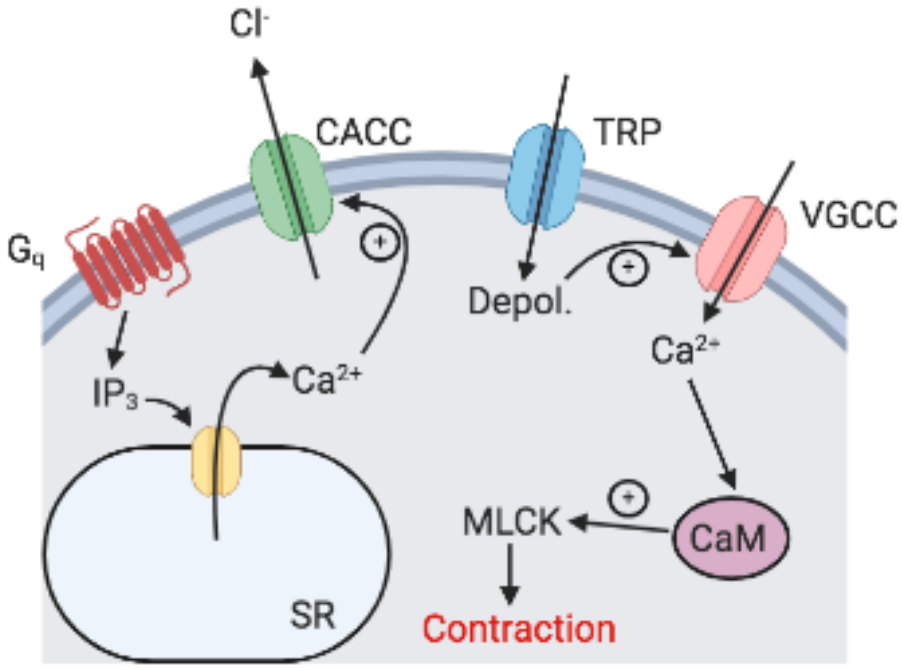


Figure 1.3.1: Mechanism of vasoconstriction of vascular smooth muscle cells

Stimulation of G_q coupled receptors, such as α_1-adreneroreceptors, leads to the generation of IP_3 and the release of Ca^{2+} from the SR via IP_3Rs. This Ca^{2+} binds to calcium-activated chloride channels (CACCs) to invoke a depolarization. Separately, an increase in intraluminal pressure can potentially open certain transient receptor potential (TRP) channels, causing a slight depolarization below the activation threshold of the L-type voltage-gated calcium channels (VGCCs), leading to Ca^{2+} influx (Ghosh et al., 2017). This Ca^{2+} binds calmodulin (CaM), which then activates myosin light chain kinase (MLCK), to galvanize the contractile machinery, as noted above.

1.4 Endothelial control of vascular function

The vascular endothelium was initially thought to be an inert barrier, but over the past three decades a body of evidence has emerged showing otherwise. The endothelium forms a barrier operated by both adherens and tight junctions formed between ECs, which function to reduce the permeability of the endothelial layer, creating a rigidly bound structure. The permeability of this layer relies upon the number of cell-cell connections; as the tightness of the barrier increases, only smaller and smaller molecules are able to traverse it (Komarova & Malik (2010).

In conjunction with this, the presence of homocellular gap junctions allows the passage of small water-soluble molecules between neighbouring ECs. Within ECs these are formed from three well-documented connexion proteins: Cx37, Cx40 and Cx43 (Yeh et al., 1998). Homocellular gap junctions are also found between SMCs (Little et al., 1995a ; Kruger et al., 2000), whilst at the MEJ there are heterocellular gap junctions to be found also. There is evidence to suggest that gap junctions located at the MEJ are constructed by varying combinations of Cx40/43 (Isakson & Duling, 2005). These junctions between ECs and SMCs allow for the movement of small molecules, as well as for the propagation of current that allows variations in membrane potential to be communicated cell-cell, therefore allowing for harmonised responses to spread throughout the artery, and as dye transfer experiments observed, the movement was completely one-directional, from the ECs to SMCs (Little et al., 1995b; as reviewed by Dora (2001)).

Furchgott and Zawadzki (1980) first published evidence that the endothelium was more than an inert layer that merely formed a barrier, as they demonstrated that the presence

of an intact endothelium was essential for ACh induced vasorelaxation. The unidentified agent was determined to be a released factor rather than an electrical current due to the sensitivity of the vasodilation to a calcium ionophore, which was determined to be acting on a Ca^{2+} sensitive enzyme to affect release of the factor (Furchgott, 1983). This factor was termed endothelium-derived relaxing factor (EDRF) and is explained in further detail below (**Chapter 1.4.I**). In addition to this discovery, a second endothelium-derived pathway for vasorelaxation has also been described as endothelium-derived hyperpolarization (EDH) (Garland et al., 2011) and is examined in **Chapter 1.4.II**. In addition to these vasodilatory pathways, the endothelium has also been reported to secrete a variety of other factors including vasoconstrictors, inflammatory signalling agents, and anti-thrombotic factors (Galley & Webster, 2004).

1.4.I Endothelium-derived relaxing factor(s)

As noted above (**Chapter 1.4**), Furchgott and Zawadzki first described EDRF in 1980; subsequent work concluded that EDRF was nitric oxide (NO) (Ignarro et al., 1987a; 1987b). As a tribute for their ground-breaking work, in 1998 Furchgott, Ignarro, and Murad were awarded the Nobel Prize in Physiology or Medicine.

NO is generated through the conversion of L-arginine and molecular oxygen by the enzyme nitric oxide synthase (NOS), with L-citrulline as the by-product formed. Three known isoforms of NOS exist: neuronal-NOS (nNOS), which was first identified in the brain (Bredt & Snyder, 1990); inducible-NOS (iNOS), which is not actively expressed, but can be induced upon the addition of bacterial lipopolysaccharide (Stuehr et al., 1991);

endothelial-NOS (eNOS), the most relevant to this thesis, is expressed in ECs (Forstermann et al., 1994)).

In addition to NO, the endothelium also produces prostacyclin, which was discovered to dilate blood vessels prior to the identification of EDRF as nitric oxide (Moncada et al., 1976; Moncada et al., 1977). Prostacyclin is produced by the primary conversion of arachidonic acid to prostaglandin H_2 by cyclooxygenase (COX), and a subsequent conversion of prostaglandin H_2 by prostacyclin synthase to prostacyclin (PGI_2) (reviewed by Luo et al., (2016)). Although PGI_2 has been observed as a potent vasodilator in some arteries (Zhao et al., 1995), this is far from ubiquitous, as in some smaller resistance arteries it has been reported to play a more minor role (Garland & McPherson, 1992). This supports the literature that its primary role is anti-aggregatory action on platelets (Moncada & Vane, 1979).

1.4.II Endothelium-derived hyperpolarization

Endothelium-derived hyperpolarizing factor (EDHF) was the result of the discovery that there was evidence of an additional endothelium-derived relaxing factor, separate from EDRF, with hyperpolarizing properties on vascular smooth muscle.

It was observed that ACh could contract rabbit mesenteric arteries, whilst also producing hyperpolarization of vascular SMCs (Kuriyama & Suzuki, 1978). This was then expanded upon to suggest that the hyperpolarization produced in response to M_3 muscarinic stimulation seemed to originate in the endothelium (Bolton et al., 1984). These discoveries were further developed on to demonstrate that EDH occurred as a response to ACh, distinct from prostacyclin-mediated responses, and in the presence of

nitric oxide scavengers, demonstrating that these observations were separate from EDRF (Chen et al., 1988). This effect was perceived to be resistant to the actions of indomethacin, methylene blue and haemoglobin.

The identification of K^+ efflux as an ion of interest in generating what was at that time referred to as EDHF sparked the study of the various potassium channels in the EDHF pathway. K_{ATP} channels were ruled out due to an insensitivity of the hyperpolarization to glibenclamide (Garland & McPherson, 1992; Plane & Garland, 1993). Likewise, a role for K_v channels was similarly ruled out (Adeagbo & Triggle, 1993). It was soon discovered that the hyperpolarization was mediated by both the small conductance (S)K_{Ca} channels and the intermediate conductance (I)K_{Ca} channels, when inhibitors for both were applied in tandem (Waldron & Garland, 1994). It was further reported that the inhibitor of BK_{Ca} channels, iberiotoxin, could not prevent the ACh mediated hyperpolarization, a trait that was maintained when used in combination with apamin also, hence appearing to demonstrate that BK_{Ca} channels were not involved in EDH (Zygmunt & Hogestatt, 1996). Further investigation of SK_{Ca} and IK_{Ca} by determined that both channels were located on the endothelium and activated by ACh (Edwards et al., 1998). The activation of SK_{Ca} and IK_{Ca} sparked an increase in K^+ in the myoendothelial space, promoting the activation of Na^+/K^+-ATPases and inwardly rectifying K^+ channels (K_{IR}) located on SMCs, hence generating hyperpolarization in the SMC associated with the expected EDHF response, identifying K^+ as a likely EDHF. Successive studies in various animal species have verified the importance of K^+ in EDH (Beny & Schaad, 2000; Dora & Garland, 2001; Edwards et al., 2001; Nelli et al., 2003). Following on from this, it was shown that myoendothelial gap junctions allow for the direct transduction of hyperpolarization

between the endothelium and SMCs (Dora et al., 2003). Other processes within the ECs have been reported to act in as initiators of EDH, including localised Ca^{2+} "pulsars" originating from IP_3Rs within the myoendothelial projections, which have been described to co-localise with IK_{Ca} channels to initiate hyperpolarization also (Ledoux et al., 2008). Similarly, TRPV4 channels, clustered towards the end of the cells as well as the myoendothelial projections, within the ECs have been observed to produce "sparklets" to initiate activation of the SK_{Ca} and IK_{Ca} channels in GCaMP2 mouse mesenteric arteries, causing a subsequent hyperpolarization (Sonkusare et al., 2012).

1.5 Nitric oxide and its role in the resistance vasculature

As noted above (**Chapter 1.4.I**), in endothelial cells NO is produced via the conversion of L-arginine to L-citrulline by eNOS (Li & Forstermann, 2000). The process requires several co-factors including (6R)-5,6,7,8-tetrahydrobiopterin (BH_4), which forms part of the rate-limiting stage in the production of NO (Wever et al., 1997).

Although there are several substances that can activate eNOS through diverse pathways, one of the major pathways as far as is relevant to this thesis is of activation though the increase of intracellular calcium via the activation of G-protein coupled receptors (GPCR), which activate phospholipase-C (PLC). The increase in intracellular calcium initiates the binding of calmodulin to eNOS, in turn originating the generation of NO (Forstermann et al., 1990). Phosphorylation of two separate serine residues (1177 and 635) on eNOS, by protein kinase A (PKA), protein kinase B (Akt), or shear stress (in

a PKA-dependent manner), also lead to eNOS activation and the subsequent production of NO (Zhao et al., 2015).

NO mediated vasorelaxation is chiefly attained through the activation of soluble guanylyl cyclase (sGC), leading to the conversion of guanosine triphosphate to cyclic guanosine monophosphate (cGMP) (see **Figure 1.5.1**). cGMP will then act as a secondary messenger, activating protein kinase G (PKG), which catalyzes the phosphorylation of many targets to enable vasodilation (Murad, 1986). It has also been reported that NO can activate a variety of potassium channels both directly and indirectly, resulting in hyperpolarization (Bolotina et al., 1994; Lin et al., 1994; Mistry & Garland, 1998; Sampson et al., 2001).

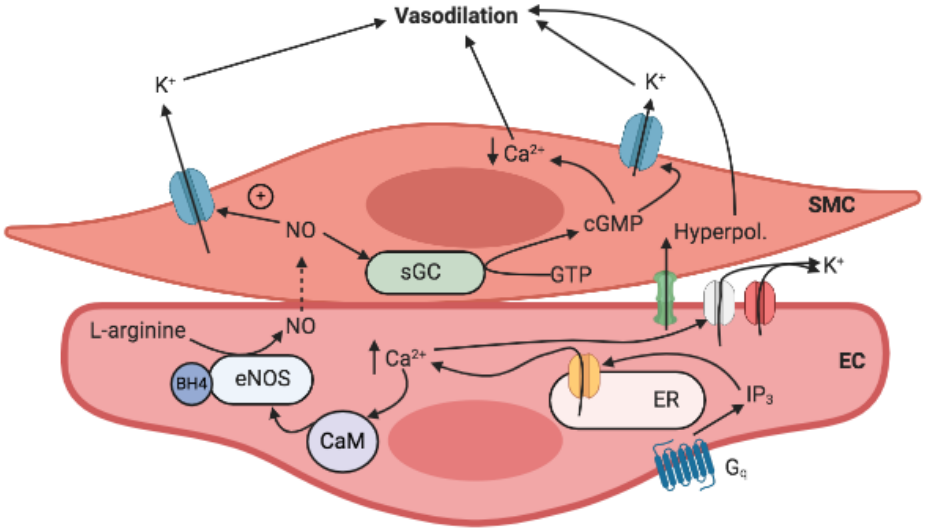


Figure 1.5.1: Endothelium-mediated relaxation of vascular smooth muscle

Stimulation of a G_q coupled receptor, such as M_3 muscarinic receptors, leads to the generation of IP_3 and the release of Ca^{2+} from the ER via IP_3Rs. This Ca^{2+} binds to CaM, which then activates eNOS, prompting the conversion of L-arginine to NO with L-citrulline as a by-product (not shown). NO transfers across into the SMC, directly activating BK_{Ca} channels, and acting to stimulate sGC. sGC the catalyzes the production of cGMP, leading to activation of PKG, and the lowering of intracellular calcium, as well as other mechanisms to effect vasodilation. The Ca^{2+} released in the endothelium will also activate the IK_{Ca} and SK_{Ca} channels in myoendothelial projections, effecting a K^+ efflux into the extracellular space. This efflux drives a hyperpolarizing inward current, which is then transferred to the smooth muscle via gap junctions.

1.6 The physiological significance and basis of vasomotion

Various resistance arteries are capable of generating regular vasomotion upon vasoconstrictor-mediated stimulation, consisting of alternate periods of vasoconstriction and vasodilation. This phenomenon was first discovered *in vivo* in bat wings in the mid-19th Century (Jones, 1853). Although there has been much evidence of vasomotion *in vivo*, that it can be elicited in excised arteries seemingly confirms that the oscillations are independent of central neuronal input and blood flow, and appear to be intrinsic to the vascular smooth muscle (Peng et al., 2001). In terms of a physiological rationale, previous modelling suggests that an oscillating vessel will conduct blood at a higher average flow through the lumen than an equivalent vessel with an equal width fixed diameter (Meyer et al., 2002). Vasomotion has also been linked to ensuring a greater equability in any changes in blood flow, crucial in the resistance vessels that exhibit the phenomenon in preventing tissue damage downstream of the location of oscillation, and can result from phase delay in the myogenic response (Ursino et al., 1996). Some prior studies have attempted to link vasomotion to tissue oxygenation, showing that the high blood flow permitted by low frequency vasomotion leads to a far greater level of oxygenation downstream (Tsai & Intaglietta, 1993). However further theoretical studies by another group have raised doubt on the effect this would have on muscle oxygenation, claiming that the supposed benefit would only be available at low levels of myoglobin (Goldman & Popel, 2001). A further theoretical model has been used to probe the relation of vasomotion to capillary function, but proved inconclusive (Iida, 1990).

Although the direct physiological function of vasomotion remains somewhat vague, what is clear is that the dysfunction of it is linked to many pathophysiologies, and the increase in overall peripheral resistance resulting from these. Observations have shown that in human patients across both type I and type II diabetes the regular vasomotion pattern is disrupted (Benbow & Williams, 1997). The same occurrence has also been observed *in vivo* in hamster (Bouskela et al., 1997) and rat (Renaudin et al., 1999) models. Further to this, animal models of hypertension have also shown dysfunctional vasomotion (Liu et al., 2017). Both essential and pulmonary hypertension have been linked to the disrupted vasomotion resulting from endothelial dysfunction, with the suggestion that the loss of the vasodilatory functions within the vessels worsens these disorders (Perticone et al., 2001; Budhiraja et al., 2004). Whether or not the loss of vasomotion is a driving or contributory factor, it is apparent that the loss of intrinsic ability to autoregulate will exacerbate the disorder.

Various models of the initiation of vasomotion have been proposed, with these grouped together by Aalkjaer & Nilsson (2005) into three main proposed categories: cytosolic oscillators, membrane oscillators, and metabolic oscillators. In the proposed cytosolic oscillator model, vasomotion occurs due to fluctuations in calcium, whereby as intracellular calcium concentration oscillates and forms propagating waves that are coordinated along the smooth muscle cells in the vascular wall (Lee et al., 2002). In this model the driving force is the release of calcium from the sarcoplasmic reticulum and the subsequent re-uptake which cycles to form the oscillation (Lee et al., 2001; Ruehlmann et al., 2000). This is thought to rely on the activation of the IP_3 receptors to drive the calcium release (Boittin et al., 1999), although the activation of other calcium-

releasing channels, such as the ryanodine-sensitive receptors, amongst others, are suspected to be involved in the initiation of the cycles (Boittin et al., 2002; McCarron et al., 2004). Interestingly, it has also been proposed that there exists a form of pacemaker cells embedded in the vascular wall near the bifurcations of resistance arteries and arterioles (Colantuoni et al., 1985; Goligorksky et al., 1995). However, these findings have not been replicated in subsequent studies, and do not appear to explain how excised arteries taken away from the bifurcations can exhibit vasomotion intrinsically.

The metabolic oscillator model is suggested to be precipitated by changes in glycolysis, leading to fluctuations in the cellular concentration of ATP. This then leads to a change in activity of the sodium/potassium pump, triggering an oscillation in its activity, and therefore driving oscillations in the membrane potential of the cell (Siegel, 1983; Aalkjaer & Nilsson, 2005). The blockade of ryanodine-sensitive receptors and the sarcoplasmic reticulum Ca^{2+}-ATPase led to regular oscillations, indicating that a more nuanced picture was beginning to emerge, where the various potential oscillators worked in unison (Omote et al., 1992). Building on this, these residual waves removed by the BK_{Ca} channel blockers iberiotoxin and charybdotoxin, further adding credence to the more complex picture of an entwined oscillator mechanism, although these compounds are not completely selective for the BK_{Ca} channels (Omote et al., 1993). It has also been observed that corresponding membrane potential changes are also required, and these membrane potential oscillations have been observed at the same frequency as the calcium concentration changes (Hill et al., 1999; Yuill et al., 2010). It had also been reported prior to this that membrane potential oscillations were mandatory for the oscillations in tone to appear (Gustafsson et al., 1993). Evidence has

also been described of bursts of action potentials leading to rhythmic contractions and relaxations, although both of the studies reporting this phenomenon were utilising potentially endothelium-compromised arteries, from disease models animals and patients (Lamb & Webb, 1989; Gokina et al., 1996).

An important feature of vessels with vasomotion is the robust intercellular Ca^{2+} signalling between the vascular smooth muscle cells and the endothelial cells, and the ensuing feedback via endothelial projections (Haddock & Hill, 2005). A key messenger in this instance, from the VSMCs to the ECs, has been shown to be Ca^{2+} (Garland et al., 2017) and potentially also inositol 1,4,5-trisphosphate (IP_3), the movement of which, through myoendothelial gap junctions (Kansui et al., 2008; Ledoux et al., 2008), via holes in the internal elastic laminar, will cause nitric oxide (NO) production (Dora et al., 1997), endothelium-dependent hyperpolarization (EDH), and a subsequent vasodilation. This mechanism of feedback is crucial to the propagation of vasomotion, and inhibition will prevent oscillations in vessel tone from spontaneously appearing (Garland et al., 2017).

Chapter 2

Methods & Materials

2.1 Tissue isolation

Male Wistar rats (7-8 weeks old, 200-250 g, Charles River, UK) were used in this study, and housed in individually ventilated cages and kept on a 12:12 hour light and dark cycle. Standard chow and water were available *ad libitum*. Animals were killed by rising carbon dioxide exposure followed by cervical dislocation, as defined by Schedule 1 of the Animals (Scientific Procedures) Act 1986, UK. The mesentery and heart were removed from the rat and placed in ice-cold MOPS-buffered solution (see **section 2.5** for composition) before transferral to the laboratory. Tissue was subsequently pinned out in a re-usable Sylgard coated Petri dish, filled with ice-cold MOPS-buffered solution within 1 hour of removal.

Third and fourth order branches (180 µm – 360 µm diameter) of the superior mesenteric artery were dissected away from the neighbouring vein and cleared of surrounding adipose and connective tissue (**Figure 2.1.1**). For wire myography and electrophysiology experiments, arterial segments were cut to 2 mm in length. Intra-septal coronary arteries were cleaned carefully of any surrounding cardiomyocytes. Tissue was kept at 4 °C in the dissection dish so further arteries could be dissected if required. After use, the dissection dish was cleaned using 70 % ethanol followed by Milli-Q distilled water. Intra-septal coronary arteries were prepared using the same method, but extra care was taken to ensure 2 mm was freed from surrounding cardiomyocytes prior to threading the first wire through the lumen, as these vessels had a greater degree of longitudinal stretch.

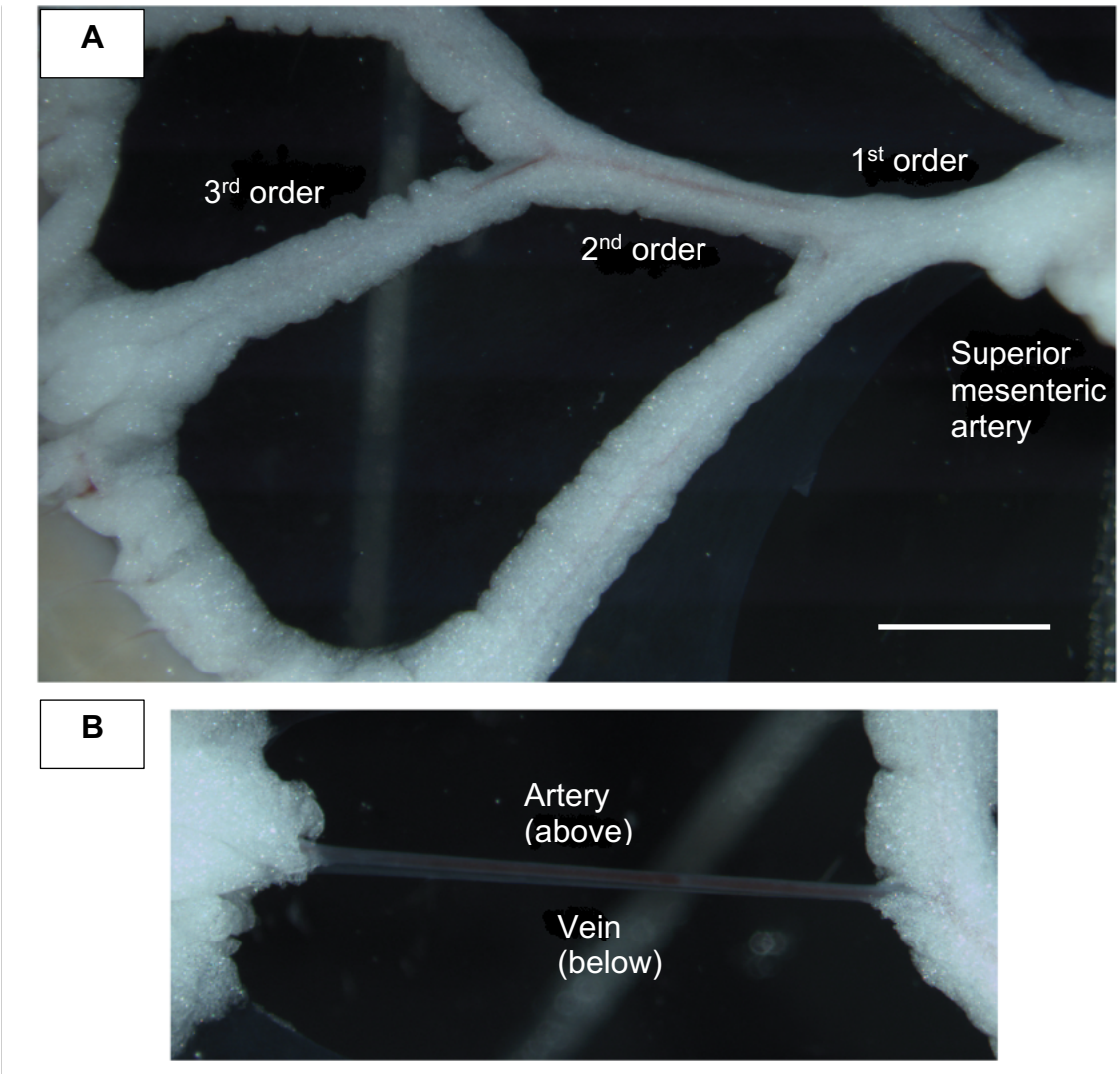


Figure 2.1.1: Dissection of rat mesenteric arteries

Mesentery pinned down in dissection dish (A) with order of vessels highlighted. (B) Parallel third order artery and vein, with the artery above as viewed. Scale bar, 2 mm.

2.2 Wire myography

First described by Bevan and Osher (1972), wire myography was advanced by Mulvany and Halpern (1977) to enable the studying of the contractile properties of small resistance arteries. Wires are inserted carefully through the lumen of an artery and screwed down onto two parallel jaws, one of which is attached to a transducer, the other a micrometer (**Figure 2.2.1**). This configuration allows for the measurement of vasoconstriction under isometric conditions. Prior to functional studies, each artery was stretched stepwise and tension readings recorded and fitted to an exponential curve, in order to generate a length-tension relationship. This allows for the optimal resting tension of the vessel to be calculated. It was determined the optimal resting tension to be equivalent to 0.8 x the internal diameter of the vessel at 100 mmHg (Mulvany & Halpern, 1977).

2.2.I Mounting arteries for wire myography

Segments of third order mesenteric artery or intra-septal coronary arteries, prepared as described in **section 2.1**, were mounted luminally using two 25 µm diameter gold-plated tungsten wires, in the chamber of a Mulvany-Halpern myograph (model 400A, 10 ml chamber, for single recordings; or model 610M, 5 ml chamber, for multiple recordings; DMT Denmark) in cold Krebs solution (see **section 2.5** for composition). An equilibration period of ~30 min was allowed whilst the chamber was warmed to 37°C. Following this, arteries were normalized by constructing a passive diameter-tension curve, as described by Mulvany and Halpern (1977), to a resting tension equivalent to that generated at 0.9 x the diameter of the vessel at 70 mmHg.

Arteries were left to equilibrate, at their optimal resting tension, for a minimum of 20 min before their viability was assessed. Contractility was assessed using phenylephrine (PE), an α_1-adrenergic agonist, and endothelial viability was determined using acetylcholine (ACh), a muscarinic M_3 receptor agonist. Only arteries that maximally contracted to PE (1-10 µM) and achieved ≥ 95% relaxation to ACh (10-100 nM) were considered to be viable and used for experimentation. Bath temperature was maintained at 37°C throughout the experiment and the Krebs solution was replaced approximately every 30 min to reduce the chance of Ca^{2+} precipitation, and the Krebs solution was bubbled continuously with 5% CO_2/21% O_2/balance N_2 to enable buffering and ensure the full distribution of any drugs in the solution.

2.2.II Analysis of wire myography data

Relaxation is expressed as a % of the maximal level of tone achieved immediately prior to the addition of the test compound according to the following calculation:

$$\frac{recorded\ tension - resting\ tension}{maximum\ tension - \ resting\ tension}\ x\ 100$$

The level of pre-constriction was determined by first constructing a PE dose-response curve (1-10 µM) and then calculating the approximate concentration required to achieve 70% maximal tone. This concentration was then used to pre-constrict the artery and increased if necessary to achieve ~70% tone.

For constriction experiments, maximum tension was determined from the maximal response to 45 mM KCl in addition to 10 µM PE, which was applied at the end of the dose-response experiment.

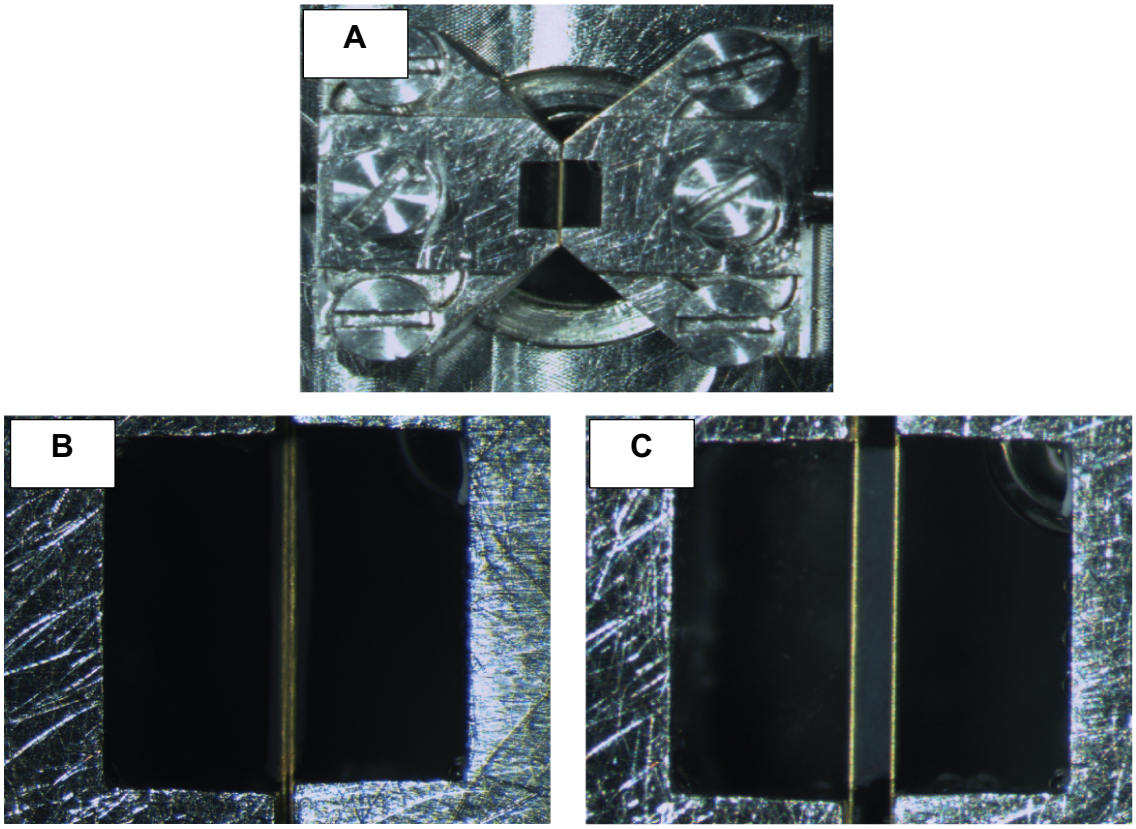


Figure 2.2.1: Wire myograph preparation setup with two wires through the arterial lumen

A Wire myograph jaws within a 10 mL chamber of a two channel myograph (model 400A, DMT) with force transducer, micrometer and screws required to secure the mounting wires labelled. **B** Mesenteric artery with wires threaded through lumen and secured without tension applied. **C** The same artery with optimal tension applied post-normalisation. Artery is approximately 2 mm in length.

2.3 Sharp microelectrode intracellular recording

The use of sharp glass microelectrodes to record the membrane potential of smooth muscle cells in intact resistance arteries has previously been described by Garland and McPherson (1992). Utilising both a wire myograph to mount the artery and a sharp microelectrode, a synchronised recording of both tension and membrane potential can be made. This allows for the electrical activity to be compared to observed vasomotor effects from the tension data.

2.3.I Preparation of arteries

Arteries were prepared and mounted, as above (**Chapter 2.1 & 2.2**), in a two channel 10 ml myograph. Extra care was taken, when dissecting, to ensure that all connective tissue was removed, as any excess connective tissue will cause difficulties with impalement and maintaining a stable recording.

2.3.II Preparation of microelectrodes

The sharp microelectrodes were made on the day of use. Borosilicate glass capillaries with an internal filament (30-0044; Harvard Apparatus, MA, USA) were pulled using a pre-defined programme on a pipette puller (model P-1000; Sutter Instrument, CA, USA). The electrodes were then backfilled with 2 M KCl and inserted into an electrode holder and attached to the headstage of the electrophysiology rig. The electrode was tested to ensure that the tip impedance was between 60-100 MΩ. If the tip impedance was not suitable, the temperature and/or pull force on the pipette puller were adjusted and a new electrode was pulled, and impedance tested.

2.3.III Determination of successful intracellular recordings

To gain an intracellular recording of a single smooth muscle cell, the electrode was advanced in 1.5 μm steps towards the mounted artery using a Burleigh Inchworm motor and 6000 series controller (Burleigh, USA). An impalement was considered successful if the resting membrane potential was approximately -50 mV and remained stable for a minimum of 30 seconds. Smooth muscle membrane potential was recorded through a pre-amplifier (Neurolog system, Digitimer Ltd., U.K.) linked to a MacLab data acquisition system (AD Instruments Model 4e, acquisition at 100 Hz).

2.4 Calcium imaging

2.4.I Preparation of arteries for calcium imaging

Rat third order mesenteric arteries were dissected and mounted as above (**Chapter 2.1 & 2.2**) on a Mulvany-Halpern wire myograph with a window at the bottom of the bath to enable confocal microscopy. The viability of the smooth muscle and endothelium was tested as above (**Chapter 2.2**), and only vessels that met this requirement were used to proceed to experimentation.

2.4.II Measurement of smooth muscle intracellular calcium

Change in intracellular $[Ca^{2+}]_i$ was imaged following incubation of arteries in HEPES buffer containing 2 μM Calbryte 520AM (AAT Bioquest) and 0.02% pluronic F-127 (Thermo Fisher Scientific) for 30 min at 30^{O}C. Calbryte 520AM has an excitation wavelength of 493 nm, an emission wavelength of 515 nm, a quantum yield of 0.75, and a dissociation constant (K_d) of 1200 nM. HEPES contained (in mmol/L): 130 NaCl, 5 KCl, 1.2 $MgCl_2$, 1 $CaCl_2$, 2 pyruvate (Na salt), 10 $HEPES_2$ and 10 glucose. Arteries were then incubated in Krebs buffer for 30 min to allow de-esterification. Confocal images were obtained using a x40 (0.8 NA, Olympus) water immersion objective and iXon 887 EMCCD camera (Andor Technology, UK) coupled to a Nipkow spinning disk confocal head (CSU22, Yokogawa, Japan) and inverted microscope (IX70, Olympus, Japan). Fluorescence intensity at 513-563 nm (excitation 488 nm) was acquired from the bottom surface of arteries at 40 Hz (Andor iQ v 3.5, Andor Bioimaging Division, UK). Experiments were performed in the presence of L-NAME (100 μM) at 36.6^{O}C. Fast Ca^{2+} events (Ca^{2+}

flashes, duration at 50% < 339±11ms, n=5) synchronized between neighbouring cells were induced by phenylephrine (0.3 μM) and acquired from 430x420 pixels. Data are expressed either as relative fluorescence (F/F_0) from the full field of view or the frequency of Ca^{2+} events observed per minute.

2.5 Solutions and drugs

All wire myography and sharp microelectrode experiments were performed using a Krebs solution containing (mM): NaCl, 118; KCl, 3.6; $MgSO_4.7H_2O$, 1.2; KH_2PO_4, 1.2; D-glucose, 11; $NaHCO_3$, 25; CaCl, 2.5; at 37°C; continuously bubbled with 5% CO_2/21% O_2/balance Nitrogen. All dissection was completed in a MOPS-buffered solution containing (mM):NaCl, 145;KCl, 4.7; $CaCl_2$ 2; $MgSO_4.7H_2O$, 1.17; MOPS, 2; NaH_2PO_4, 1.2; D-glucose, 5; pyruvate, 2; EDTA, 0.02; NaOH, 2.75; at 37°C (on ice for dissection); pH = 7.4 ± 0.02 adjusted using 1 M or 4 M NaOH.

Details of suppliers of drugs and chemicals are given in **Table 2.5.**

Drug/Chemical	Product code	Supplier	Stock conc	Stock solvent
ADMA	D4268	Sigma-Aldrich (UK)	100 mM	Milli-Q
Acetylcholine (Ach)	A6625	Sigma-Aldrich (UK)	10 mM	Milli-Q
Apamin	L8407	Latoxan	0.1 µM	Milli-Q
Apocynin	4663	Tocris	100 mM	DMSO
Bay 41-2272	4430	Tocris	100 mM	DMSO
Bay K8644	B112	Sigma-Aldrich (UK)	100 mM	Milli-Q
CaCl2	E506	VWR	1 M	Milli-Q
D-Glucose	G/0500/60	Fisher	NA	NA
Hypoxanthine	H9377	Sigma-Aldrich (UK)	100 mM	Formic acid
KCl	P/4240/53	Fisher	2 M	Milli-Q
KH2PO4	26936.236	VWR	NA	NA
KT 5823	K1388	Sigma-Aldrich (UK)	100 mM	Ethyl acetate
L-arginine	A5006	Sigma-Aldrich (UK)	100 mM	Milli-Q
L-NAME	N5751	Sigma-Aldrich (UK)	100 mM	Milli-Q
MgSO4.7H2O	25165.26	VWR	NA	NA
MOPS	M5162	Sigma-Aldrich (UK)	NA	NA
NaCl	194090010	Acros Organics	NA	NA
NaH2PO4	102454R	VWR	NA	NA
NaHCO3	14707	Alfa Aesar	NA	NA
NaOH	28244.262	VWR	NA	NA
NiCl2	339350	Sigma-Aldrich (UK)	2 M	Milli-Q
Nifedipine	N7634	Sigma-Aldrich (UK)	10 mM	Ethanol
NNC 55-0396	2268	Tocris	100 mM	Milli-Q
ODQ	880	Tocris	20 mM	DMSO
Paxilline	P2928	Sigma-Aldrich (UK)	10 mM	DMSO
Phenylephrine (PE)	P6126	Sigma-Aldrich (UK)	10 mM	Milli-Q
Pyruvate	P2256	Sigma-Aldrich (UK)	NA	NA
Ryanodine	559276	Sigma-Aldrich (UK)	10 mM	Milli-Q
Tempol	176141	Sigma-Aldrich (UK)	100 mM	DMSO
TRAM-34	T6700	Sigma-Aldrich (UK)	10 mM	DMSO
TTA-A2	T-140	Alomone Labs	10 mM	Milli-Q
U46619	16450	Cayman Chemical (USA)	10 mM	DMSO
Xanthine oxidase	X4376	Sigma-Aldrich (UK)	NA	Milli-Q

Table 2.5.1: Origin and stock details of drugs and chemicals used in this thesis

2.6 Statistical analysis

All data are expressed as mean ± SEM, analysed using Microsoft Excel and GraphPad Prism 5.0. *n* values refer to the number of animals used. Depending on the data sets to be analysed, either a one-way or two-way ANOVA was performed, followed by a Tukey test post-hoc to analyse individual points. Where only two sets of data were compared, a two-tailed Student's *t*-test was performed. Statistical significance was defined by $P < 0.05$. For vasomotion waveform analysis a proprietary MATLAB (MathWorks) script was used to ascertain the frequency of and characterise the waveform, based upon Fourier transforms and subsequent integration of the resulting power spectra to calculate a signal to noise ratio.

Chapter 3

Assessing nitrosylation and sGC-mediated mechanisms of vasomotion

3.1 Introduction

Vascular smooth muscle within various resistance arteries is capable of generating tone in an oscillatory manner upon vasoconstrictor-mediated stimulation, consisting of periods of vasoconstriction and vasodilation, and forming the phenomenon known as vasomotion (Nicholl & Webb, 1955). The concept of vasomotion has been recognised for over 160 years, since it was discovered in blood vessels from bat wings (Jones, 1853). The phenomenon is the regular and uniform oscillation of the resistance arteries independently of heartbeat or blood pressure and generated entirely from within the vessel. The complete physiological function remains the subject of debate (Tsai & Intaglietta, 1993), but there is evidence to suggest that an oscillating vessel will conduct blood at a higher average flow through it than the same vessel with a static diameter of the same mean width (Meyer et al., 2002), and also that vasomotion may ensure a much greater moderation of any changes in flow, a form of buffer against swings in blood pressure to the downstream tissue and the subsequent damage that could cause. This idea is supported by *in vivo* experiments concerning the effects of vasomotion on oxygenation in perfused rat hind limbs (Rucker et al., 2000). NADH fluorescence was used as a marker of the metabolic performance of the tissue; in animals and preparations where vasomotion was induced there was a higher NADH concentration, hence showing a greater level of oxygenation than the preparations without vasomotion. Also telling and consistent was that a reduction in the volume of perfused blood appeared to initiate vasomotion.

The most researched resistance arteries with respect to vasomotion are the smaller

arteries of the mesenteric arcade, attractive due to their robustness and the ease at which they develop vasomotion when stimulated with an adrenergic agonist (Dora et al., 2000; Nausch et al., 2012). Other resistance vessels develop myogenic tone in response to physiological intraluminal pressure (Bagher et al., 2012), such as cerebral and coronary arteries. Both in vessels with vasomotion and those with myogenic tone, the intercellular Ca^{2+} signalling between the vascular smooth muscle cells and the endothelial cells, and the subsequent feedback via endothelial projections is crucial to the governing of peripheral blood flow (Haddock & Hill, 2005). A key messenger in this instance, from the VSMCs to the ECs, has been shown to be Ca^{2+} (Garland et al., 2017) and potentially also inositol 1,4,5-trisphosphate (IP_3), the movement of which, through myoendothelial gap junctions (Kansui et al., 2008; Ledoux et al., 2008), enabled by holes in the internal elastic laminar, will cause nitric oxide (NO) production (Dora et al., 1997), endothelium-dependent hyperpolarization (EDH), and a subsequent vasodilation.

3.1.I Proposed mechanisms of vasomotion

As alluded to above the exact cellular mechanisms responsible for vasomotion have been debated, with various models proposed, and as reviewed by Aaljkaer & Nilsson (2005) distilled down to three broad categories. The first two types of cellular oscillators were categorised by Berridge & Rapp (1979), and are cytosolic oscillators and membrane oscillators, whilst the third was added in the later review by Aalkjaer & Nilsson (2005) and is the metabolic oscillator.

The proposed cytosolic oscillator model centres around fluctuations in calcium, as intracellular calcium concentration can oscillate and form propagating waves along smooth muscle cells (Lee et al., 2002). This reflects the release of calcium from the sarcoplasmic reticulum and the subsequent re-uptake which cycles to form the oscillation (Lee et al., 2001; Ruehlmann et al., 2000). This has been hypothesised to rely on the activation of the IP_3 receptors to drive the calcium release (Boittin et al., 1999), although the activation of other channels such as the ryanodine-sensitive receptors, amongst others, are suspected to be involved in the propagation of the waves (Boittin et al., 2002; McCarron et al., 2004).

The proposed metabolic oscillator is theorised to be initiated by changes in glycolysis, leading to fluctuations in the concentration of ATP. This in turn may affect the activity of the sodium/potassium pump, triggering an oscillation in its activity, and therefore driving oscillations in the membrane potential of the cell (Aalkjaer & Nilsson, 2005). Studies utilising rabbit arteries and the blockade of ryanodine-sensitive receptors and the sarcoplasmic reticulum Ca^{2+}-ATPase showed persistent oscillations, perhaps demonstrating the deficiency in the cytosolic oscillator hypothesis alone (Omote et al., 1992). Further studies by the same group (Omote et al., 1993) showed these residual waves removed by the BK_{Ca} channel blockers iberiotoxin and charybdotoxin, although these toxins may also impact other gated potassium channels. Griffith & Edwards (1997) showed complete removal of oscillations with cyclopiazonic acid, an inhibitor of sarcoplasmic reticulum Ca^{2+}-ATPase, suggesting a balance of both of the above types of oscillators may be required for vasomotion (Aalkjaer & Nilsson, 2005).

Regardless of the mechanism of initiation, a crucial component of the global mechanism is the ability of cells to synchronise and propagate the oscillations along the length of arteries. For this reason, it is believed that the electrical coupling between individual cells is fundamental. It has also been observed that membrane potential fluctuation is also required and oscillates at the same frequency as the calcium concentration changes (Hill et al., 1999; Yuill et al., 2010).

3.1.II Dysfunction of vasomotion

The importance of vasomotion to the control of regular blood flow was alluded to above, and the alteration of it from a regular oscillation to a degenerated form has been linked with multiple pathophysiologies. The same is true for the increase in myogenic tone stemming from endothelial dysfunction in many conditions. It has been shown that in patients across both type I and type II diabetes the regular vasomotion pattern is disrupted (Benbow & Williams, 1997). The phenomenon has also been observed in hamster (Bouskela et al.,1997) and rat (Renaudin et al., 1999) models *in vivo*. Hypertensive animal models of disease also show compromised vasomotion (Liu et al., 2017). Endothelial dysfunction has been strongly linked to essential hypertension (Perticone et al., 2001) and pulmonary hypertension (Budhiraja et al., 2004), with the implications that accompany losing the protective effect of endogenous NO production in acerbating these disorders. It is clear then that whether the endothelial dysfunction is the initial cause for the increase in blood pressure or not, the main physiological vasodilator factory, the endothelium, being compromised will only reinforce the

increase.

The focus of this initial stage of the project was to firmly establish the link between the loss of endogenous NO production and the subsequent degeneration of vasomotion, and whether and to what extent the cGMP pathway was solely involved, or if direct nitrosylation by NO could potentially also play a role. I then attempt to quantify this connection in a novel way for the field, designed to try and remove ambiguity surrounding the waveform of regular physiological vasomotion, as well as establishing a standard for pharmacologically disrupted vasomotion. With the link cemented, the focus shifted latterly to investigating whether endothelial dysfunction in myogenic active arteries had a marked effect on tone levels.

3.2 Methods & Materials

3.2.I Wire myography

Third order mesenteric artery segments from rats were mounted and normalised in an isometric wire myograph as previously described (**Methods & Materials section 2.1 & 2.2**) and exposed to a rising cumulative concentration of PE, to elicit an increasing vasoconstriction. Except for L-NAME, all drugs were added directly to the bath and L-NAME and ODQ were pre-incubated for a minimum of 30 minutes before PE was introduced, 5 minutes for SNOG and Bay 41-2272. Drugs were mixed through gentle bubbling in the chamber. Isolated rat intra-septal coronary artery segments were mounted on 15 μm diameter tungsten wire and normalised as referred to previously.

For full details on the set up for wire myography studies please refer to **Methods & Materials section 2.2**.

3.2.II MATLAB analysis and Fourier transforms

Fourier transforms were performed on the raw data to provide a quantitative analysis of the waveforms resulting from various treatments. This was carried out through a proprietary MATLAB script (**Appendix 1**), written and tailored to the demands of the analysis. This afforded a frequency comparison of the different waveforms, as well as a visual depiction of the aggregated mean experiments per treatment. It also allowed comparisons to be drawn between treatments through the signal to noise ratio, calculated as the mean peaks of the Fourier spectra 25% above the basal frequencies, in effect giving a measurement for the symmetricity of the waveform.

3.3 Results

Corruption of vasomotion to chaotic vasomotion with L-NAME

To achieve control vasomotion PE was added to the chamber stepwise, until vasomotion was achieved at 80% of the maximal constriction, as expanded on above. A Fourier transform of aggregated control vasomotion presented as a waveform with a primary frequency of 0.22 ± 0.01Hz (n=5) (**Figure 3.3.1**). The addition of L-NAME (100 µM) led to a collapse of the primary waveform, resulting in a chaotic vasomotion with a frequency of 0.13 ± 0.03Hz (n=5) (**Figure 3.3.1)**. This was immediately observable by the distinct change in the tension profile of the vessel under these conditions, with the previously neat and repeating profile disrupted, and a more prolonged, higher amplitude, and less repeatable waveform emerging. The addition of NO donor SNOG (1 µM) in addition to the maintained L-NAME concentration complete reversed this effect, and restorated the primary waveform at 0.23 ± 0.01Hz (n=5).

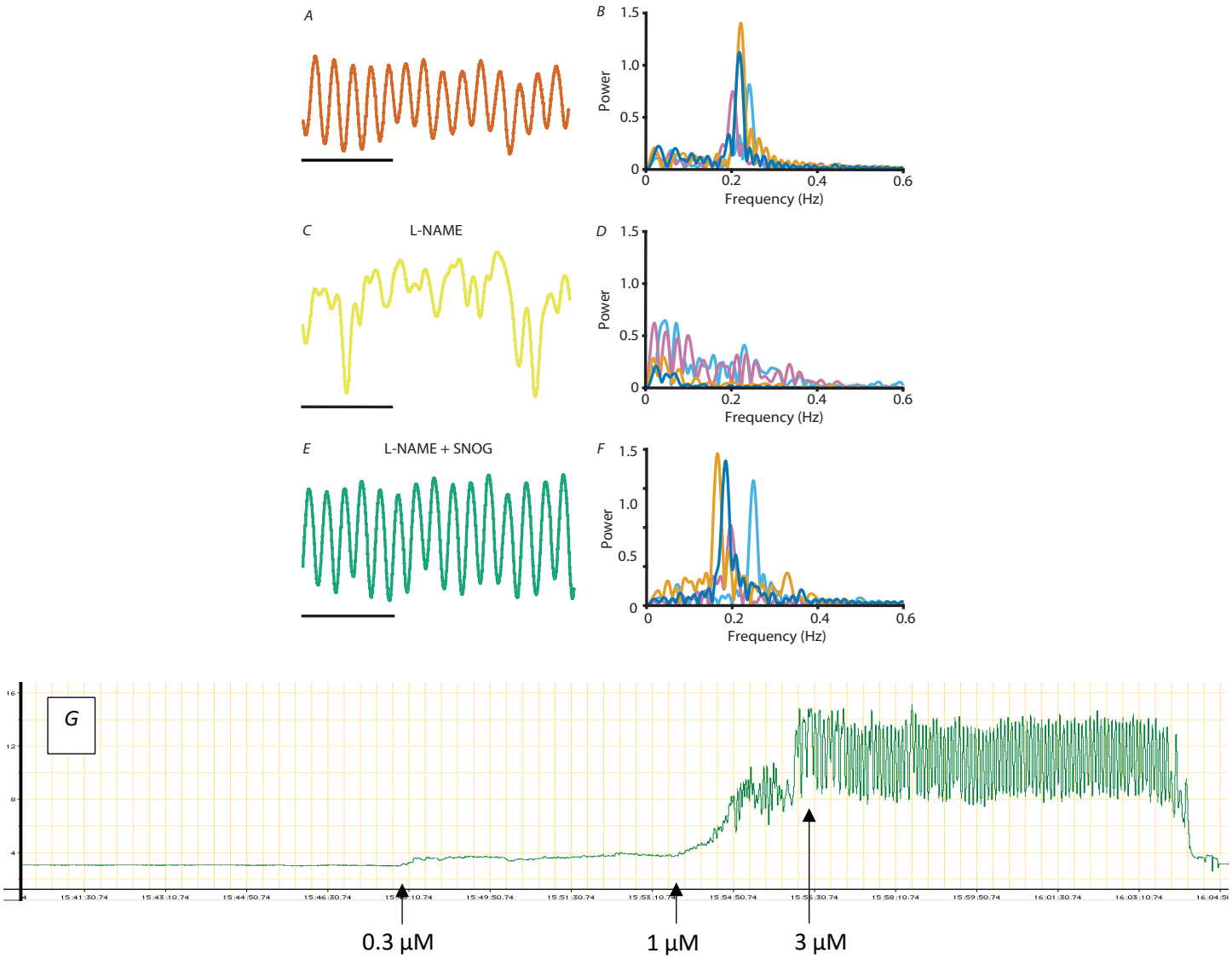


Figure 3.3.1: Comparison between control vasomotion and L-NAME treated vessels, with SNOG mediated reversal.

Aggregated Fourier spectra of individual experiments with control vasomotion (B), L-NAME (D) and L-NAME + SNOG (F). The frequencies shown are for 30 second segments to establish a quantitative measurement of the waveform. Inset in both (A), (C) and (E) are representative tension traces from corresponding single experiments. Scale bars represent 20 seconds. (G) Representative trace of initiation of regular vasomotion which is subsequently sustained for 8 minutes. Time stamp of recording in minutes along x-axis, and tension in mN on y-axis.

Corruption of vasomotion to chaotic vasomotion with ODQ

In a similar manner to that above, control vasomotion was disrupted with the guanylyl cyclase inhibitor, ODQ (10 μM). As with L-NAME, this caused a similar (not statistically different) collapse in the primary waveform to a frequency of 0.12 ± 0.03Hz (n=5) (**Figure 3.3.2**). The key difference arises upon the further addition of 1 μM SNOG (**Figure 3.3.2**); no restoration of the previous control primary waveform was achieved (0.13 ± 0.01Hz) (n=5). This was also repeated at higher concentration of SNOG, but again without a restorative effect.

This effect, as well as the previously shown effect of L-NAME/SNOG, is further illustrated by reference to the signal to noise ratios (**Figure 3.3.3**), with the method by which these are generated detailed above (**Methods & Materials 3.2.III**). This shows a stark and statistically significant difference between control vasomotion and L-NAME, ODQ, and ODQ + SNOG treated vessels. The treatment with L-NAME, and the ODQ-based treatments exhibited no difference in the waveforms, suggesting a degradation of vasomotion due to the same pathway. In contrast the application of the sGC stimulator Bay 41-2272 to L-NAME treated vessels ensured a return to a similar signal to noise ratio as the control, with the same true for the addition of SNOG to L-NAME.

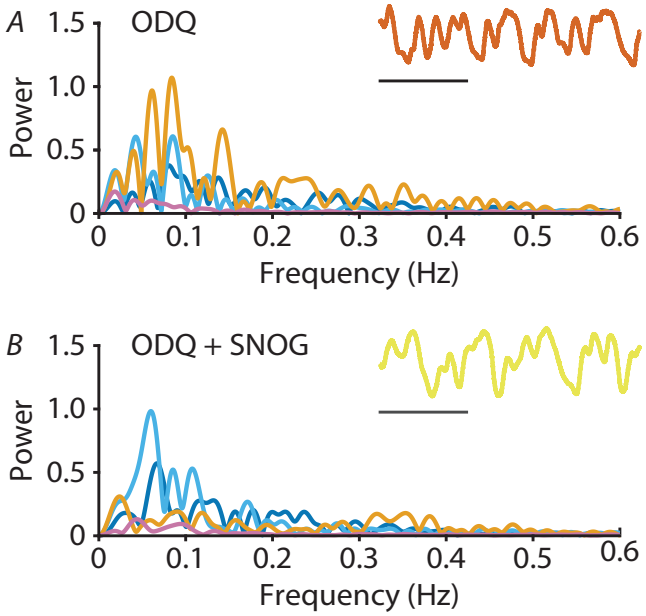


Figure 3.3.2: Comparison between ODQ treatment and the subsequent addition of SNOG.

Aggregated Fourier spectra of individual experiments with ODQ (A) and ODQ + SNOG (B). The frequencies shown are for 30 second segments that were measured to establish a quantitative measurement of the waveform. Inset in both (A) and (B) are representative tension traces from corresponding single experiments. Scale bar represents 20 seconds.

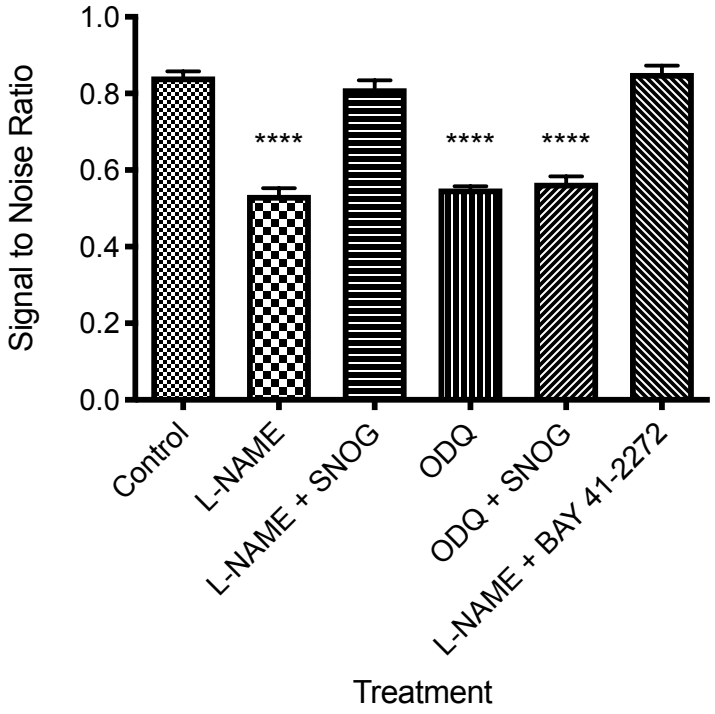


Figure 3.3.3: The signal to noise ratios of various treatments against control vasomotion.

L-NAME (100 µM; 0.53, n=5) significantly reduced the signal to noise ratio metric compared to control vasomotion (0.84, n=5). L-NAME + SNOG (1 µM; 0.82, n=5) restored this to a statistically similar level to control. The addition of ODQ to control (10 µM; 0.55, n=5) significantly reduced the signal to noise ratio, whilst the subsequent addition of SNOG (1 µM; 0.57, n=5) could not reverse this. The addition of Bay 41-2272 (1 µM; 0.85, n=4) to L-NAME treated vessels achieved a reversal statistically similar to the effect SNOG had. ****P<0.0001 compared to control.

Probing the soluble guanyl cyclase mediated pathway further

To investigate further the sGC-mediated contribution to vasomotion, as opposed to the nitrosylation-based pathway, the sGC stimulator Bay 41-2272 (1 μM) was added to vessels treated with L-NAME (100 μM) that exhibited chaotic vasomotion (0.13 ± 0.03Hz) as a result (**Figure 3.3.4**). The addition of Bay 41-2272 restorated regular vasomotion at 0.23 ± 0.01Hz (n=5), compared to control vasomotion at 0.22 ± 0.01Hz (n=5), a non-statistically significant difference.

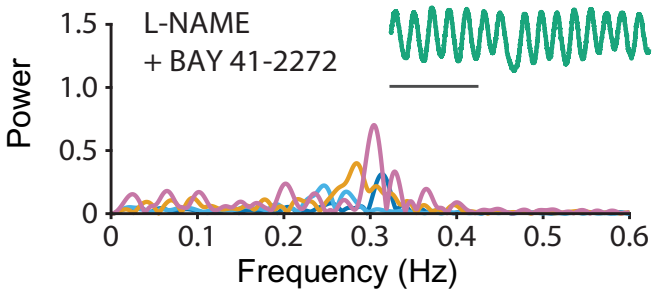


Figure 3.3.4: Effect on vasomotion of Bay 41-2272 on L-NAME treated vessels.

Bay 41-2272 (1 µM) was added to L-NAME (100 µM) treated vessels. Shown on the main axes are an aggregation of individual experiments showing the Fourier spectra after FFT application upon 30 second segments of Bay 41-2272-mediated vasomotion. The inset waveform is a representative tension trace of one of these experiments. Scale bar represents 20 seconds.

Application to a myogenically-active artery type

Rat intra-septal coronary arteries were normalised, and maximal constriction ascertained as detailed above (**Methods & Materials 3.2.I**) and myogenic tone was measured after a period of 30 minutes. This myogenic tone 22.8 ± 2.6% (n=5) was disrupted with L-NAME (100 μM), leading to an increased level of tone (79.6 ± 3.6%). The subsequent addition of T-type channel inhibitor NNC 55-0396 lowered the tone back to a statistically similar level as that of myogenic tone (24.2 ± 3.0%). The addition of the L-type channel inhibitor nifedipine to L-NAME disrupted vessels led to a complete relaxation of the vessel and loss of all tone (0.0%).

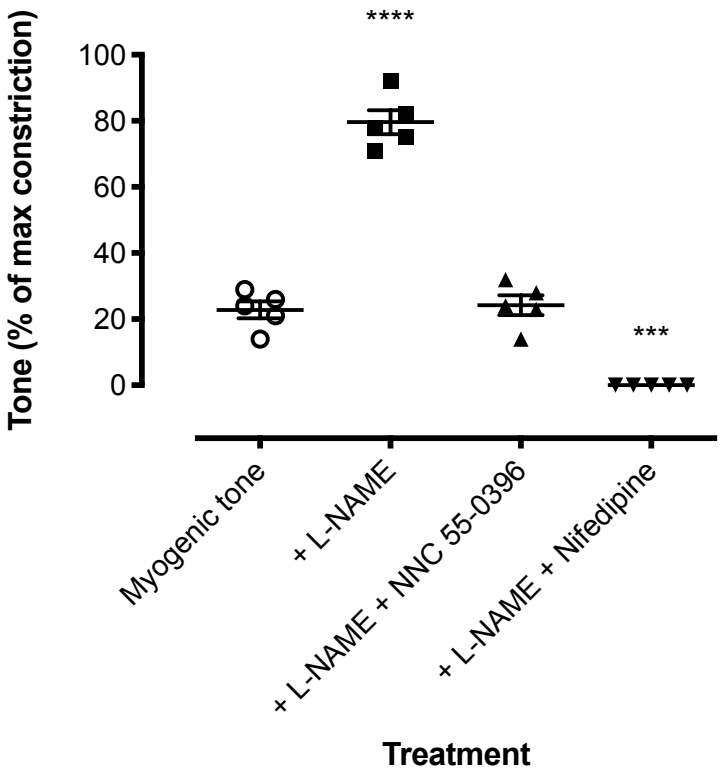


Figure 3.3.5 Effect of eNOS blocking treatment on tone levels in rat intra-septal coronary arteries.

The addition of L-NAME to vessels with spontaneous myogenic tone led to the development of greatly increased tone. Additional application of NNC 55-0396 reduced this tone to a comparable level to myogenic tone. Nifedipine added to L-NAME treated vessels resulted in a statistically significant block of all tone. ***P<0.001, ****P<0.0001, compared to control.

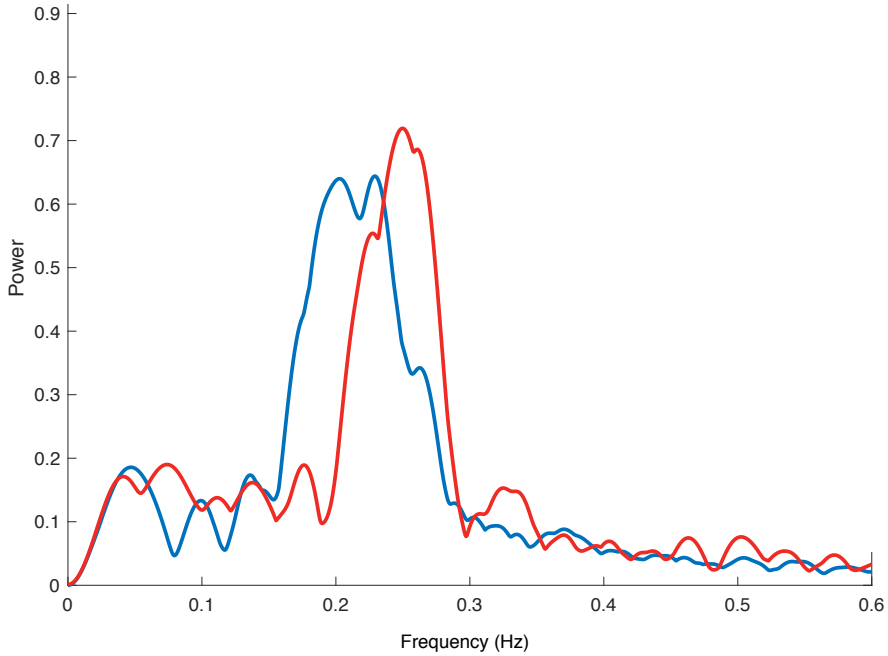


Figure 3.3.6 Comparison of control vasomotion with the addition of nickel chloride.

The mean power spectra of control vasomotion resulted in the above profile (red). This compares similarly to the mean power spectra of control vasomotion (n=5) with the addition of nickel (n=5), a $Ca_v3.2$ specific T-type calcium channel blocker. As clearly visible, the profile has not changed significantly, and represents evidence of no impact of nickel (50 µM) on control vasomotor function.

3.4 Discussion

The rationale for the experiments performed in this chapter was to discover if the loss of vasomotion observed upon restriction of endogenous nitric oxide production (Gustafsson et al., 1993; Jackson et al., 1991) is due to a direct effect of nitric oxide or mediated via soluble guanyl cyclase. The observations described above suggest cGMP is the chief route to NO mediated vasomotion; that a distinct profile of reactivity could be re-established repeatedly by promoting formation of cGMP is a clear indication of this.

Regarding the generation of regular vasomotion, a low concentration of PE was used to prevent over-constriction of the vessel, as interestingly vessels developing higher tension appear to have a far more irregular vasomotion, though there were exceptions to this observation. 3 μM PE was found to give a standard response at approximately 80% of the maximal constriction, as detailed above (**Methods & Materials section 2.3**). Vasomotion was generally observed in the majority of arteries with a functional endothelium and healthy smooth muscle and it was the exception for an otherwise healthy vessel not to produce vasomotion under control conditions, consistent with recent literature concerning endothelial feedback (Garland et al., 2017). The suggestion is the endothelium has a crucial role in response to VSMC depolarization by Ca^{2+} entering the ECs via projections through holes in the internal elastic lamina, facilitating opening of IP_3 receptors to amplify Ca^{2+} levels. These increased Ca^{2+} levels initiate raise the open probability of IK_{Ca} channels, hyperpolarizing passing back to the smooth muscle cells and dilating the vessel.

For the L-NAME based experiments, 100 μM was used as this has been reported previously (Line et al., 1984) to completely block endothelial NOS in rat mesenteric arteries. The disruption of signal seen in the Fourier spectra of L-NAME treated vessels (**Figure 3.4.1.(D)**) compared to the control (**Figure 3.4.2.(B)**) is due to the degradation of an almost sine wave signal into a non-repeating chaotic waveform. The representative trace (**Figure 3.4.3.(C)**) shows how this removal of endogenous nitric oxide results in the vessel spending the majority of stimulated time in spasm, with brief periods of dilation, but very little approaching a regular pattern of vasomotion. The reversal of the L-NAME mediated waveform degradation using SNOG provides further evidence of the key role of nitric oxide in enabling vasomotion in healthy arteries (Jackson et al., 1991; Peng et al., 2001). This raised the question of whether the effect seen thus far was a result of direct nitrosylation by nitric oxide. There is some evidence to indicate the S-nitrosylation of specific residues within some charybdotoxin-sensitive K_{Ca} channels, whilst sGC is blocked with methylene blue, can affect a vasodilation in rabbit aorta (Bolotina et al., 1994). This appears to agree with prior studies (Bouskela & Grampp, 1992) that showed an abolition of vasomotion when hamster cheek pouch arterioles were treated with pinacidil, a K^+ channel activator. Together with the evidence of direct S-nitrosylation of the charybdotoxin-sensitive K_{Ca} channels, these observations could indicate a direct effect of nitric oxide on vasomotion. However, the previous studies failed to take into account the effect of drastically changing the membrane potential on addition of potassium channel activators, and no control was provided to account for this effect. Other studies into the role of K_{ATP} channels (Gustafsson et al., 1994) and K_V channels (Edwards & Griffiths, 1997) in vasomotion have also found they play a minor role. The restoration of L-NAME-induced dysfunction with an sGC

stimulator (**Figure 3.4.4**) also appears to contradict the direct nitrosylation of potassium channels theory of vasomotion.

The ODQ treated vessels were almost identical in profile to those exposed to L-NAME (**Figure 3.4.2.(A)**), an observation we predicted and necessary if we are to discount a contribution of direct S-nitrosylation by NO. This is further characterised by an inability to reverse the effect of ODQ with SNOG (**Figure 3.4.2.(B)**), and appears to confirm the suggestion that sGC activity is the necessary mechanism for generating vasomotion (Aalkjaer et al., 2011; Peng et al., 2001). The Bay 41-2272 experiments support this assumption, as it selectively stimulates sGC enzyme (Koglin et al., 2002). I found this reversed the effects due to NOS block, and interestingly also affected regular vasomotion in vessels that had not previously developed vasomotion, but that had shown a strong endothelial vasorelaxation, indicating good functionality (not shown).

The script used to analyse these data was written in MATLAB and uses a Fast Fourier Transform (FFT) as the starting point for analysis. The FFT is an established technique for converting a waveform into its constituent frequencies, and their corresponding power – a measure of each frequency's contribution to the overall waveform profile. From the power spectra generated by the FFT a signal to noise ratio was designed to integrate every individual curve and, separately, the most prominent peaks with each curve. This allowed a direct comparison of each individual trace, with the emphasis on how the signal to noise ratios clustered (**Figure 3.4.4**) with each experimental treatment.

$$X(\omega) = \int_{-\infty}^{+\infty} x(t)e^{-j\omega t}\, dt$$

Figure 3.4.1.: Algebraic representation of Fast Fourier transform.

The above equation is the algebraic definition of a Fast Fourier transform, and highlights how the function of time $x(t)$ is transformed into a function of frequency $X(\omega)$, using the integral limits defined by the waveform with respect to the change in time dt. The underlying theory behind a Fourier transform is the Fourier series. This explains how a function of time, regardless of shape or profile, can be composed of the sum of sinusoidal functions, that is to say sine and cosine waves. This, if applied only on the scale of one sine or cosine cycle (the fundamental harmonic), would clearly result in an unsatisfactory interpretation of the waveform due to an imperfect oscillation profile being measured. What was required to ensure an accurate measurement of the vasoconstriction waveforms was to apply further harmonic series to the data. This can be thought of as increasing the number of sine/cosine waves measured per oscillation, so the waveform can effectively be broken down in more minute constituent parts.

This required the script developed to be able to adapt to the waveform presented, as this would increase the efficiency of analysis, as opposed to changing the parameters of the Fourier transform with every individual tension profile measured. Also critical to the analysis was the subsequent signal to noise ratio generated post-Fourier transform. As presented above (**Figure 3.3.3**) this proved an invaluable metric in calculating the differences in vasomotion profile between treatments. This was completed by developing the script to measure a baseline with variance parameters for each power

spectra for individual experiments. This, in addition to a smoothing function built in, accounted for the natural deviances in vasoconstriction over the course of a recording, and allowed false peaks to be filtered, so as to not mask the true primary frequencies. This signal to noise ratio further functioned as a proxy for the wavelength, as a higher oscillation would produce a greater peak on the power spectrum, which would then have the noise filtered to show a larger ratio measurement.

The coronary artery experiments were to ascertain the effect of L-NAME in a vessel with spontaneous myogenic tone and to probe a possible contribution of T-type Ca^{2+} channels after loss of NO. As shown (**Figure 3.4.5**), L-NAME potentiated myogenic tone, greatly increasing it. This seems to be attributed to the involvement of T-type Ca^{2+} channels, as NNC 55-0396, a selective blocker (Huang et al., 2004), caused a vasorelaxation to a significantly similar level as spontaneous myogenic tone. In other words, NNC reversed the increase in vasoconstrictor tone evoked by block of NO synthase with L-NAME. Subsequent addition of the L-type VGCC blocker, nifedipine reduced tone further, to basal pre-myogenic tone levels. This confirms prior studies that show evidence L-type calcium channels are required for myogenic tone, as reviewed by Davis & Hill (1999) and Hill et al (2001). A suggested link between NOS inhibition and the appearance of T-type Ca^{2+} channel activity had been observed previously in cerebral arteries but not fully characterised (McNeish et al., 2010). That it is possible to block these channels but sustain tone equivalent to normal levels of myogenic tone is of considerable interest. The use of the coronary arteries is important moving forward, as it will allow any link between T-type Ca^{2+} channels and endogenous NO production, and by extension cGMP, to be drawn without the requirement of a pharmacological pre-

constriction agent as the vessels are myogenically active. They also of course represent a key therapeutic target.

3.5 Conclusion

To conclude, these data indicate that the main signalling pathway for the ability of nitric oxide to sustain vasomotion in non-myogenically active vessels is downstream of soluble guanyl cyclase, allowing for the focus of the investigation to now shift to uncovering what may underlie the phenomenon. The effect in the myogenically active intra-septal coronary vessel is of interest as it both identifies a vessel that can be studied going forward without a need to evoke background vasoconstriction, and also indicates that a loss of endogenous nitric oxide production activates the T-type calcium channels. This could provide for a model of endothelial dysfunction of direct clinical relevance and warrants further investigation to define the vascular smooth muscle electrical activity responsible for the chaotic effects. Another point raised for further investigation is the role of the endothelium beyond nitric oxide production, and whether the physical removal of the endothelium, as opposed to simple loss of NO synthase activity, will yield altered effects due to the further loss of EDH.

Chapter 4

T-type calcium channel involvement in endothelial dysfunction

4.1 Introduction

As established above, withdrawal of endogenous nitric oxide caused an sGC-dependent dysfunction of vasomotion such that it changed to a chaotic form, with increased mean levels of tone, and a substantial increase in tone in mesenteric arteries and myogenically active coronary arteries. Within the coronary arteries blockade of the T-type calcium channels appeared to reverse this effect, with further blockade of the L-type channels abolishing any residual tone. The next stage of the investigation therefore focused on the effects of T-type calcium channel inhibitors on pharmacologically, and physically, altered vessels, and the relation with the functional role of the L-type calcium channels. First an insight into the normal electrical activity of the vascular smooth muscle cells of the affected arteries was required, and only once this was established could further experiments be designed.

It has been established previously in patch clamp experiments that nitric oxide can regulate vascular smooth T-type calcium channels via cGMP (Harraz et al., 2014; Quignard et al., 1997). T-type current was blocked both by the addition of nitric oxide and PKG activators. These data were supported with functional experiments in rat cerebral arteries (Harraz et al., 2014). T-type channels have also been observed previously to be regulated by S-nitrosylation (Lee et al., 2013), and by oxidative stress (Howitt et al., 2013). The molecular physiology and activation window of T-type channels makes them targets of interest for research into activity at more polarized membrane potentials, compared to L-type channels (as review by Perez-Reyes, 2003). Indeed, the importance of T-type channels has also been demonstrated in arterial

diameter control at higher levels of hyperpolarization (Abd El-Rahman et al., 2013; Jensen et al., 2009).

4.1.I T-type calcium channels and their connection to the vasculature

T-type calcium channels are divided into three sub-types: $Ca_v3.1$, $Ca_v3.2$ and $Ca_v3.3$, with the $Ca_v3.2$ sub-type being the most commonly reported and investigated sub-type as far as vascular smooth muscle is concerned (Perez-Reyes, 2006). The α_1H subunit forms the main anchor for the channel and creates the transmembrane pore (Iftinca, 2011). It is composed of four domains, I-IV, each domain containing six transmembrane segments, S1-S6, with S4 responsible for voltage sensing, and opening or closing the channel pore accordingly (Catterall, 2011). Absent from the channels are the α_2 and β subunits, that regulate the kinetics and conductance, and the γ subunit that modulates voltage sensitivity in other types of voltage-gated calcium channels, perhaps suggesting the $Ca_v3.2$ channels are merely made from the α_1H subunit (Perez-Reyes, 2003).

Direct T-type channel involvement has been shown in the regulation of arterial tone in previous studies (Navarro-Gonzalez et al., 2009; McNeish et al., 2010; Abd El-Rahman et al., 2013; Harraz et al., 2014), and have been depicted in a range of different scenarios. They have been described in rat mesenteric resistance arteries (Braunstein et al., 2008), a key artery bed of interest to this study, as well as observed to have a role in generating myogenic tone in rat middle cerebral arteries (Lam et al., 1998; McNeish et al., 2010), as well as in rat basilar arteries (Navarro-Gonzales et al., 2009), and rat cremasteric arteries (VanBavel et al., 2002). All of the studies listed here were performed in arteries that generated spontaneous myogenic tone, and research with non-myogenically active

vessels is very limited, although Braunstein et al (2008) did use calcium imaging to describe T-type involvement during calcium influx in response to the addition of potassium chloride to rat mesenteric arteries.

Several inhibitors of the $Ca_v3.2$ T-type calcium channels have been described: Ni^{2+} (Harraz et al., 2013; Harraz et al., 2014; Lee et al., 1999), NNC 55-0396 (Huang et al., 2004; Li et al., 2005), TTA-A2 (Kraus et al., 2010), and Efonidipine (Harada et al., 2003). In addition to these experimental compounds a small molecule therapeutic drug was designed and released: Mibefradil (Mishra & Hermsmayer, 1994). The release by Roche in 1997 quickly led to several cases of serious interactions with existing drugs therapeutics, and the drug was pulled from the market a year later (Mullins et al., 1998). It was later determined that the drug was not as specific for T-type channels over other targets as previously thought and this had led to dangerous adverse effects when used in combination with other drugs, on already ill patients, sometimes resulting in heart block (Krayenbuhl et al., 1999). It also exhibited high levels of cytochrome P450 34A block rapidly after administration (Foti et al., 2011). If the T-type channels are involved with the dysregulation of arterial tone, then more specific inhibitors could be an invaluable novel therapeutic class.

The focus of this intermediate stage of the project was to investigate the electrical basis for the dysfunction observed previously in response to nitric oxide withdrawal, and once that had been established, and the potential link with T-type channels been elucidated, characterise their action and effect on the mesenteric vessels under varying conditions. The aim here was to determine whether it was solely nitric oxide withdrawal that was

initiating the chaotic vasomotion and vasospasm, or if other endothelial actions, such as EDH, also played a role. Once established, any additional interaction with the L-type channels could be investigated to see if they acted in unison with, or played a separate role to, the T-type channels.

4.2 Materials & Methods

4.2.I Wire myography

Third order mesenteric artery segments from rats were mounted and normalised in an isometric wire myograph as previously described (**Methods & Materials section 2.1 & 2.2**) and exposed to a rising concentration of PE stepwise to elicit an increasing level of vasoconstriction. Except for L-NAME, all drugs were added directly to the bath and L-NAME and ODQ were pre-incubated for a minimum of 30 minutes before PE was introduced, 5 minutes for SNOG and Bay 41-2272. Drugs were mixed through gentle bubbling in the chamber. Isolated rat intra-septal coronary artery segments were mounted on 15 μm diameter tungsten wire and normalised as referred to previously.

For full details on the set up for wire myography studies please refer to **Methods & Materials section 2.2**.

4.2.II Sharp microelectrode studies of membrane potential

Rat third order mesenteric arteries were mounted and normalised to resting tension in an isometric wire myograph as previously described (**Methods & Materials section 2.1 & 2.2**). The resting membrane potential (Em) of a single smooth muscle cell was recorded by impalement with a sharp borosilicate microelectrode back-filled with a 2M KCl solution. Inhibitors were added 30 minutes prior to impalement of the cell, and once an impalement had been successfully achieved (**Materials & Methods section 2.3.III**) increasing concentrations of PE were introduced. Drugs were mixed through gentle bubbling in the chamber.

For full details on the set up for sharp microelectrode studies please refer to **Methods & Materials section 2.3**.

4.3 Results

The electrical basis for chaotic vasomotion and vasospasm

With the application of L-NAME (100 µM) the electrical profile of the vascular smooth muscle cells in rat mesenteric arteries changed such that bursts of action potentials occurred (**Figure 4.3.1**) at a frequency of 0.68 ± 0.08Hz (n=8). In marked contrast, in control arteries vasomotion was recorded with oscillations in depolarization linked to vasoconstriction, and at lower frequency (0.22 ± 0.01Hz, n=6). After destruction of the endothelium by physical denudation, the profile was one of continuous spiking, at a frequency of 1.13 ± 0.15Hz (n=8). This was observed despite an equal mean level of depolarization as control and treatment with L-NAME (**Figure 4.3.2**). The mean amplitude of the vasomotion oscillations was 13.59 ± 0.9 mV, in contrast to the much larger amplitude (and faster) L-NAME-facilitated action potentials (29.26 ± 1.7 mV) and the denudation-induced action potentials (21.84 ±2.5 mV). The control vasomotion required 3 µM PE, but both with the denuded and L-NAME treated arteries only required 0.3 µM PE, as described in **Chapter 3.3**.

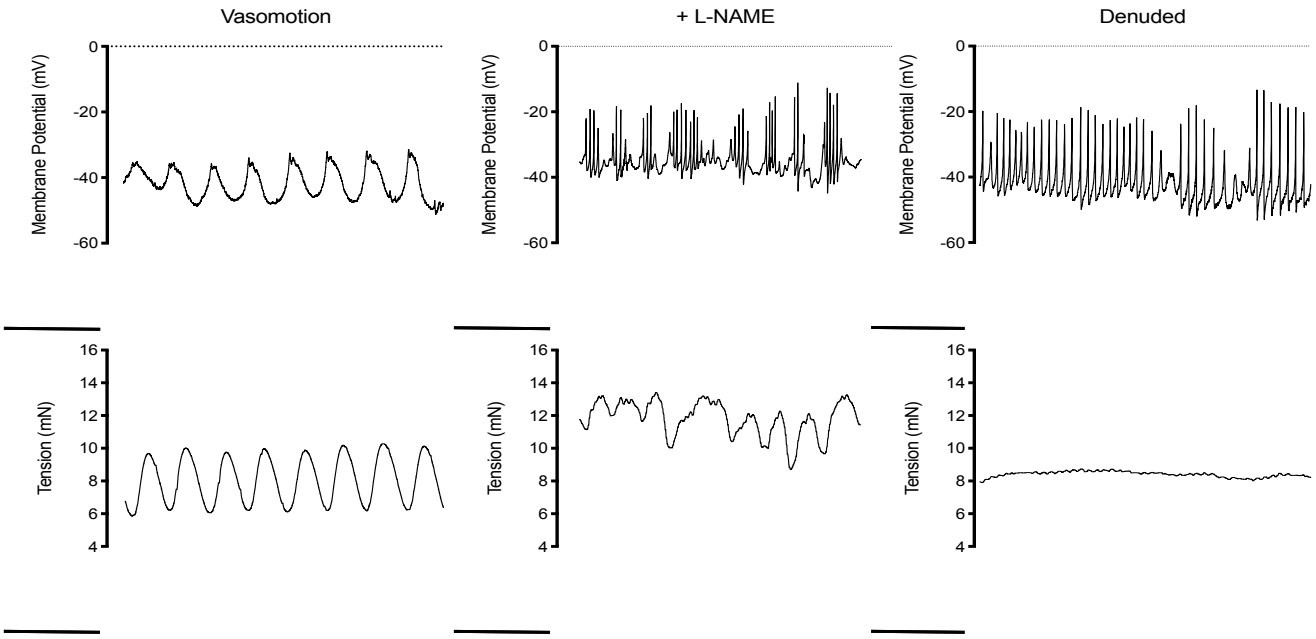


Figure 4.3.1: Representative membrane potential and tension traces for control vasomotion, L-NAME treatment, and physical denudation.

Representative traces of membrane potential and corresponding tension profiles of control vasomotion (n=6), L-NAME (100 µM, n=8) treatment, and physical denudation (n=8) (**Methods & Materials 3.2.III**). The electrical profile clearly changes from an oscillating wave during vasomotion, to bursts of action potentials with L-NAME treatment, to continuous action potentials with physical denudation. Scale bars represent 20 seconds.

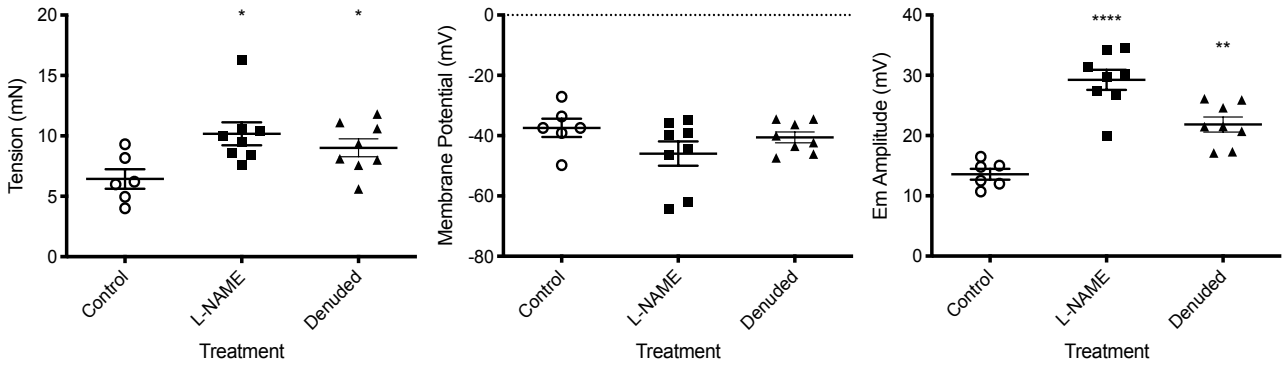


Figure 4.3.2 Quantification of the different levels of endothelial function with regards to membrane potential and tension.

The clear increase in tension mediated either by L-NAME or denudation is compared to control vessels, despite the use of lower PE concentrations (0.3 µM PE as opposed to 3 µM). The slight, but not statistically significant, decrease in vasoconstriction for denuded compared to L-NAME could be due to physical trauma to the smooth muscle during the denudation process. The mean membrane potentials with all three groups did not differ statistically in the level of depolarization. But both L-NAME treatment and denudation resulted in the generation of large amplitude action potentials to PE, compared to the slower oscillations of vasomotion in healthy arteries. * $P<0.05$ compared to control, *** $P<0.001$

Action potential sensitivity to T-type calcium channel inhibitors

The action potentials generated with L-NAME present (100 µM) or after denudation once 0.3 µM PE was applied, were sensitive to T-type calcium channel inhibition. All inhibitors were added at least five minutes prior to the addition of PE to constrict the arteries. Nickel (50 µM) reduced the vasoconstriction with 1 µM PE to 5.74 ± 0.40 mN (n=5) (**Figure 4.3.3**), NNC 55-0396 (0.3 µM) reduced the tension to 6.21 ± 0.52 mN (n=5) with 1 µM PE added, and TTA-A2 (0.3 µM) reduced the vasoconstriction to 6.44 ± 1.29 mN (n=5) with 1.3 µM PE added. This was down from the 10.17 ± 0.95 mN measured with L-NAME treatment. Across all three T-type inhibitors, and treatment with L-NAME, a similar level of depolarization was achieved (**Figure 4.3.3**), as well as with denudation (not shown). Frequency measurements showed a complete abolition of action potentials in response to all T-type inhibitors (**Figure 4.3.3**).

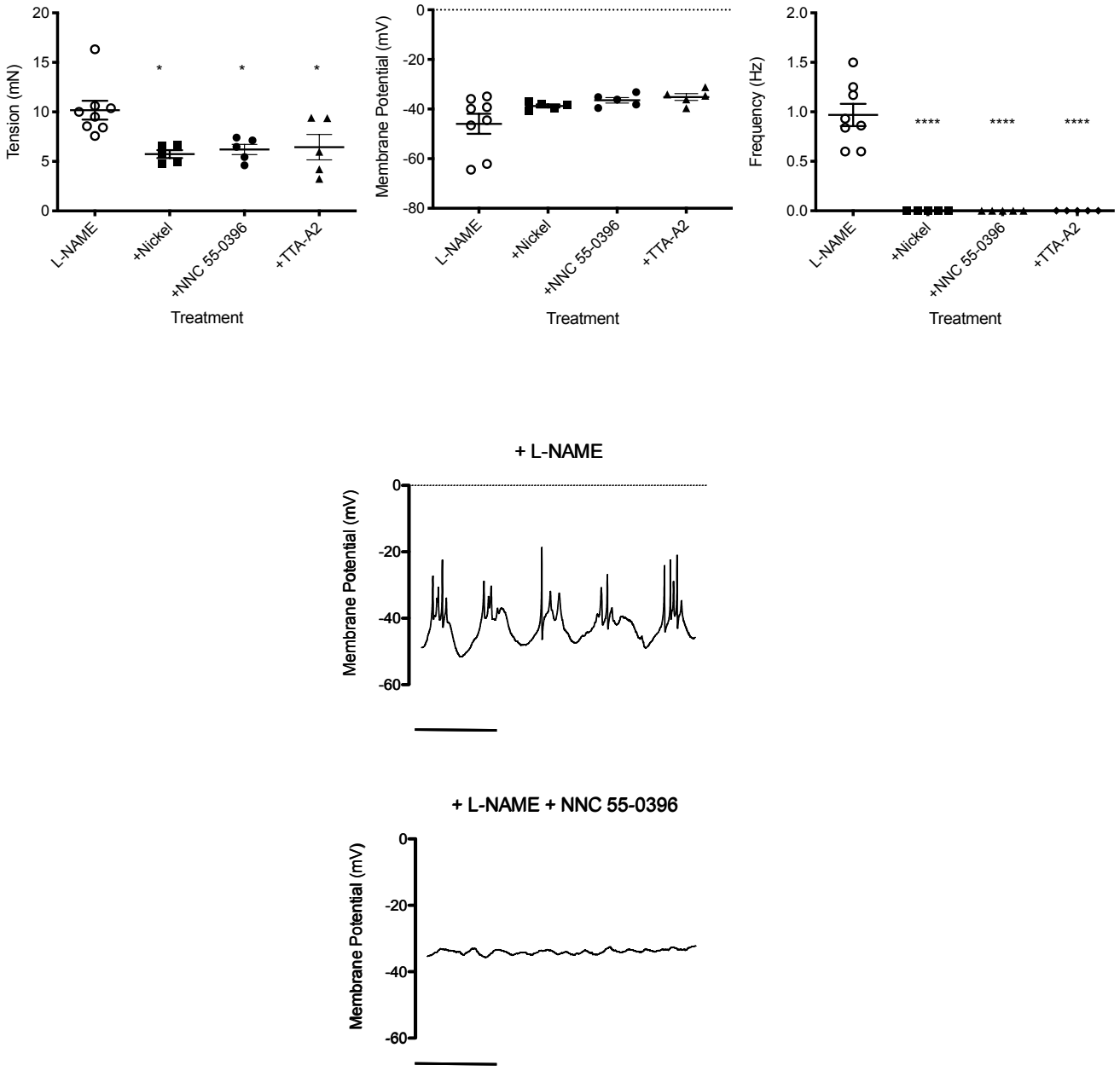


Figure 4.3.3 The effect of T-type calcium channel inhibitors on L-NAME-treated arteries.

100 µM L-NAME and 0.3 µM PE was used to generate action potentials as above, and the application of T-type channel blockers resulted in a reduction in tension, and completely abolished the action potentials, even though depolarization to PE was similar. A representative membrane potential trace of action potentials following incubation with L-NAME and pre-constriction with PE, and a trace from the same artery following incubation with 0.3 µM NNC 55-0396. Scale bars represent 10 seconds. * P<0.05 compared to control, *** P<0.001

Effect of EDH blockade on the electrical activity of vascular smooth muscle cells

The EDH inhibitors SK_{Ca} inhibitor Apamin (100 nM) and the IK_{Ca} inhibitor TRAM-34 (1 µM) were added to the bath one hour and thirty minutes prior, respectively. They are required in combination to block EDH (Crane et al., 2003). They were added to assess if loss EDH might also lead to action potential triggering. Without block of eNOS, inhibition of EDH alone did not generate action potentials during vasoconstriction with PE (0.3 µM) (**Figure 4.3.4**), although they did abolish vasomotion.

Only when L-NAME was added in addition to EDH block were action potentials observed, with L-NAME + TRAM-34 (n=5) yielding an overall frequency of 0.82 ± 0.05Hz for action potentials, and 0.056 ± 0.013Hz for frequency of bursts of spikes. L-NAME + Apamin (n=5) gave an overall frequency of 0.80 ± 0.08Hz, and a frequency of bursts of 0.061 ± 0.009Hz. When both EDH blockers were used in combination with L-NAME (n=5) the result was no change to the overall frequency, which measured 0.80 ± 0.03Hz.

Figure 4.3.5 clearly shows the change observed, for the different stages of endothelial function inhibition, on the membrane potential and vasocontrcition profile. Compared to control vasomotion (**Figure 4.3.1**) the electrical profile is erratic in the presence of TRAM-34 solely, and the vasomotion is correspondingly degraded. This is in contrast to the effect observed when both EDH blockers are added in tandem, which results in the abolition of vasomotion and is noted by the absence in the membrane potential of any oscillation. This is due to the reported feedback the I/SK_{Ca} channels provide in perpetuating vasomotion (Garland et al., 2017). That blockade of only one of these

channels types does not achieve this is testament to the critical role both channels are known to play.

The further addition of apamin and L-NAME to TRAM-34 led rise to action potentials that were strikingly similar in profile to the action potentials observed in physically denuded arteries (**Figure 4.3.1**), and as presented below (**Figure 4.3.4**) were not significantly different in frequency. The profile was a continuous spiking, resulting in a vasospasm when tension recordings were performed.

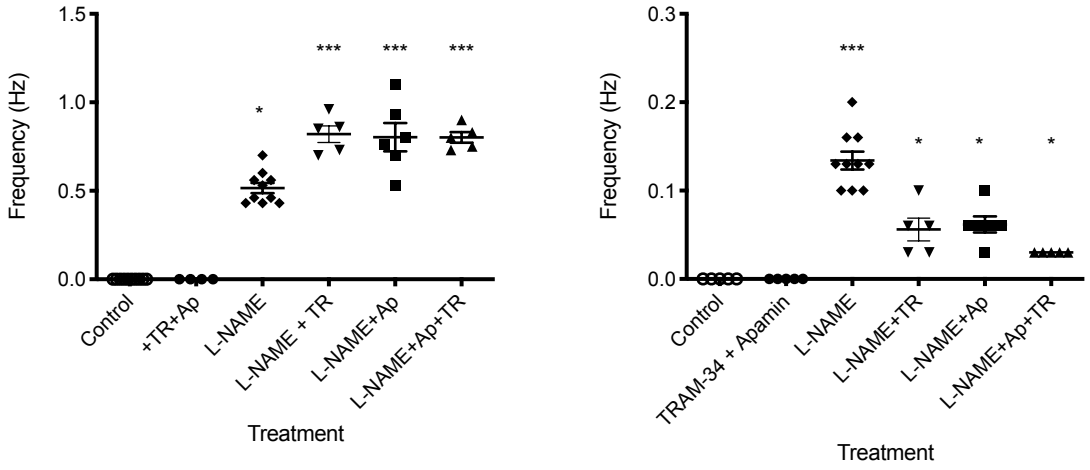


Figure 4.3.4: Examination into whether EDH blockade could induce action potentials.

(A) The addition of TRAM-34 and Apamin to control vasomotion, and stimulation with 0.3 µM PE led to no change with regards to action potentials, but when added in combination with L-NAME they elicited an increase in the frequency of action potentials and the frequency of bursts of action potentials (B), compared to L-NAME alone. * P<0.05 compared to control, *** P<0.001. L-NAME + TRAM-34 data set was acquired by Professor Christopher Garland.

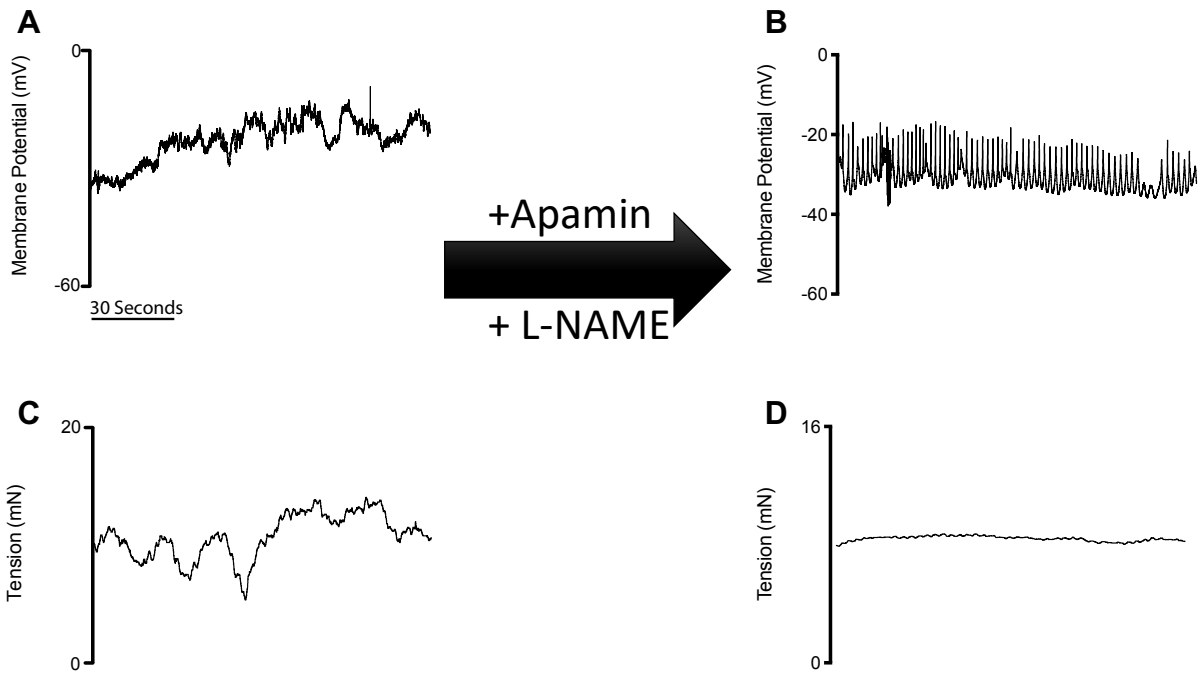


Figure 4.3.5: Representative traces of two different stages of EDH inhibition.

(A) The addition of TRAM-34 to control vasomotion leads to the corruption of the control waveform to a chaotic vasomotion, but (B) without the appearance of spikes. (C) Further addition of apamin and L-NAME cause the initiation of action potentials, (D) and the vasoconstriction profile to enter a vasospasm.

Effect of NNC 55-0396 on sensitivity to PE

0.3 μM NNC 55-0396 reversed the left-shift in the PE concentration-response curve that followed L-NAME (**Figure 4.3.6**), and this also occurred in denuded arteries. However, the effect was not observed with NNC 55-0396 after EDH inhibitors, and the concentration response curve remained left-shifted. The EDH inhibitors left-shifted the curve to a statistically similar degree as the treatments compromised the activity of eNOS. The EC50s for the respective treatments are displayed in the table below.

Treatment	**LogEC50**
Control	-5.833
L-NAME	-6.473
L-NAME + NNC	-6.010
Denuded	-6.465
Denuded + NNC	-6.003
TRAM-34 + Apamin	-6.361
TRAM-34 + Apamin + NNC	-6.185
L-NAME + TRAM-34 + Apamin	-6.472
L-NAME + TRAM-34 + Apamin + NNC	-6.019

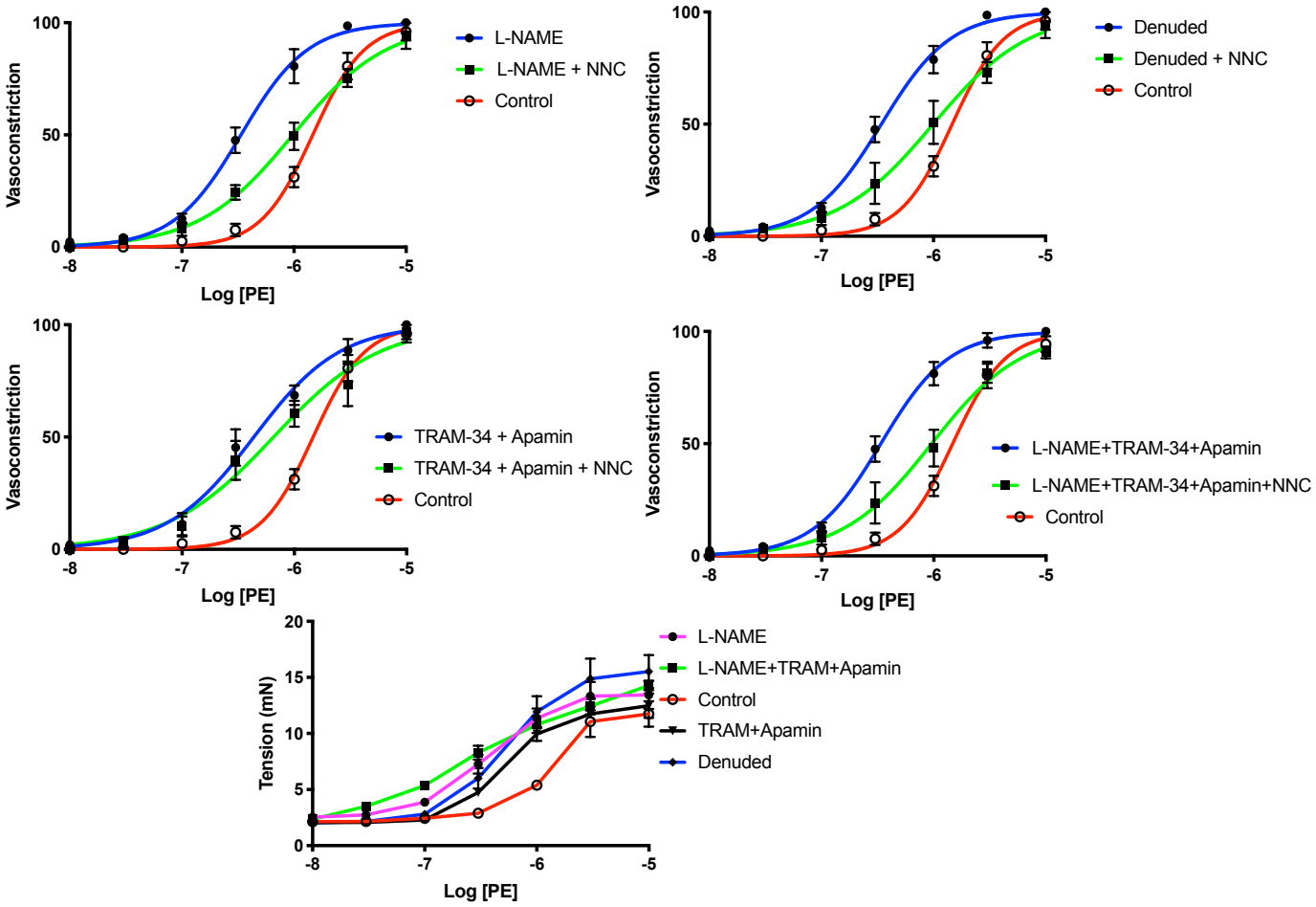


Figure 4.3.6 Dose-response curves showing the impact of NNC 55-0396 on various disruptions of the endothelial function.

Various treatments compromising aspects of the endothelium's dilatory function and their effect on the dose-response curve to PE. Vasoconstriction expressed as a percentage of maximal constriction to 30 µM PE and 45 mM hypertonic KCl (see **Methods & Materials section 2.3**). Raw tension data of treatments also shown. n=5 for all treatments.

Examination of the role of T-type calcium channels in response to action potentials in the coronary arteries

Rat intra-septal coronary arteries were normalised, maximal constriction ascertained, and myogenic tone established as detailed above (**Methods & Materials 4.2.I**). The membrane potential was then recorded (-38.7 ± 2.76 mV, n=5) (**Figure 4.3.7**), and the frequency of any oscillations measured (0.14 ± 0.08Hz). Some small oscillations were observed during myogenic tone, but these were not ubiquitous and only infrequently recorded. Incubation for 30 minutes with L-NAME, led to an observed change that did not reach significance, with a mean depolarization of -33.3 ± 1.76 mV (n=5), and a frequency of action potentials of 0.65 ± 0.15Hz. The subsequent addition of the T-type antagonist NNC 55-0396 completely abolished all action potentials, but without altering depolarization to PE (-33.5 ± 0.56 mV, n=5).

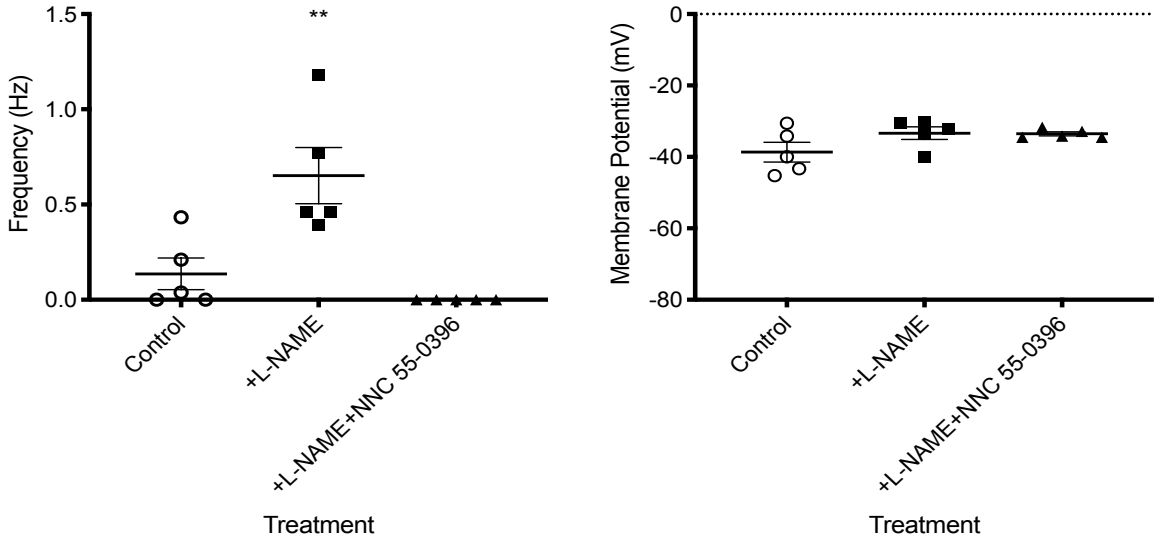


Figure 4.3.7 Electrical activity of eNOS blockade on intra-septal coronary arteries, and recovery with NNC 55-0396.

The addition of L-NAME increased the frequency of action potentials (A), with NNC 55-0396 abolishing them entirely. This is despite the depolarization of the smooth muscle cells to a similar membrane potential (B). ** P<0.01 compared to control

Provoking action potentials via the L-type calcium channels

Endothelium denuded third order rat mesenteric arteries exposed to Bay K8644 (10-30 nM) (**Figure 4.3.8)** generated robust action potential firing (n=6). The APs had a mean amplitude of 21.80 ± 0.83 mV and had a mean frequency of 1.17 ± 0.07Hz. Upon addition of the T-type channel antagonist NNC 55-0396 (n=5), the mean spike amplitude (23.00 ± 1.53 mV), and frequency (1.17 ± 0.11Hz) were unchanged. This was similar with Nickel (n=5) to denuded Bay K8644 treated vessels, which had action potentials with a mean amplitude of 21.54 ± 1.44 mV and a mean frequency of 1.13 ± 0.10Hz. Nifedipine (0.3 µM) abolished all residual action potentials (n=4). Controls were performed to ascertain the effect of Nifedipine on vasomotion and membrane potential, and on denuded arteries (not shown). It was found to abolish vasomotion in intact arteries, and block the denudation-derived spikes in denuded vessels, but still allow for depolarization to similar levels (under than -40 mV) with 3 µM PE in both cases.

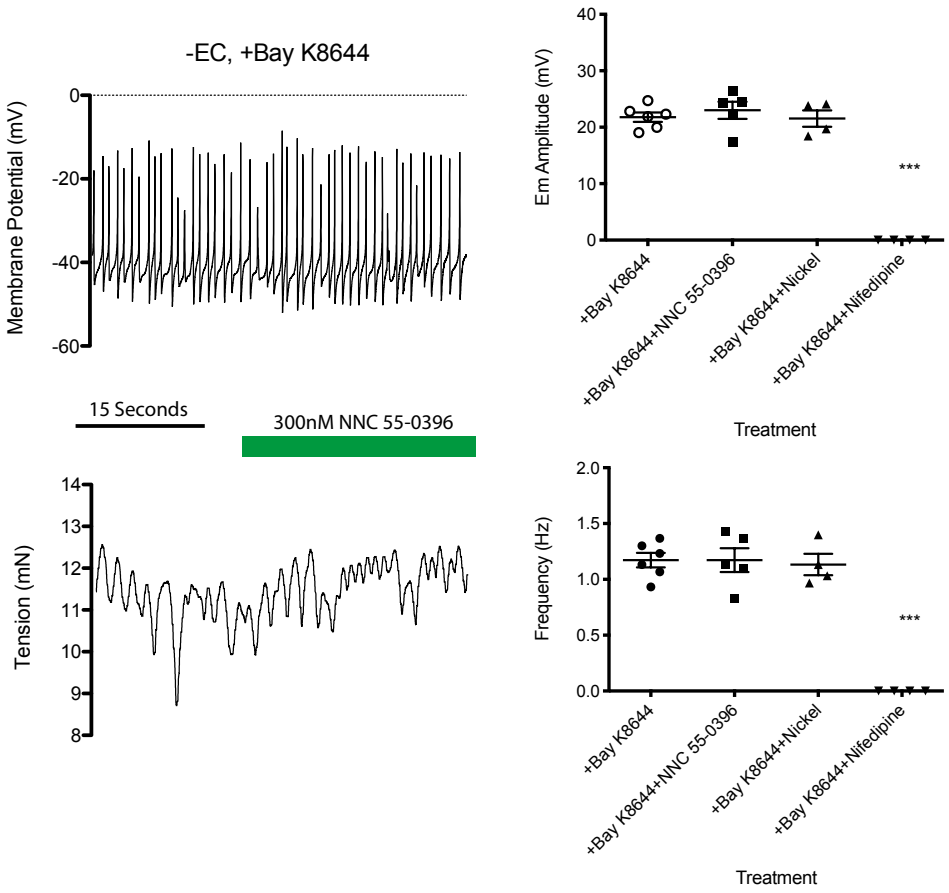


Figure 4.3.8 Effect of the L-type calcium channel opener Bay K8644 on denuded mesenteric arteries.

(A) Representative membrane potential and tension (C) traces of denuded mesenteric artery with exposure to 10 nM Bay K8644 (n=6), and lack of reversal with NNC 55-0396 (0.3 µM, n=5). (B) Mean amplitude ± SEM of action potentials from denuded vessels with Bay K8644 and various VGCC inhibitors. (D) Mean frequency ± SEM of action potentials from denuded vessels with Bay K8644 and various VGCC inhibitors. *** P<0.001 compared to control. Partial data sets of Bay K8644+Nickel and Bay K8644+NNC 55-0396 were acquired by Professor Christopher Garland.

4.4 Discussion

The rationale for the experiments performed for this chapter was to ascertain the electrical basis responsible for the disruption noted above (**Chapter 3.3**), and once membrane electrical activity was defined, pharmacologically to probe the provenance of the action potentials observed. The initial findings suggest the activation of the T-type calcium channels underlies the action potentials seen, and that it is critical for them to appear and disrupt the vasomotion profile recorded with control vessels.

It is clear from the above data (**Figure 4.3.1**) that in response to eNOS blockade, or physical stripping of the vascular endothelium, small rat mesenteric arteries have the ability to generate action potentials when depolarization was stimulated with 0.3 μM PE. This is important as apart from a small number of notable exceptions (Spencer & Greenwood, 2003; McNeish et al., 2010) vascular smooth muscle is usually electrically quiescent, showing a slow smooth depolarization, as opposed to rapid spiking observed in smooth muscle in other tissue beds such as the gut. Sensitivity to PE stimulation increased by approximately a factor of 10 as noted above (**Chapter 3.4**), and although mean tension was observed at a higher level for L-NAME treated and denuded arteries, the mean change in membrane potential (**Figure 4.3.2**) was not statistically significant, so the same level of depolarization occurred in both cases against control vasomotion. A slightly lower mean in denuded artery tension was observed compared to L-NAME treatment, but this was not statistically significant, and may reflect the trauma associated with denudation. From the amplitude data (**Figure 4.3.2**) we can observe the scale of the change from the vasomotion oscillations to the action potentials, the amplitude having almost doubled.

Having observed what was underlying the degeneration in the vasomotion waveform, the next stage was to apply the observations regarding the T-type channel blocker in the coronary arteries (**Figure 3.3.3**) to mesenteric vessels. The suggestion that blocking nitric oxide could be responsible for activating the T-type channels, leading to action potentials, was based on prior observations in middle cerebral arteries (Yuill et al., 2010; McNeish et al., 2010) that observed nifedipine-insensitive spikes resulting from eNOS blockade with L-NAME (100 μM). Patch-clamp electrophysiology studies in isolated vascular smooth muscle cells have also observed nifedipine-insensitive calcium channel currents that correspond with T-type channel activation and inactivation profiles (Lam et al., 1998; Morita et al., 1999; Morita et al., 2002; VanBavel et al., 2002; Navarro-Gonzalez et al., 2009). However, as in many ways cerebral arteries may differ from those in the periphery, it was important to study the latter, that form the microcirculation.

Once action potentials were generated with L-NAME, nickel chloride (50 μM), NNC 55-0396 (0.3 μM), or TTA-A2 were added, with no blocker added to a vessel another had been added to, as all the inhibitors proved irreversible. All T-type blockers reduced the level of tension observed (**Figure 4.3.3**) in the presence of L-NAME, even with a higher concentration of PE added (1-1.3 μM). This was in addition to reducing action potential frequency to zero – whilst depolarization with PE was similar level as with L-NAME. Combined these data indicate a return to the electrical profile, and vasoconstriction levels, of a healthy control artery, although vasomotion did not return in the majority of vessels. This was perhaps due to a latent role for T-type channels in vasomotion, or maybe a minor effect of these blockers on L-type channels, although previous studies indicate high selectivity for $Ca_v3.2$ at these concentrations over L-type channels (Lee et

al., 1999; Huang et al., 2004; Kraus et al., 2010), as well as internal controls showing no significantly different effect of these T-type blockers on control vasomotion waveform (not shown).

Once the link between T-type channels and the action potentials was established, the focus shifted to deciphering the difference between the response to eNOS blockade via L-NAME, and that seen by physical denudation. The responses, as shown in **Figures 4.3.1** and **4.3.2**, differ in that the L-NAME response shows bursts of action potentials, and periods of repolarization and dilation, but the denuded response shows constant spiking and no repolarization or dilation. There are two key factors to consider when comparing the treatments. The first is the lack of cell to cell signalling, shown to propagate coordinating waves along lengths of artery (Borysova et al., 2018); preliminary experiments were performed with the gap junction blocker carbenoxolone (n=3, not shown), but this proved too non-specific and was abandoned. The second, and more relevant, is the complete lack of EDH in physically denuded vessels. This therefore precipitated an investigation into the effects of blocking IK_{Ca} and SK_{Ca} channels on the action potentials.

As presented (**Figure 4.3.4**) TRAM-34 and Apamin, to block IK_{Ca} and SK_{Ca} respectively, increased the sensitivity to PE, and abolished vasomotion, as would be expected due to the feedback system thought to underlie the membrane potential oscillations (Garland et al., 2017). They failed however to elicit action potentials when endogenous nitric oxide production was intact. The addition of each, or both, of the EDH blockers was found to both increase the frequency of overall spikes, and reduce the frequency of bursts of spikes, indicating a shift towards the profile seen with denuded vessels, as

might be expected. There was a residual difference between the eNOS and EDH blocked vessels, and the denuded ones, one that may be explained by the gap junction propagation. But in general these data indicate that ECs mediate the bursting pattern.

Control concentration response experiments were performed to test the effect of the T-type blocker NNC 55-0396 against the sensitivity to PE, in control and dilatory-compromised vessels (**Figure 4.3.5**). Observed was an expected left-shift in response to the compromising treatments, and a right-shift back with the addition of 0.3 μM NNC 55-0396. The exception to this however was in the solely EDH blocked vessels, which exhibited a non-significant shift back from the compromising treatment.

Coronary arteries were next to be examined to see whether the T-type channels appeared to underlie the increase in tone seen with L-NAME application (**Figure 3.3.5**). As shown in the previous chapter, the removal of nitric oxide precipitated a large increase in vascular tone, which was then reduced back to myogenic tone levels with NNC 55-0396 (0.3 μM). Electrophysiological impalements of intra-septal coronary arteries were performed, with a heightened level of depolarization compared to complete relaxation. Some vessels exhibited slow-wave and low amplitude oscillations in membrane potential at myogenic tone, but most were latent. It has been previously reported in rat coronary arteries that nitric oxide greatly supresses myogenic tone (Szekeres et al., 2004), and this appeared to be supported by these data (**Figure 4.3.6**). The application of L-NAME led to the formation of action potentials, almost constant in profile and more akin to the profile seen with denuded mesenteric vessels than the L-NAME treated ones, perhaps a function of the lower membrane potential in coronary arteries more readily falling in the activation range for the T-type channels, as mean

membrane potential difference between myogenic tone and L-NAME treatment, and therefore spike development, was not significantly different (**Figure 4.3.6**). The same held true for the additional application of NNC 55-0396, which did not significantly change the mean membrane potential, despite abolishing action potentials in all cases.

The final strand to investigate in this chapter was the contribution of the L-type calcium channels to the action potentials, if any, and whether they could act in concert with the T-type channels or otherwise to initiate or propagate spiking behaviour. Experiments were performed with intact mesenteric arteries, L-NAME treated arteries, and denuded arteries. The endothelium intact vessels showed no action potentials with stimulation by PE and, in fact, the vasomotion was often enhanced in these vessels, presumably due to the increased activity of $Ca_V1.2$ channels, which contribute to the phenomenon, as cited above (**Chapter 3.1**). In denuded vessels the L-type channel opener Bay K8644 depolarized the membrane potential to cause constriction and action potentials without the aid of PE (**Figure 4.3.7**). As presented the T-type blockers nickel and NNC 55-0396 had no impact on either the amplitude or frequency of the action potentials, but the addition of the L-type blocker Nifedipine abolished spikes completely. This shows that whilst the native action potentials in response to reduced nitric oxide availability are mediated via the T-type channels, the L-type channels are capable of instigating action potentials, even once the T-type channels are inhibited, confirming nitric oxide appears to supress L-type activation as previously reported (Yuill et al., 2010; Harraz et al., 2015). Control experiments were performed with depolarization in intact arteries with PE (not shown), in the presence of Nifedipine to block the L-type channels. These controls showed it was possible to depolarize the membrane potential to the same degree with

the L-type channels blocked, but all vasomotion had been abolished, further giving credence to the theory that L-type channels underpin calcium entry for vasomotion. A parallel set of controls showed vasomotion uninhibited by nickel, suggesting the T-type channels play a small or non-existent role in healthy conditions, although this is a source of debate (Jensen & Holstein-Rathlou, 2009; Bjorling et al., 2013).

4.5 Conclusion

To conclude, the experiments and evidence above indicates that the disruption to regular 'physiological' vasomotion observed in **Chapter 3** is due to the initiation of action potentials, and these require T-type calcium channels input for triggering, but also require the L-type channels. The key difference between the two VGCCs is that input from the T-type channels is not observed in vasomotion, suggesting their activation in the absence of NO. EDH plays a role in repolarizing the smooth muscle cells when the endothelium is still present but not producing nitric oxide, but does not contribute towards the generation of action potentials. L-type channels are capable of producing action potentials in the absence of T-type input, but this seems to be the case under artificial conditions, and not what would be expected to be the case in normal endothelial dysfunction. Application of this theory to myogenically-active vessels showed the T-type channels were crucial to the increase in tension, and blockade may potentially offer a path for novel therapeutics.

Chapter 5

Investigating alternative pathways for the initiation of action potentials in vascular smooth muscle

5.1 Introduction

As observed above withdrawal of endogenous nitric oxide can lead to the generation of high frequency action potentials in both myogenically active, and non-myogenically active vascular smooth muscle and further, these are ostensibly mediated via T-type voltage-dependent calcium channels. The next stage of the investigation was designed therefore to confirm whether calcium events occurred in the arteries at the same frequency and manner as the observed action potentials.

If this was established, it seemed only logical to ensure that the earlier findings regarding components downstream of sGC were the responsible agents for recruiting or activating the T-type channels. Previous studies have provided evidence for the effect of downstream pathways of sGC on T-type channels; with the suggestion that direct activation of protein kinase G in cultured rat cerebral arterial SMCs led to a suppression of T-type currents, measured using patch-clamping electrophysiology (Harraz et al., 2014). Another investigation into the connection between T-type channels and their regulation by cGMP found, also using patch-clamping, that permeable analogues of cGMP could suppress T-type currents, and that this effect was mimicked with nitric oxide donors. The study in question used rat coronary myocytes (Quignard et al., 1997).

A review into the effects of T-type channel knockout models concluded that $Ca_v3.2$ channel deletion can lead to a lower vasodilatory ability *in vivo* (Hansen, 2015). Global knockouts of $Ca_v3.2$ have been achieved with encouraging survival rates, but a specific vascular smooth muscle knockout has yet to be reported (Chen et al., 2003).

5.1.I Alternative regulators of the T-type channels

Data presented earlier (**Chapter 4.4**) indicate a clear role for L-type calcium channels in the generation of smooth muscle action potentials. As mentioned previously, nitric oxide is known to suppress L-type calcium channel currents but has also been observed to enhance BK_{Ca} channel action directly (Bolotina et al., 1994; Mistry & Garland, 1998), via a cGMP-dependent mechanism (Robertson et al., 1993; Archer et al., 1994; Mandala et al., 2007), and via ryanodine receptor mediated calcium release (Yuill et al., 2010; McNeish et al., 2010). Both of these mechanisms therefore represented potential contributors to the action potentials seen now and could be tested with regard to their respective potential input.

Other regulators of different types of T-type channels have been described. For example, $Ca_v3.1$ in cardiac myocytes is known to be modulated via protein kinase A (Li et al., 2012), as are $Ca_v3.2$ channels in cerebral arterial smooth muscle (Harraz & Welsh, 2013). Also reported has been the regulation of neuronal $Ca_v3.2$ channels by S-nitrosothiols (Lee et al., 2013). This effect relied upon a redox mechanism, whereby cysteine residues on repeats I and II of the channels were nitrosylated by nitric oxide donors, and these effects were found to be insensitive to sGC blockade, suggesting a direct effect of nitric oxide to depress the activity of the channels. As observed in **Chapter 1**, the direct effect of nitrosylation on the variance of vasomotion has already been discounted in this study, and so was considered by this stage to be an unlikely consideration with regard to the action potentials. This study was also performed with reliance on the non-specific alkylating agent N-ethylmaleimide, which affects multiple targets. This compound is known to have the effect of blocking SNARE mediated

exocytosis in various cells (Puri et al., 2003; Yoon et al., 2007), and so could provide unreliable, non-specific outcomes in whole vessel myography experiments.

Another potential vascular smooth muscle pathway for the regulation of T-type channel relies upon oxidative stress reflecting an increase in activity of NADPH oxidases (Drummond et al., 2011; Streeter et al., 2013). In this scenario, increased concentrations of superoxide, produced by NADPH oxidases, scavenge nitric oxide and reduce tetrahydrobiopterin (Miller et al., 2010), This effect has been suggested to be relevant for an increase in the activation of T-type channels, or potentially their insertion into the cell membrane in arterial smooth muscle (Howitt et al., 2013).

5.1.II An endogenous inhibitor of eNOS

Asymmetric dimethylarginine has been described as an endogenous inhibitor of eNOS in the vasculature (Leone et al., 1992; Vallance & Leiper, 2004). It is a variant of methylarginine, formed by protein hydrolysis of protein arginine methyltransferases and transported via the same mechanism as the majority of L-arginine into endothelial cells, due to the similarity in structure (Fickling et al., 1993; Greene et al., 1993). It is suspected that the probable mechanism by which ADMA actions its effects is through competitive antagonism at the catalytic site with L-arginine (Boger & Ron, 2005). This raises the question of whether the effects can be reversed with an appropriate concentration of L-arginine, as this may represent a potential therapeutic avenue, but has only previously been explored *in vivo* (Perticone et al., 2005). If ADMA was to cause action potentials due to the block of eNOS, in a similar fashion to L-NAME, it could also be of therapeutic value if L-arginine could be used to restore endothelial functionality, as the physiological tolerance to this is well characterised (Melik et al., 2017).

5.2 Methods & Materials

5.2.I Wire myography

Third order mesenteric artery segments from rats were mounted and normalised in an isometric wire myograph as previously described (**Methods & Materials section 2.1 & 2.2**) and exposed to rising cumulative concentrations of PE to elicit an increasing level of vasoconstriction. Except for L-NAME, all drugs were added directly to the bath and L-NAME and ODQ were pre-incubated with arteries for a minimum of 30 minutes before PE was introduced, 5 minutes for SNOG and Bay 41-2272. Drugs were mixed through gentle bubbling in the chamber. Isolated rat intra-septal coronary artery segments were mounted on 15 μm diameter tungsten wire and normalised as referred to previously.

For full details on the set up for wire myography studies please refer to **Methods & Materials section 2.2**.

5.2.II Sharp microelectrode studies of membrane potential

Rat third order mesenteric arteries were mounted and normalised to resting tension in an isometric wire myograph as previously described (**Methods & Materials section 2.1 & 2.2**). The resting membrane potential (Em) of a single smooth muscle cell was recorded by impalement with a sharp borosilicate microelectrode back-filled with a 2M KCl solution. Inhibitors were added 30 minutes prior to impalement of the cell, and once an impalement had been successfully achieved (**Materials & Methods section 2.3.III**) increasing concentrations of PE were introduced. Drugs were mixed through gentle bubbling in the chamber.

For full details on the set up for sharp microelectrode studies please refer to **Methods & Materials section 2.3**.

5.3 Results

The effect of eNOS blockade and VGCC blockers on intracellular calcium levels

Experiments were performed to ascertain the intracellular calcium activity within the smooth muscle whilst condition from earlier electrophysiological experiments were replicated (**Figure 5.3.1**). It was found that under condition where action potentials were previously observed, calcium events were happening. Under treatment with L-NAME (100 µM, n=5) and stimulation with PE (0.3 µM) this led to a mean F/F_0 of 1.25 ± 0.03, a mean tension of 8.59 ± 0.54 mN, and a mean frequency of events of 0.45 ± 0.08Hz. This frequency was interestingly not significantly different from action potential frequency (**Chapter 4.3.3**). The addition of NNC 55-0396 (0.3 µM, n=5) reduced the mean F/F_0 to 1, the tension to 6.80 ± 1.05 mN, and the frequency of events to 0, still with 0.3 µM PE used as a pre-constrictor. The presence of Bay K8644 (30 nM, n=5) in addition to the conditions noted above, and the presence of 1 µM PE, led to a mean F/F_0 of 1.47 ± 0.06, a mean tension of 10.07 ± 0.99 mN, and a mean frequency of 0.57 ± 0.09Hz. The subsequent addition of the L-type channel blocker nifedipine (0.3 µM, n=5) led to a reduction of mean F/F_0 to 1, a reduction of tension to basal levels (1.86 ± 0.27 mN), and abolished calcium events. A representative image and quantification of the flashes is shown in **Figure 5.3.2**.

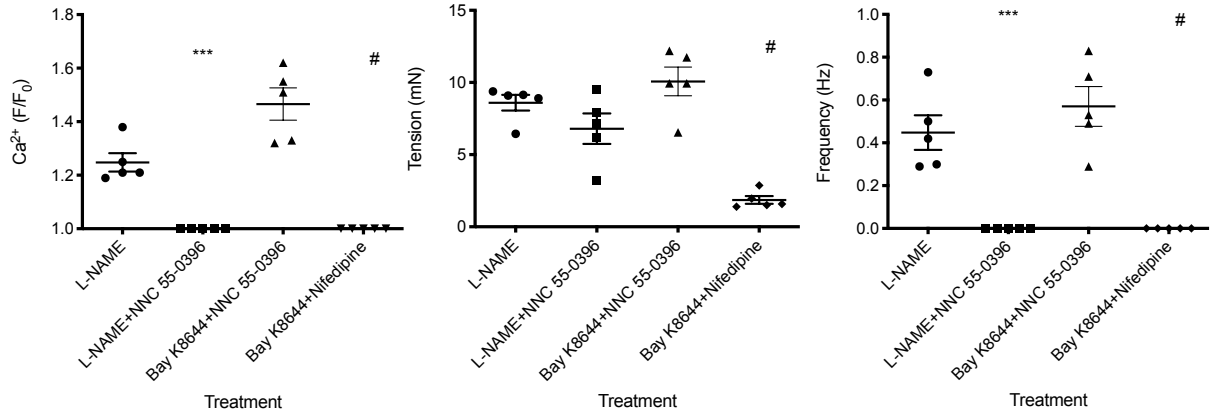


Figure 5.3.1: Quantification of calcium imaging of spike generation

(A) Mean F/F_0 amplitude from calcium imaging various treatments in response to PE (0.3 µM) stimulation. (B) Corresponding mean tension recordings during the same period as calcium recordings. (C) Mean frequency of the calcium events. *** P<0.001 compared to L-NAME. # P<0.001 compared to Bay K8644+NNC 55-0396. Experiments were set up by myself, performed and analysed by Dr Lydmyla Borysova, and Professor Kim Dora.

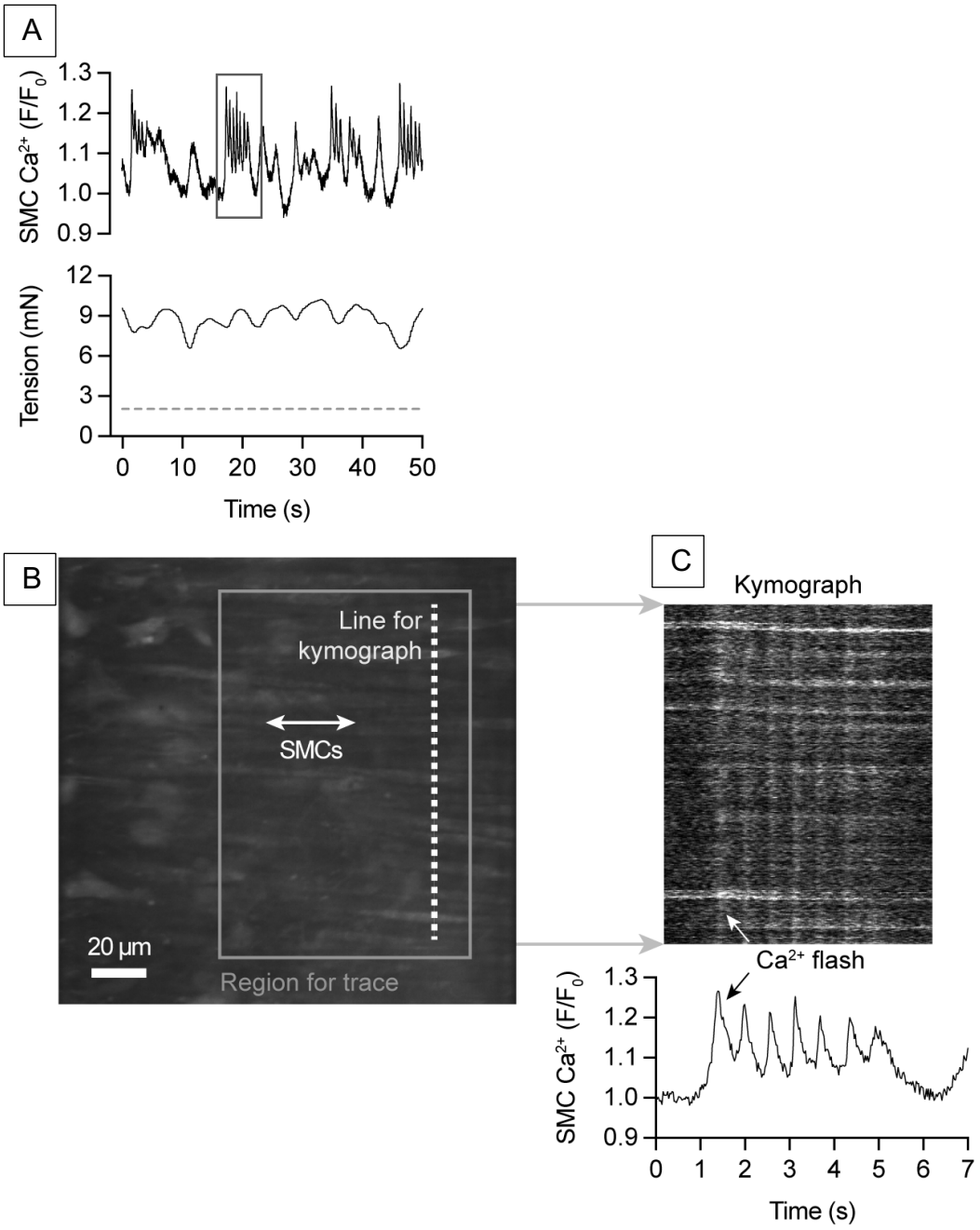


Figure 5.3.2: Representative calcium imaging trace and time lapse recording of spike generation

(A) Representative F/F_0 amplitude from calcium imaging in response to PE (0.3 µM) stimulation in the presence of L-NAME (100 µM). (B) Region of arterial smooth muscle imaged for the representative trace. (C) Kymograph showing a time lapse with an x-axis of time, corresponding with plot below, showing the flashes recorded from the broken line from (B) over 7 seconds. Image was composed by Professor Kim Dora.

Probing the effect of cGMP on action potentials

The next stage of the investigation was to investigate the impact downstream of sGC with regard to the spikes observed (**Figure 5.3.3**). The PKG inhibitor KT 5823 (1 µM, n=5) was used in an attempt to provoke action potentials, in conjunction with 2 µM PE. This led to a mean tension of 9.74 ± 0.51 mN, compared to a mean tension with the subsequent addition of ODQ (10 µM, n=5) of 10.03 ± 0.34 mN, when pre-constricted with 0.3 µM PE. Membrane potential measurements were equally statistically similar, at -35.50 ± 2.25 mV for KT 5823 treated vessels, and -37.84 ± 0.94 for ODQ treated ones. However, the divergence became clear when the action potential readings were taken: KT 5823 failed to elicit any action potentials across all experiments, regardless of time of exposure, whereas ODQ always stimulated them, and at a mean frequency of 0.59 ± 0.11Hz, so statistically similar level to those induced by L-NAME.

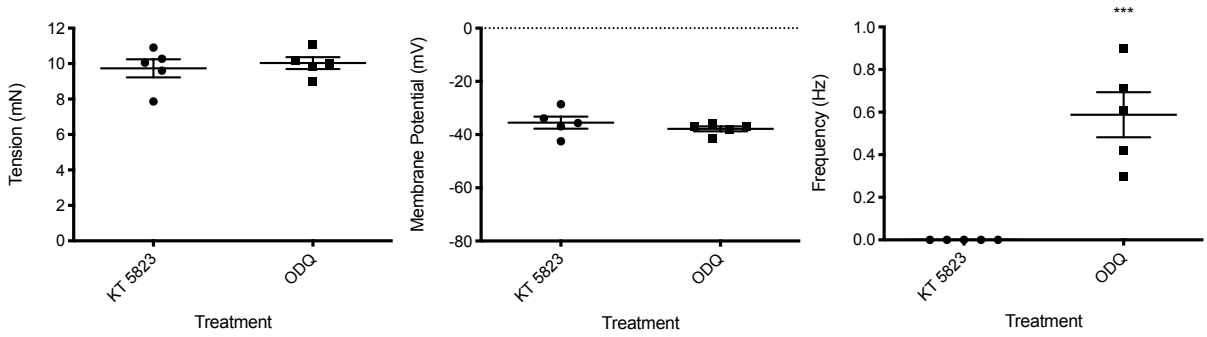


Figure 5.3.3: Effect of PKG and sGC blockade on tension and membrane potential

Mean tension and membrane potential across KT 5823 and ODQ treated vessels were statistically similar, showing a similar level of depolarization and stimulation, but the KT 5823 failed to provoke spikes, which were later generated in all case by the subsequent addition of ODQ. *** $P<0.001$.

Involvement of the BK_{Ca} channels and ryanodine receptors on action potentials

Due to the impact discussed previously (**Chapter 4.4**) of nitric oxide on BK_{Ca} channels and ryanodine receptors, it was decided to pharmacologically probe their function with respect to the spiking. The BK_{Ca} blocker paxilline (0.1 μM) was added to intact and healthy rat mesenteric arteries, stimulated with PE (1 μM, n=5), and the response measured. Although a slight sensitisation to PE was observed (not shown) the impact on membrane potential profile was uneventful (**Figure 5.3.4**), and depolarization was achieved to a level usually able to elicit spikes. Upon the addition of L-NAME (100 μM) however, although the mean membrane potential was not changed (-35 ± 1.29 mV, n=5), action potentials were generated at a frequency of 1.43 ± 0.10Hz, a huge increase on what was observed with L-NAME alone. Similarly, when ryanodine (1 μM, n=5) was utilised to block the ryanodine receptors, and hence outward repolarizing currents, in conjunction with L-NAME (100 μM) and PE (0.3 μM), the frequency of action potentials was measured at 0.87 ± 0.05Hz, an increase over the frequency observed with L-NAME alone.

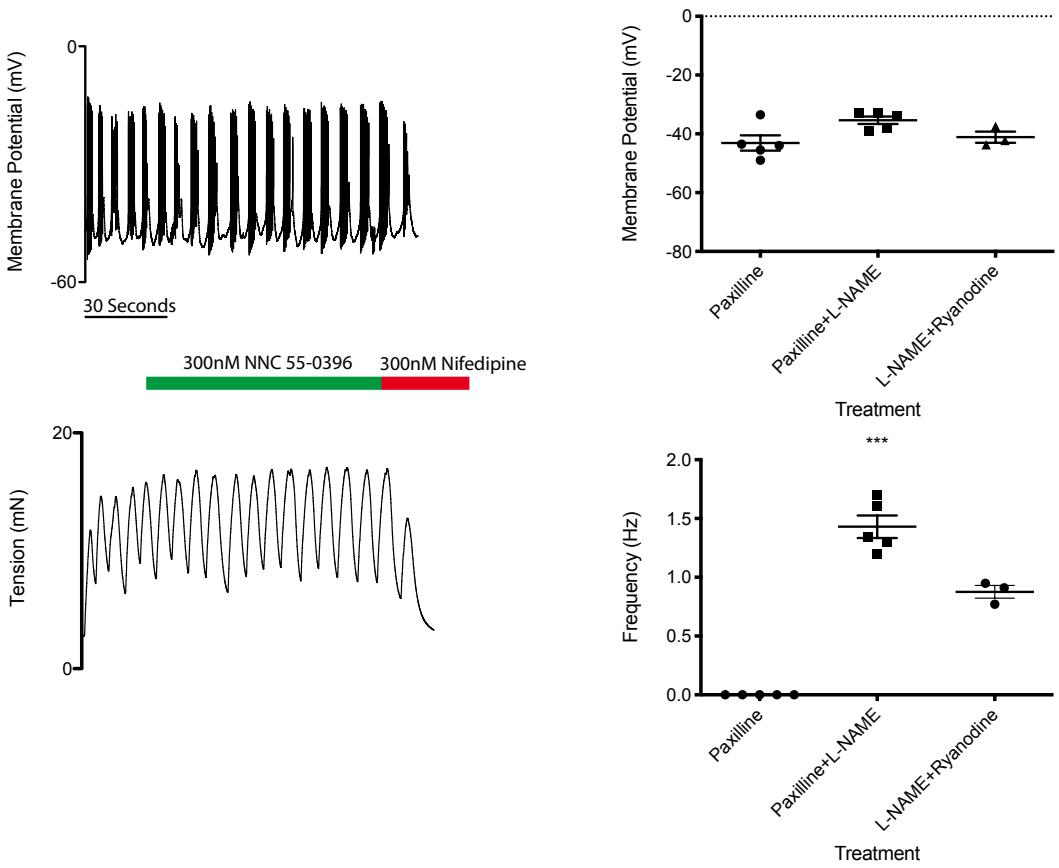


Figure 5.3.4: The effect of paxilline and ryanodine on membrane potential

The amplitude of oscillations in ryanodine and L-NAME treated vessels was amongst the largest observed, both in membrane potential and tension. Representative traces of both membrane potential and tension shown. Mean membrane potential and frequency of spikes for paxilline with and without L-NAME, and ryanodine with L-NAME. *** P<0.001.

The effect of NADPH oxidase blockade and superoxide formation and scavenging on action potential generation

Another potential pathway for activation of the T-type channels, is through superoxide formation (**Figure 5.3.5**). 10 µM TEMPOL was therefore used to inhibit superoxide dismutase, as well as to scavenge any residual superoxide, and was added once action potentials had been established with L-NAME (100 µM) and PE (0.3 µM), which stimulated a mean tension of 10.49 ± 0.71 mN (n=5), and a mean membrane potential of -38.55 ± 1.11 mV. The mean frequency of action potentials in this series was 0.50 ± 0.02Hz, which was not statistically different to the frequency generated with L-NAME alone. This was followed with an attempt to increase the levels of superoxide, to see if this would generate action potential firing in intact and healthy vessels without a need to block eNOS. Hypoxanthine (250 µM) and xanthine oxidase (3 U) were added to the bath 1 hour prior to experimentation to achieve this. The results of this treatment were not significantly different from any of the others shown below. PE (3 µM) was added to constrict the arteries; mean tension was observed to be 9.48 ± 0.48 mN (n=5), and mean membrane potential was -39.54 ± 1.16 mV. No spikes were observed across any experiment. The final treatment in this experimental series was the introduction of apocynin (500 µM) to inhibit NADPH oxidase, and therefore generate action potentials if this was the mechanism of generation, as opposed to cGMP mediation. No experiments with apocynin (n=5) showed any signs of spikes, with all of the vessels generating spikes subsequently with the blockade of eNOS. This was despite depolarization to a level beyond that where action potentials will usually be generated (-38.35 ± 1.09 mV), and negative controls were established to ensure no detrimental effect on healthy vessel contractility (n=2).

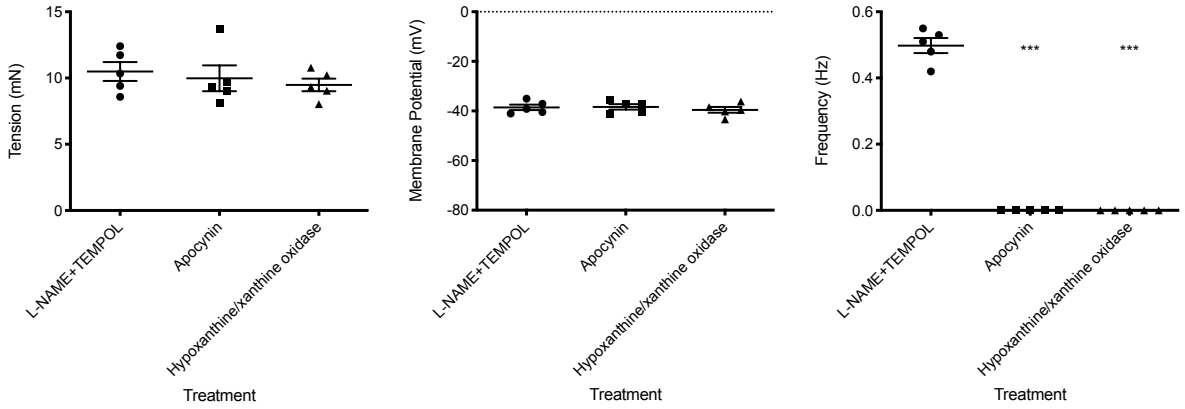


Figure 5.3.5: The effect of NADPH oxidase and superoxide inhibition.

Mean tension, mean membrane potential, and mean action potential frequency upon exposure to treatments that blocked superoxide generation and scavenged residual superoxide (TEMPOL), that instigated blockade of NADPH oxidase (apocynin), and generated excess superoxide (hypoxanthine/xanthine oxidase). *** = $p<0.001$.

The effect of an endogenous eNOS inhibitor on membrane potential and spikes

The final investigation for this chapter investigated an endogenous inhibitor of eNOS, ADMA. Exogenous ADMA (300 µM) was added to intact and healthy vessels, with PE (1 nM – 30 µM, n=5) used to determine a concentration-response relationship (**Figure 5.3.6**). ADMA caused a left-shift, as would be predicted, but when the experiments were repeated in denuded arteries, no significant shift occurred (**Figure 5.3.6**). A concentration-response relationship to ACh (1 nM- 3µM, n=5) was also established, and a right-shift observed, also as may have been predicted. Interestingly the subsequent addition of L-arginine (1 mM) returned the vasorelaxation curve to ACh back to a similar level as the control (n=5), and the addition of L-arginine alone failed to elicit a statistically significant shift in the curve leftwards.

The next step was to use electrophysiological experiments to measure membrane potential and action potential generation. 300 µM ADMA was pre-incubated with arteries for a minimum of 30 minutes prior to impalements being achieved, and then PE (0.3 µM) was added to depolarize the vessels. This was carried out with ADMA (n=3), and also with NNC 55-0396 present (n=3). The ADMA treated vessels had a mean membrane potential of -40.57 ± 1.73 mV, compared to a mean of -37.30 ± 1.13 mV with the subsequent addition of NNC 55-0396. With regards to action potential generation, ADMA treated vessels developed action potentials at an average frequency of 0.75 ± 0.09Hz, and these were abolished with NNC 55-0396 present.

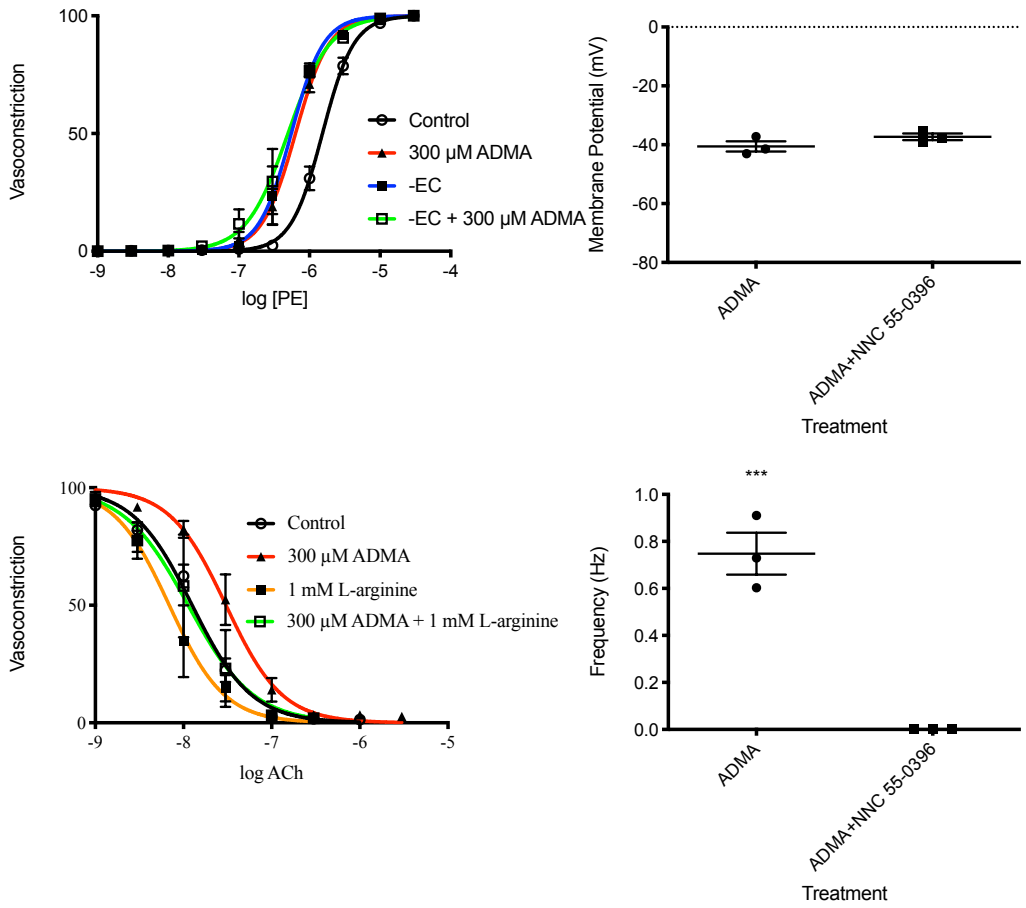


Figure 5.3.6: The effect of ADMA and L-arginine on tension and membrane potential.

(A) Concentration-response relationship between various treatments against PE, showing a left-shift for the addition of 300 µM ADMA against control, and no impact when using denuded vessels. (B) Membrane potential means for ADMA against the subsequent addition of NNC 55-0396, showing no difference between the two treatments. (C) Concentration-response relationship between various treatments and ACh, showing a right-shift with the addition of 300 µM ADMA, and a reversal with 1 mM L-arginine added. (D) Frequency of action potentials in ADMA treated vessels, and the subsequent addition of NNC 55-0396, which abolished them. *** = $p<0.001$. Concentration-response experiments were performed by James Alden, some electrophysiology experiments were set up by James Alden, and all were performed and data were analysed by myself.

5.4 Discussion

The aim of the experimental sets presented above was to probe and characterise the nature of the action potentials induced with PE and the mechanisms for induction to show whether there was an alternative or additional pathway operating, compared to the evidence presented in **Chapter 4**.

Calcium imaging (**Figure 5.3.1 & 5.3.2**) provided a clear insight that the driving force behind the action potentials was indeed calcium entry, as the signals had similar frequency and sensitivity to T-type channel blockers as the action potentials. That the flashes could then be redeveloped with the introduction of the L-type channel activator Bay K8644, in the presence of NNC 55-0396, also gives credence to the observation prior (**Figure 4.3.7**) whereby stimulation of the L-type channels can produce action potentials in eNOS-compromised vessels, that are insensitive to T-type channel blockade. The F/F_0 of the Bay K8644 induced flashes proved to be greater than those instigated by L-NAME alone, reflecting perhaps the increased open probability of the L-type channels with Bay K8644 present.

The next experimental data set also provided interesting and additional insight (**Figure 5.3.3**), as these data showed a disconnect between the observed effects of inhibiting sGC and inhibiting PKG, something that would only be expected if cGMP was having a direct effect, and not merely acting as a secondary messenger to activate PKG. The KT 5823 data were something of an anomaly then, considering the literature supports a role for PKG regulation of T-type channels (Quignard et al., 1997; Harraz et al., 2014), supporting the data presented above (**Figure 5.3.3**) for ODQ. Very limited evidence

exists to show direct an action by cGMP on targets other than PKG, especially within the vascular system, where its effects and signal transduction are well established, although the potential for cross-activation of PKA by cGMP within the vasculature has been observed previously (Lohmann et al., 1997; Cornwell et al., 1994).

Experiments with mice mesenteric vessels were also carried out (n=3, not shown), but these arteries were electrically unexcitable and failed to respond to any treatment to induce action potentials. Pharmacological treatments included L-NAME (100 μM) to block eNOS, paxilline (0.1 μM) to block BK_{Ca} channels, and 4-aminopyridine (1 mM) to block K_v channels (Harder & Sperelakis, 1979). This was unfortunate, as global knockout models for $Ca_v3.2$ are available (Chen et al., 2003) and have shown promising results previously (Harraz et al., 2015).

The role of smooth muscle BK_{Ca} channels and ryanodine receptors was investigated in rat arteries to define any contribution, in action potential generation (**Figure 5.3.4**). Using patch-clamp electrophysiology it has been reported previously that BK_{Ca} channel activity is directly enhanced by nitric oxide (Bolotina et al., 1994; Mistry & Garland, 1998), so paxilline was added to control arteries to probe this possibility and see whether action potentials were evoked without any other pharmacological interrogation. Despite depolarization to the level previously shown to active action potentials in L-NAME treated or denuded vessels, none followed paxilline alone. However, on addition of L-NAME to block eNOS (**Figure 5.3.4**), high frequency spike firing occurred. This observation doesn't rule out a role for the BK_{Ca} channels in action potential generation however, as it has been reported that BK_{Ca} channel currents can be enhanced by a cGMP-dependant mechanism (Robertson et al., 1993; Archer et al., 1994;

Mandala et al., 2007). Also tested was the effect of blocking ryanodine receptor induced calcium release, as these receptors have previously been reported to be directly activated by nitric oxide (Yuill et al., 2010; McNeish et al., 2010) and could therefore play a role in action potential initiation. The application of ryanodine led to a large increase in amplitude of spikes observed compared to L-NAME, and a slight increase in frequency. This could be due to the lack of feedback on the BKCa-RyR axis, and therefore the loss of spontaneous transient outward currents (STOCs), which are known to provide a feedback mechanism with Ca^{2+} sparks produced by the RyRs leading to activation of the nearby BK_{Ca} channels and the associated K^+ efflux to repolarize the cell (Perez et al., 2001). Interestingly, it has been observed that, due to the effect of caveolin1 within caveolae, $Ca_v3.2$, RyRs and BK_{Ca} channels may form co-localised complexes (Hashad et al., 2018). This study was performed with mouse mesenteric arteries, which as mentioned above (**Chapter 5.4**), we found not to generate action potentials, which may be pertinent as the study in question suggested a role for them in governing Ca^{2+} sparks, and therefore negative feedback, potentially the opposite of what is reported in this thesis.

An alternative pathway for generating action potentials is through the NADPH oxidase and superoxide pathway (**Figure 5.4.1**), which has been shown to activate vascular smooth muscle T-type channels through superoxide ion (Howitt et al., 2013). The same study also suggested that upon withdrawal of nitric oxide, T-type channels migrated to the cell membranes, presumably in order to be available to activate current passage. The rationale then for experiments with TEMPOL (**Figure 5.3.5**), which is both a superoxide dismutase inhibitor and a radical scavenger, was to measure the effect of

superoxide withdrawal on action potentials *in situ*. TEMPOL failed to affect the frequency of spikes, and no changes in either membrane potential or tension were recorded when added onto a vessel already producing action potentials. One study raised the possibility that exposure of vascular smooth muscle to L-NAME resulted in trafficking of $Ca_v3.1$ channels to the cell membrane from the cytosol (Howitt et al., 2013). This was initially presented as immunohistochemistry on rat basilar VSMCs, but the quantification process requires optimisation as the corresponding experiments in whole artery staining were less than conclusive.

Similarly negative were data derived from the opposite approach: hypoxanthine and xanthine oxidase were incubated with arteries for an hour prior to experiments with PE, and these also failed to show any impact on action potential production. If such an impact was to be seen, it would be due to the increase in hypoxanthine and xanthine oxidase producing a larger than usual level of superoxide, which would therefore activate the T-type channels if it had a role to play. The final experiments in this set were performed with apocynin, a direct inhibitor of the NADPH oxidases. This should have also theoretically produced action potentials if increased superoxide production due to nitric oxide blockade of the enzymes prevented T-type activation. However once again action potentials were not elicited. Taken together these data support the previous mechanism of T-type channel mediated action potential invoking cGMP acting directly downstream of sGC.

Finally, an endogenous inhibitor of eNOS (Leone et al., 1992; Vallance & Leiper, 2004) was utilised to discover whether it had the ability to evoke action potentials similar to synthetic compounds. In concentration-response experiments, ADMA left-shifted the

response to PE compared to a control (**Figure 5.3.6**) and had no effect upon the curve of physically denuded vessels. Similarly, ADMA also right-shifted the response to ACh compared to control experiments, with this effect being recovered with L-arginine, showing the competitive nature of ADMA as an antagonist (Boger & Ron, 2005). Electrophysiology experiments showed ADMA producing NNC 55-0396-insensitive action potentials, at a statistically similar level to those generated by L-NAME.

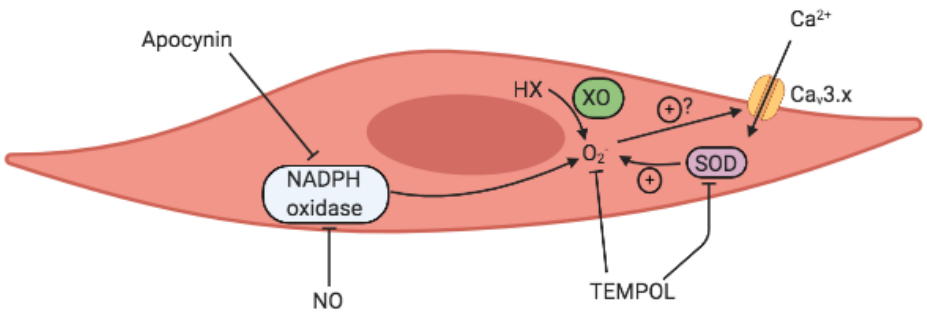


Figure 5.4.1: The potential NADPH oxidase facilitated pathway of $Ca_v3.x$ activation

NADPH oxidase is responsible for the production of superoxide (O_2^-), which some literature suggests can activate T-type channels (Howitt et al., 2013). This pathway can be inhibited with apocynin or NO. Hypoxanthine (HX) can also produce O_2^- in tandem with the enzyme xanthine oxidase (XO). Finally, superoxide dismutase can produce O_2^-, and this enzyme can be blocked with TEMPOL, which is also a known reactive oxygen species scavenger.

5.5 Conclusion

This chapter has demonstrated that an increase in intracellular calcium underlies the action potentials observed. It has also presented data that by exclusion sure up the the sGC pathway appears as the most likely mechanism for activation of T-type channels after the withdrawal of nitric oxide. These data show the NADPH oxidase pathway was unable to initiate action potentials when the most active components of the pathway were suppressed or enhanced. Finally, data in this chapter has also demonstrated an endogenous inhibitor of eNOS has the capacity to generate spikes, and the effects of it can be reversed with the application of a greater concentration of L-arginine. This suggests a potential therapeutic route to overcome any effects that may be ascribed to elevated levels of ADMA in life. One small-scale study has already gathered evidence of an increased ADMA blood plasma concentration in essential hypertensive patients; the same study found that the infusion of L-arginine increased the vasodilatory capacity of these hypertensives significantly more than for normotensive subjects (Perticone et al., 2005).

Chapter 6

Summary and future directions

This thesis examines the role that NO and its downstream pathways play in governing vasomotion, and the input when endogenous nitric oxide production is curtailed, either pharmacologically or by physical removal of the endothelium. Functional experiments were performed in order to test the hypotheses outlined within the experimental chapters above and were centred around collecting vasoconstriction and membrane potential data via wire myography and sharp electrode electrophysiology respectively. Small mesenteric resistance arteries were the main source of data, but intra-septal coronary arteries were also utilised. The fundamental hypothesis of this thesis was that the pharmacological prevention of endothelial nitric oxide production leads to an activation of the T-type calcium channels, appearing to be mediated downstream of cGMP, that leads to action potentials, and this underlies the disruption of healthy vasomotion observed in these compromised vessels, with inhibition of these channels promoting a restorative effect on vascular smooth muscle function.

In **Chapter 3** it was demonstrated that the disruption to vasomotion when endogenous nitric oxide production was withdrawn was due to effects downstream of sGC.

L-NAME was used to achieve eNOS inhibition and led to chaotic vasomotion that could be reversed with application of the synthetic nitric oxide donor SNOG. A similar reversal was not observed with the sGC inhibitor ODQ, and Fourier transform analysis of the waveforms confirmed the similarities between blockade of both enzymes in terms of the chaotic vasomotion induced, suggesting a common pathway. Further probing of this pathway with an sGC stimulator supported these observations. These findings were replicated to a degree in myogenically-active coronary small arteries, with interesting preliminary findings using a non-dihydropyridine T-type calcium channel antagonist,

NNC 55-0396, to reverse the effect of eNOS inhibition, as opposed to exogenous nitric oxide.

The focus of **Chapter 4** was to uncover the electrical basis for the disruption observed in **Chapter 3**. Membrane potential recordings showed that withdrawal of endothelial nitric oxide synthesis led to the generation of action potentials within the smooth muscle cells. These, along with the noted effects of nitric oxide withdrawal on various targets, had the effect of preventing the smooth and regular oscillations in membrane potential, or vasomotion, seen under control conditions and accounted for the greater levels of vasoconstriction with a chaotic, unstable profile. Removal of EDH, a major route to vasodilation in small arteries, abolished residual repolarization during chaotic vasomotion and led to vasospasm, due to continuous action potential spiking, rather than bursts of the spikes seen after eNOS blockade. In both cases, the action potentials were sensitive to T-type calcium channel inhibitors, of which three structurally different compounds were used.

Next an L-type calcium channel component was established, through the use of a dihydropyridine blocker for these channels, nifedipine, as well as a structurally related opener. This proved that L-type contribution was crucial as an accessory for the appearance of action potentials, and NNC 55-0396-insensitive action potentials were able to be mediated through the use of an L-type channel opener, but this phenomenon was not replicated under standard impairment of the endothelium, as would be expected physiologically. Tellingly, T-type channel inhibition in arteries with a healthy endothelium showed no effect on the vasoconstriction profile of vasomotion, whereas L-type inhibition under the same circumstances abolished vasomotion. These findings

were once again supported in myogenically-active coronary arteries, with the spikes mediated by eNOS inhibition removed by T-type blockade, sustaining a return to a control level of myogenic tone and corresponding membrane potential, which was then reduced to basal tone and resting membrane potential by L-type inhibition as expected. No pre-constrictor was required for these coronary artery experiments.

Chapter 5 initially investigated the calcium basis for the action potentials and showing that a spike in intracellular calcium underlies their appearance. Calcium imaging data supported the electrophysiological recordings by showing a lack of calcium events in the presence of NNC 55-0396 in vessels treated with L-NAME, but that the application of an L-type channel opener, in tandem with PE, would cause nifedipine-sensitive action potentials, despite the presence of NNC 55-0396.

High frequency and amplitude spikes were observed after depolarization in the presence of BK_{Ca} and ryanodine inhibitors, with spikes generated from the former sensitive to the pre-incubation with NNC 55-0396. This was interesting as it appeared to indicate a role for BK_{Ca} channels, in concert with the T-type channels, in facilitating the action potentials. Block of BK_{Ca} channels alone failed to elicit action potentials during pre-constricted with PE however, underlining the apparent critical role downstream of nitric oxide in activating the T-type channels. This supports what is known regarding the interaction of BK_{Ca} channels and ryanodine receptors, and it does not discount a role for these channels in the action potential mechanism, only that they are not the primary drivers of such electrical activity.

Another prospective target of nitric oxide, the NADPH oxidase pathway, was probed as previous studies had suggested this as a mechanism for the activation of vascular T-type

channels. The production of superoxide was prevented, or stimulated, in turn in separate arteries. The NADPH oxidase enzyme was also inhibited. None of these three treatments had any significant impact the production or sustenance of action potentials, further giving credit to the sGC-mediated pathway as the main route to suppress T-type channel activation.

Finally, an endogenous inhibitor of eNOS was investigated, both in vasoconstriction and membrane potential experiments to indicate whether physiological changes might influence NO synthesis and alter vasoreactivity. Concentration-response studies to PE and ACh demonstrated a left-shift in the former, and right-shift in the latter. The latter could be reversed on application of L-arginine, the enzyme substrate with which ADMA competes to occupy the eNOS catalytic site. Electrophysiological data showed the generation of NNC 55-0396-sensitive action potentials with ADMA present during stimulation with PE, showing it to be very similar to L-NAME.

Experimental results across all chapters were encouraging, and the evidence gathered strongly suggests the withdrawal of nitric oxide causes disruption to vasomotion via the generation of T-type channel mediated action potentials, with the T-type channels usually inhibited downstream of cGMP, or a target of it independent of PKG. This effect is exacerbated by the further loss of EDH, as no repolarization can take place, resulting in a constant vasospasm upon stimulation in mesenteric resistance arteries. With regards to the next steps of the investigation, work has already begun on testing the equivalent arteries from more advanced aged animals, to observe any changes in electrical excitability with age; as well as investigating the prospective of arteries from spontaneously hypertensive rats producing spontaneous action potentials, perhaps

aiding our understanding of some of the pathophysiology observed with that animal model. Further experiments to be performed on tissue types used across the course of this thesis would include biochemical characterisation of the individual ion channels involved, and any possible co-localisation, to produce the observations from this thesis. This includes immunohistochemistry experiments, especially concerning the interaction between T-type and L-type calcium channels, and other agents responsible for ion flux, such as the BK_{Ca} channels and ryanodine receptors, as some evidence exists to suggests there may be a microdomain that could aid feedback involving the aforementioned channels. Therefore, a proximity ligation assay, or a similar co-localisation technique, could be utilised to confirm this.

Further functional experiments could include sharp electrode impalements in pressurised arteries, to uncover whether the same electrical activity is present under isobaric conditions, but also to potentially enable the simultaneous recording of membrane potential and intracellular calcium. A useful technique to discover the nature of the action potentials would be patch-clamping electrophysiology studies, although the practical prohibitions of performing said technique on intact tissue are great, due to issues forming an effective seal directly on the vascular smooth muscle cells, with the surrounding adventitia and detritus. Pursuing the ADMA pathways could include interfering with other mechanisms either upstream or downstream of endogenous ADMA, however this is limited somewhat by the availability of compounds acting specifically on the intended targets. L-arginine could also be used in membrane potential recordings, to ascertain whether its addition is able to reverse the action potentials, as

this may provide a relatively benign therapeutic route for patients with various cardiovascular disorders.

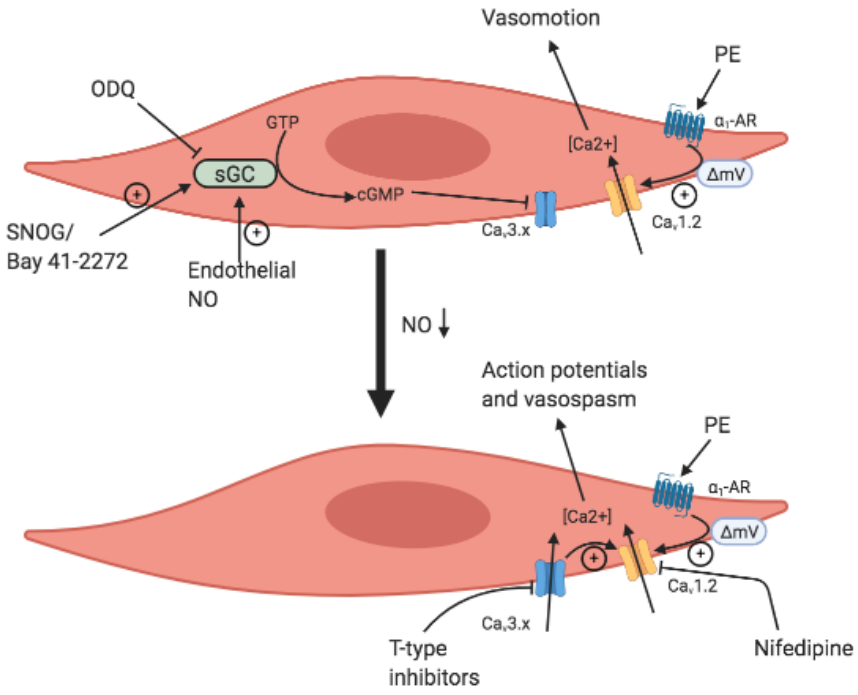


Figure 6.1.1: The proposed pathway for action potential generation

cGMP, produced from GTP with sGC catalysis, inhibits T-type calcium channels, preventing the generation of action potentials by limiting the reinforcing action from the T-type channels onto L-type channels. PE evoked depolarization is required to activate L-type channels and the result is vasomotion. In arteries where endothelial NO has been compromised, physiologically or pharmacologically, the production of cGMP is halted, leading to the activation of the T-type channels and subsequent action potentials and vasospasm. Not shown here are the interactions with BK_{Ca} channels and RyRs (discussed in **Chapter 5.4**).

References

A., M. A., Michael, D. S. T., P., J. C., Henry, D., R., D. G., & G., S. C. (2010). Augmented superoxide production by Nox2-containing NADPH oxidase causes cerebral artery dysfunction during hypercholesterolemia. *Stroke*, *41*(4), 784–789.

Aalkjær, C., Boedtkjer, D., & Matchkov, V. (2011). Vasomotion–what is currently thought? *Acta Physiologica*, *202*(3), 253–269.

Aalkjær, C., & Nilsson, H. (2005). Vasomotion: cellular background for the oscillator and for the synchronization of smooth muscle cells. *British Journal of Pharmacology*, *144*(5), 605–616.

Albert, A. P., & Large, W. A. (2003). Store-operated Ca^{2+}-permeable non-selective cation channels in smooth muscle cells. *Cell Calcium*, *33*(5), 345–356.

Amberg, G. C., Navedo, M. F., Nieves-Cintrón, M., Molkentin, J. D., & Santana, L. F. (2007). Calcium sparklets regulate local and global calcium in murine arterial smooth muscle. *The Journal of Physiology*, *579*(Pt 1), 187–201.

Amberg, G. C., & Navedo, M. F. (2013). Calcium dynamics in vascular smooth muscle. *Microcirculation (New York, N.Y.: 1994)*, *20*(4), 281–289.

Andreas, B., F., G. M., Karl, D., Shang-Zhong, X., Mikael, A., J., B. D., Jonas, B., Per, H., & Karl, S. (2003). Cholesterol depletion impairs vascular reactivity to endothelin-1 by reducing store-operated Ca^{2+} entry dependent on TRPC1. *Circulation Research*, *93*(9), 839–847.

Archer, S. L., Huang, J. M., Hampl, V., Nelson, D. P., Shultz, P. J., & Weir, E. K. (1994). Nitric oxide and cGMP cause vasorelaxation by activation of a charybdotoxin-sensitive K channel by cGMP-dependent protein kinase. *Proceedings of the National Academy of Sciences*, *91*(16), 7583 LP – 7587.

Bagher, P., Beleznai, T., Kansui, Y., Mitchell, R., Garland, C. J., & Dora, K. A. (2012). Low intravascular pressure activates endothelial cell TRPV4 channels, local Ca^{2+} events, and IK_{Ca} channels, reducing arteriolar tone. *Proceedings of the National Academy of Sciences of the United States of America*, *109*(44), 18174–18179.

Bandick, N. R., & Sparks, H. V. (1970). Contractile response of vascular smooth muscle of renal hypertensive rats. *American Journal of Physiology-Legacy Content*, *219*(2), 340–344.

Benbow, S. J., & Williams, G. (1997). Impaired peripheral vasomotion. *Diabetes Care*, *20*(3), 462.

Beech, D. J. (2005). Emerging functions of 10 types of TRP cationic channel in vascular smooth muscle. *Clinical and Experimental Pharmacology & Physiology*, *32*(8), 597–603.

Beech, D. J. (2013). Characteristics of transient receptor potential canonical calcium-permeable channels and their relevance to vascular physiology and disease. *Circulation Journal*, *77*(3), 570–579.

Bény, J., & Schaad, O. (2000). An evaluation of potassium ions as endothelium-derived hyperpolarizing factor in porcine coronary arteries. *British Journal of Pharmacology*, *131*(5), 965–973.

Berridge, M., & Rapp, P. E. (1979). A comparative survey of the function, mechanism and control of cellular oscillators. *Journal of Experimental Biology*, *81*(1), 217–279.

Bevan, J. A., & Osher, J. V. (1972). A direct method for recording tension changes in the wall of small blood vessels in vitro. *Agents and Actions*, *2*(5), 257–260.

Björling, K., Morita, H., Olsen, M. F., Prodan, A., Hansen, P. B., Lory, P., Holstein-Rathlou, N., & Jensen, L. J. (2013). Myogenic tone is impaired at low arterial pressure in mice deficient in the low-voltage-activated $Ca_v3.1$ T-type Ca^{2+} channel. *Acta Physiologica*, *207*(4), 709–720.

Böger, R. H., & Ron, E. S. (2005). L-Arginine improves vascular function by overcoming deleterious effects of ADMA, a novel cardiovascular risk factor. *Altern Med Rev*, *10*(1), 14-23.

Boittin, F.-X., Macrez, N., Halet, G., & Mironneau, J. (1999). Norepinephrine-induced Ca^{2+} waves depend on $InsP_3$ and ryanodine receptor activation in vascular myocytes. *American Journal of Physiology-Cell Physiology*, *277*(1), C139–C151.

Bolotina, V. M., Najibi, S., Palacino, J. J., Pagano, P. J., & Cohen, R. A. (1994). Nitric oxide directly activates calcium-dependent potassium channels in vascular smooth muscle. *Nature*, *368*(6474), 850–853.

Bolton, T. B., Lang, R. J., & Takewaki, T. (1984). Mechanisms of action of noradrenaline and carbachol on smooth muscle of guinea-pig anterior mesenteric artery. *The Journal of Physiology*, *351*(1), 549–572.

Borysova, L., Dora, K. A., Garland, C. J., & Burdyga, T. (2018). Smooth muscle gap-junctions allow propagation of intercellular Ca^{2+} waves and vasoconstriction due to Ca^{2+} based action potentials in rat mesenteric resistance arteries. *Cell Calcium*, *75*, 21–29.

Bouskela, E., & Grampp, W. (1992). Spontaneous vasomotion in hamster cheek pouch arterioles in varying experimental conditions. *American Journal of Physiology-Heart and Circulatory Physiology*, *262*(2), H478–H485.

Bouskela, E., Cyrino, F. Z. G. A., & Wiernsperger, N. (1997). Effects of insulin and the combination of insulin plus metformin (glucophage) on microvascular reactivity in control and diabetic hamsters. *Angiology*, *48*(6), 503–514.

Bowles, D. K., Hu, Q., Laughlin, M. H., & Sturek, M. (1997). Heterogeneity of L-type calcium current density in coronary smooth muscle. *American Journal of Physiology-Heart and Circulatory Physiology*, *273*(4), H2083–H2089.

Braunstein, T. H., Inoue, R., Cribbs, L., Oike, M., Ito, Y., Holstein-Rathlou, N.-H., & Jensen, L. J. (2009). The role of L- and T-type calcium channels in local and remote calcium responses in rat mesenteric terminal arterioles. *Journal of Vascular Research*, *46*(2), 138–151.

Bredt, D. S., & Snyder, S. H. (1990). Isolation of nitric oxide synthetase, a calmodulin-requiring enzyme. *Proceedings of the National Academy of Sciences*, *87*(2), 682 LP – 685.

Briones, A. M., Daly, C. J., Jimenez-Altayo, F., Martinez-Revelles, S., Gonzalez, J. M., McGrath, J. C., & Vila, E. (2005). Direct demonstration of beta 1- and evidence against beta 2- and beta 3-adrenoceptors, in smooth muscle cells of rat small mesenteric arteries. *British Journal of Pharmacology*, *146*(5), 679–691.

Brozovich, F. V., Nicholson, C. J., Degen, C. V., Gao, Y. Z., Aggarwal, M., & Morgan, K. G. (2016). Mechanisms of vascular smooth muscle contraction and the basis for pharmacologic treatment of smooth muscle disorders. *Pharmacological Reviews*, *68*(2), 476–532.

Brueggemann, L. I., Martin, B. L., Barakat, J., Byron, K. L., & Cribbs, L. L. (2005). Low voltage-activated calcium channels in vascular smooth muscle: T-type channels and AVP-stimulated calcium spiking. *American Journal of Physiology-Heart and Circulatory Physiology*, *288*(2), H923–H935.

Budhiraja, R., Tuder, R. M., & Hassoun, P. M. (2004). Endothelial dysfunction in pulmonary hypertension. *Circulation*, *109*(2), 159–165.

Catterall, W. A. (2011). Voltage-gated calcium channels. *Cold Spring Harbor Perspectives in Biology*, *3*(8), a003947–a003947.

Chen, G., Suzuki, H., & Weston, A. H. (1988). Acetylcholine releases endothelium-derived hyperpolarizing factor and EDRF from rat blood vessels. *British Journal of Pharmacology*, *95*(4), 1165–1174.

Chen, Y., Lu, J., Pan, H., Zhang, Y., Wu, H., Xu, K., Liu, X., Jiang, Y., Bao, X., Yao, Z., Ding, K., Lo, W. H. Y., Qiang, B., Chan, P., Shen, Y., & Wu, X. (2003). Association between genetic variation of CACNA1H and childhood absence epilepsy. *Annals of Neurology*, *54*(2), 239–243.

Colantuoni, A., Bertuglia, S., & Intaglietta, M. (1985). Variations of rhythmic diameter changes at the arterial microvascular bifurcations. *Pflugers Archiv: European Journal of Physiology*, *403*(3), 289–295.

Cornwell, T. L., Arnold, E., Boerth, N. J., & Lincoln, T. M. (1994). Inhibition of smooth muscle cell growth by nitric oxide and activation of cAMP-dependent protein kinase by cGMP. *American Journal of Physiology-Cell Physiology*, *267*(5), C1405–C1413.

Cornwell, T. L., Soff, G. A., Traynor, A. E., & Lincoln, T. M. (1994). Regulation of the expression of cyclic GMP-dependent protein kinase by cell density in vascular smooth muscle cells. *Journal of Vascular Research*, *31*(6), 330–337.

Crane, G. J., Gallagher, N., Dora, K. A., & Garland, C. J. (2003). Small- and intermediate-conductance calcium-activated K^+ channels provide different facets of endothelium-dependent hyperpolarization in rat mesenteric artery. *The Journal of Physiology*, *553*(Pt 1), 183–189.

Crnich, R., Amberg, G. C., Leo, M. D., Gonzales, A. L., Tamkun, M. M., Jaggar, J. H., & Earley, S. (2010). Vasoconstriction resulting from dynamic membrane trafficking of TRPM4 in vascular smooth muscle cells. *American Journal of Physiology. Cell Physiology*, *299*(3), C682–C694.

Cueni, L., Canepari, M., Adelman, J. P., & Lüthi, A. (2009). Ca^{2+} signaling by T-type Ca^{2+} channels in neurons. *Pflügers Archiv-European Journal of Physiology*, *457*(5), 1161.

Daoyan, L., Dachun, Y., Hongbo, H., Xiaoping, C., Tingbing, C., Xiaoli, F., Liqun, M., Zhidan, L., Lijuan, W., Zhencheng, Y., Zhiming, Z., & Martin, T. (2009). Increased transient receptor potential canonical type 3 channels in vasculature from hypertensive rats. *Hypertension*, *53*(1), 70–76.

Davis, M. J., & Hill, M. A. (1999). Signaling mechanisms underlying the vascular myogenic response. *Physiological Reviews*, *79*(2), 387–423.

Dora, K. A., Doyle, M. P., & Duling, B. R. (1997). Elevation of intracellular calcium in smooth muscle causes endothelial cell generation of NO in arterioles. *Proceedings of the National Academy of Sciences*, *94*(12), 6529–6534.

Dora, K. A., Hinton, J. M., Walker, S. D., & Garland, C. J. (2000). An indirect influence of phenylephrine on the release of endothelium-derived vasodilators in rat small mesenteric artery. *British Journal of Pharmacology*, *129*(2), 381–387.

Dora, K. A. (2001). Cell-cell communication in the vessel wall. *Vascular Medicine*, *6*(1), 43–50.

Dora, K. A., Gallagher, N. T., McNeish, A., & Garland, C. J. (2008). Modulation of endothelial cell $K_{Ca}3.1$ channels during endothelium-derived hyperpolarizing factor signaling in mesenteric resistance arteries. *Circulation Research*, *102*(10), 1247–1255.

Dora, K. A., & Garland, C. J. (2001). Properties of smooth muscle hyperpolarization and relaxation to K^+ in the rat isolated mesenteric artery. *American Journal of Physiology-Heart and Circulatory Physiology*, *280*(6), H2424–H2429.

Dora, K. A., Sandow, S. L., Gallagher, N. T., Takano, H., Rummery, N. M., Hill, C. E., & Garland, C. J. (2003). Myoendothelial gap junctions may provide the pathway for EDHF in mouse mesenteric artery. *Journal of Vascular Research*, *40*(5), 480–490.

Droogmans, G., Raeymaekers, L., & Casteels, R. (1977). Electro-and pharmacomechanical coupling in the smooth muscle cells of the rabbit ear artery. *The Journal of General Physiology*, *70*(2), 129–148.

Drummond, G. R., Selemidis, S., Griendling, K. K., & Sobey, C. G. (2011). Combating oxidative stress in vascular disease: NADPH oxidases as therapeutic targets. *Nature Reviews Drug Discovery*, *10*(6), 453–471.

E., I. B., & R., D. B. (2005). Heterocellular contact at the myoendothelial junction influences gap junction organization. *Circulation Research*, *97*(1), 44–51.

Earley, S., & Brayden, J. E. (2015). Transient receptor potential channels in the vasculature. *Physiological Reviews*, *95*(2), 645–690.

Edwards, D. H., & Griffith, T. M. (1997). Entrained ion transport systems generate the membrane component of chaotic agonist-induced vasomotion. *American Journal of Physiology-Heart and Circulatory Physiology*, *273*(2), H909–H920.

Edwards, G., Dora, K. A., Gardener, M. J., Garland, C. J., & Weston, A. H. (1998). K^+ is an endothelium-derived hyperpolarizing factor in rat arteries. *Nature*, *396*(6708), 269–272.

Edwards, G., Félétou, M., Gardener, M. J., Glen, C. D., Richards, G. R., Vanhoutte, P. M., & Weston, A. H. (2001). Further investigations into the endothelium-dependent hyperpolarizing effects of bradykinin and substance P in porcine coronary artery. *British Journal of Pharmacology*, *133*(7), 1145–1153.

El-Rahman, R. R. A., Harraz, O. F., Brett, S. E., Anfinogenova, Y., Mufti, R. E., Goldman, D., & Welsh, D. G. (2013). Identification of L-and T-type Ca^{2+} channels in rat cerebral arteries: role in myogenic tone development. *American Journal of Physiology-Heart and Circulatory Physiology*, *304*(1), H58–H71.

Harraz, O. F., Brett, S. E., Anil, Z., Monica, R., Puglisi, J. L., Wilson, S. M., & G., Welsh, D. G. (2015). Genetic ablation of $Ca_v3.2$ channels enhances the arterial myogenic response by modulating the RyR-BK_{Ca} axis. *Arteriosclerosis, Thrombosis, and Vascular Biology*, *35*(8), 1843–1851.

Fickling, S. A., Leone, A. M., Nussey, S. S., Vallance, P., & Whitley, G. S. J. (1993). Synthesis of NG, NG Dimethylarginine by human endothelial cells. *Endothelium*, *1*(3), 137–140.

Förstermann, U., Closs, E. I., Pollock, J. S., Nakane, M., Schwarz, P., Gath, I., & Kleinert, H. (1994). Nitric oxide synthase isozymes. Characterization, purification, molecular cloning, and functions. *Hypertension*, *23*(62), 1121–1131.

Förstermann, U., Gorsky, L. D., Pollock, J. S., Ishii, K., Schmidt, H. H., Heller, M., & Murad, F. (1990). Hormone-induced biosynthesis of endothelium-derived relaxing factor/nitric oxide-like material in N1E-115 neuroblastoma cells requires calcium and calmodulin. *Molecular Pharmacology*, *38*(1), 7 LP – 13.

Foti, R. S., Rock, D. A., Pearson, J. T., Wahlstrom, J. L., & Wienkers, L. C. (2011). Mechanism-based inactivation of cytochrome P450 3A4 by mibefradil through heme destruction. *Drug Metabolism and Disposition*, *39*(7), 1188.

François-Xavier, B., Antony, G., & Mark, E. A. (2002). Nicotinic acid adenine dinucleotide phosphate mediates Ca^{2+} signals and contraction in arterial smooth muscle via a two-pool mechanism. *Circulation Research*, *91*(12), 1168–1175.

Friebe, A., & Koesling, D. (2003). Regulation of nitric oxide-sensitive guanylyl cyclase. *Circulation Research*, *93*(2), 96–105.

Furchgott, R. F., & Zawadzki, J. V. (1980). The obligatory role of endothelial cells in the relaxation of arterial smooth muscle by acetylcholine. *Nature*, *288*(5789), 373–376.

Furchgott, R. F. (1983). Role of endothelium in responses of vascular smooth muscle. *Circulation Research*, *53*(5), 557–573.

Galley, H. F., & Webster, N. R. (2004). Physiology of the endothelium. *BJA: British Journal of Anaesthesia*, *93*(1), 105–113.

Garland, C. J., & Dora, K. A. (2017). EDH: endothelium-dependent hyperpolarization and microvascular signalling. *Acta Physiologica*, *219*(1), 152–161.

Garland, C. J., Yarova, P. L., Jiménez-Altayó, F., & Dora, K. A. (2011). Vascular hyperpolarization to β-adrenoceptor agonists evokes spreading dilatation in rat isolated mesenteric arteries. *British Journal of Pharmacology*, *164*(3), 913–921.

Garland, C. J., Bagher, P., Powell, C., Ye, X., Lemmey, H. A. L., Borysova, L., & Dora, K. A. (2017). Voltage-dependent Ca^{2+} entry into smooth muscle during contraction promotes endothelium-mediated feedback vasodilation in arterioles. *Science Signaling*, *10*(486), eaal3806.

Garland, C. J., Hiley, C. R., & Dora, K. A. (2011). EDHF: spreading the influence of the endothelium. *British Journal of Pharmacology*, *164*(3), 839–852.

Garland, C. J., & McPherson, G. A. (1992). Evidence that nitric oxide does not mediate the hyperpolarization and relaxation to acetylcholine in the rat small mesenteric artery. *British Journal of Pharmacology*, *105*(2), 429–435.

Ghosh, D., Syed, A. U., Prada, M. P., Nystoriak, M. A., Santana, L. F., Nieves-Cintrón, M., & Navedo, M. F. (2017). Calcium channels in vascular smooth muscle. *Advances in Pharmacology (San Diego, Calif.)*, *78*, 49–87.

Gonzales, A. L., Garcia, Z. I., Amberg, G. C., & Earley, S. (2010). Pharmacological inhibition of TRPM4 hyperpolarizes vascular smooth muscle. *American Journal of Physiology. Cell Physiology*, *299*(5), C1195–C1202.

Gokina, N. I., Bevan, R. D., Walters, C. L., & Bevan, J. A. (1996). Electrical activity underlying rhythmic contraction in human pial arteries. *Circulation Research*, *78*(1), 148–153.

Goligorsky, M. S., Colflesh, D., Gordienko, D., & Moore, L. C. (1995). Branching points of renal resistance arteries are enriched in L-type calcium channels and initiate vasoconstriction. *The American Journal of Physiology*, *268*(2 Pt 2), F251-7.

Graves, J. E., Greenwood, I. A., & Large, W. A. (2000). Tonic regulation of vascular tone by nitric oxide and chloride ions in rat isolated small coronary arteries. *American Journal of Physiology-Heart and Circulatory Physiology*, *279*(6), H2604–H2611.

Greene, B., Pacitti, A. J., & Souba, W. W. (1993). Characterization of L-arginine transport by pulmonary artery endothelial cells. *American Journal of Physiology-Lung Cellular and Molecular Physiology*, *264*(4), L351–L356.

Griffith, T. M. (1996). Temporal chaos in the microcirculation. *Cardiovascular Research*, *31*(3), 342–358.

Griffith, T. M., & Edwards, D. H. (1997). Ca^{2+} sequestration as a determinant of chaos and mixed-mode dynamics in agonist-induced vasomotion. *American Journal of Physiology-Heart and Circulatory Physiology,* 272**,** H1696-1709.

Griffith, T. M., Parthimos, D., & Edwards, D. H. (2009). Vasomotion: the case for chaos. *Journal of Biorheology*, 23(1), 11–23.

Gustafsson, H., Mulvany, M. J., & Nilsson, H. (1993). Rhythmic contractions of isolated small arteries from rat: influence of the endothelium. *Acta Physiologica Scandinavica*, 148(2), 153–163.

Gustafsson, H., & Nilsson, H. (1994). Rhythmic contractions in isolated small arteries of rat: role of K^+ channels and the Na^+/K^+-pump. *Acta Physiologica Scandinavica*, 150(2), 161–170.

Gutterman, D. D. (1999). Adventitia-dependent influences on vascular function. *American Journal of Physiology-Heart and Circulatory Physiology*, 277(4), H1265–H1272.

Haas, T. L., & Duling, B. R. (1997). Morphology favors an endothelial cell pathway for longitudinal conduction within arterioles. *Microvascular Research*, 53(2), 113–120.

Haddock, R. E., & Hill, C. E. (2005). Rhythmicity in arterial smooth muscle. The *Journal of Physiology*, 566(3), 645–656.

Hansen, P. B. L. (2014). Functional importance of T-type voltage-gated calcium channels in the cardiovascular and renal system: news from the world of knockout mice. *American Journal of Physiology-Regulatory, Integrative and Comparative Physiology*, 308(4), R227–R237.

Harder, D. R. (1980). Comparison of electrical properties of middle cerebral and mesenteric artery in cat. *American Journal of Physiology-Cell Physiology*, 239(1), C23–C26.

Harder, D. R. (1984). Pressure-dependent membrane depolarization in cat middle cerebral artery. *Circulation Research*, 55(2), 197–202.

Harder, D. R., & Sperelakis, N. (1979). Action potentials induced in guinea pig arterial smooth muscle by tetraethylammonium. *American Journal of Physiology-Cell Physiology*, 237(1), C75–C80.

Harraz, O. F., Abd El-Rahman, R. R., Bigdely-Shamloo, K., Wilson, S. M., Brett, S. E., Romero, M., Gonzales, A. L., Earley, S., Vigmond, E. J., & Nygren, A. (2014). Ca_V3. 2 channels and the induction of negative feedback in cerebral arteries. *Circulation Research*, 115(7), 650–661.

Harraz, O. F., Brett, S. E., & Welsh, D. G. (2014). Nitric oxide suppresses vascular voltage-gated T-type Ca^{2+} channels through cGMP/PKG signaling. *American Journal of Physiology-Heart and Circulatory Physiology*, 306(2), H279–H285.

Harraz, O. F., Visser, F., Brett, S. E., Goldman, D., Zechariah, A., Hashad, A. M., Menon, B. K., Watson, T., Starreveld, Y., & Welsh, D. G. (2015). $Ca_v1.2/Ca_v3.x$ channels mediate divergent vasomotor responses in human cerebral arteries. *Journal of General Physiology*, 145(5), 405–418.

Harraz, O. F., & Welsh, D. G. (2013). Protein kinase A regulation of T-type Ca^{2+} channels in rat cerebral arterial smooth muscle. *Journal of Cell Science*, 126(13), 2944–2954.

Hartzell, C., Putzier, I., & Arreola, J. (2004). Calcium-activated chloride channels. *Annual Review of Physiology*, 67(1), 719–758.

Hashad, A. M., Harraz, O. F., Brett, S. E., Romero, M., Kassmann, M., Puglisi, J. L., Wilson, S. M., Gollasch, M., & Welsh, D. G. (2018). Caveolae link $Ca_V3.2$ channels to BK_{Ca}-mediated feedback in vascular smooth muscle. *Arteriosclerosis, Thrombosis, and Vascular Biology*, 38(10), 2371–2381.

Heberlein, K. R., Straub, A. C., & Isakson, B. E. (2009). The myoendothelial junction: breaking through the matrix? *Microcirculation*, 16(4), 307–322.

Hill, C. E., Eade, J., & Sandow, S. L. (1999). Mechanisms underlying spontaneous rhythmical contractions in irideal arterioles of the rat. *The Journal of Physiology*, 521(2), 507–516.

Hill, C. E., Phillips, J. K., & Sandow, S. L. (2001). Heterogeneous control of blood flow amongst different vascular beds. *Medicinal Research Reviews*, 21(1), 1–60.

Hiromitsu, M., Helen, C., Hitoshi, O., Yushi, I., & Ryuji, I. (1999). Predominant distribution of nifedipine-insensitive, high voltage–activated Ca^{2+} channels in the terminal mesenteric artery of guinea pig. *Circulation Research*, 85(7), 596–605.

Howitt, L., Kuo, I. Y., Ellis, A., Chaston, D. J., Shin, H.-S., Hansen, P. B., & Hill, C. E. (2013). Chronic deficit in nitric oxide elicits oxidative stress and augments T-type calcium-channel contribution to vascular tone of rodent arteries and arterioles. *Cardiovascular Research*, 98 (3), 449-457.

Huang, L., Keyser, B. M., Tagmose, T. M., Hansen, J. B., Taylor, J. T., Zhuang, H., Zhang, M., Ragsdale, D. S., & Li, M. (2004). NNC 55-0396 [(1S, 2S)-2-(2-(N-[(3-benzimidazol-2-yl) propyl]-N-methylamino) ethyl)-6-fluoro-1, 2, 3, 4-tetrahydro-1-isopropyl-2-naphtyl cyclopropanecarboxylate dihydrochloride]: a new selective inhibitor of T-type calcium channels. *Journal of Pharmacology and Experimental Therapeutics*, 309(1), 193–199.

Hwa, J. J., & Bevan, J. A. (1986). Dihydropyridine calcium agonists selectively enhance resistance artery myogenic tone. *European Journal of Pharmacology*, *126*(3), 231–238.

Iftinca, M. C. (2011). Neuronal T-type calcium channels: what's new? T-type channel regulation. *Journal of Medicine and Life*, 4(2), 126–138.

Ignarro, L. J., Buga, G. M., Wood, K. S., Byrns, R. E., & Chaudhuri, G. (1987). Endothelium-derived relaxing factor produced and released from artery and vein is nitric oxide. *Proceedings of the National Academy of Sciences*, 84(24), 9265 LP – 9269.

Ignarro, L. J., Byrns, R. E., Buga, G. M., & Wood, K. S. (1987). Endothelium-derived relaxing factor from pulmonary artery and vein possesses pharmacologic and

chemical properties identical to those of nitric oxide radical. *Circulation Research*, 61(6), 866–879.

Irvine, J. C., Favaloro, J. L., & Kemp-Harper, B. K. (2003). NO− activates soluble guanylate cyclase and K_v channels to vasodilate resistance arteries. *Hypertension*, 41(6), 1301–1307.

Jackson, W. F., Mulsch, A., & Busse, R. (1991). Rhythmic smooth muscle activity in hamster aortas is mediated by continuous release of NO from the endothelium. *American Journal of Physiology-Heart and Circulatory Physiology*, 260(1), H248–H253.

Jensen, L. J., & Holstein-Rathlou, N.-H. (2009). Is there a role for T-type Ca^{2+} channels in regulation of vasomotor tone in mesenteric arterioles? *Canadian Journal of Physiology and Pharmacology*, 87(1), 8–20.

Jones, T. W. (1853). Discovery that the veins of the bat's wing (which are furnished with valves) are endowed with rhythmical contractility, and that the onward flow of blood is accelerated by such contraction. *Edinburgh Medical and Surgical Journal*, 79(195), 367–373.

Kampa, B. M., Letzkus, J. J., & Stuart, G. J. (2006). Requirement of dendritic calcium spikes for induction of spike-timing-dependent synaptic plasticity. *The Journal of Physiology*, 574(1), 283–290.

Kansui, Y., Garland, C. J., & Dora, K. A. (2008). Enhanced spontaneous Ca^{2+} events in endothelial cells reflect signalling through myoendothelial gap junctions in pressurized mesenteric arteries. *Cell Calcium,* 44, 135–146.

Keef, K. D., Hume, J. R., & Zhong, J. (2001). Regulation of cardiac and smooth muscle Ca^{2+} channels ($Ca_v1.2$) by protein kinases. *American Journal of Physiology. Cell Physiology*, *281*(6), C1743-56.

Knot, H. J., & Nelson, M. T. (1998). Regulation of arterial diameter and wall [Ca^{2+}] in cerebral arteries of rat by membrane potential and intravascular pressure. *The Journal of Physiology*, *508 (Pt 1)* (Pt 1), 199–209.

Koglin, M., Stasch, J.-P., & Behrends, S. (2002). BAY 41-2272 activates two isoforms of nitric oxide-sensitive guanylyl cyclase. *Biochemical and Biophysical Research Communications*, 292(4), 1057–1062.

Komori, K., & Vanhoutte, P. M. (1990). Endothelium-derived hyperpolarizing factor. *Journal of Vascular Research*, 27(2–5), 238–245.

Kraus, R. L., Li, Y., Gregan, Y., Gotter, A. L., Uebele, V. N., Fox, S. V, Doran, S. M., Barrow, J. C., Yang, Z.-Q., & Reger, T. S. (2010). In vitro characterization of T-type calcium channel antagonist TTA-A2 and in vivo effects on arousal in mice. *Journal of Pharmacology and Experimental Therapeutics*, 335(2), 409–417.

Krayenbühl, J. C., Vozeh, S., Kondo-Oestreicher, M., & Dayer, P. (1999). Drug–drug interactions of new active substances: mibefradil example. *European Journal of Clinical Pharmacology*, 55(8), 559–565.

Kruger, O., Plum, A., Kim, J. S., Winterhager, E., Maxeiner, S., Hallas, G., Kirchhoff, S., Traub, O., Lamers, W. H., & Willecke, K. (2000). Defective vascular development in connexin 45-deficient mice. *Development*, 127(19), 4179 LP – 4193.

Kuriyama, H., & Suzuki, H. (1978). The effects of acetylcholine on the membrane and contractile properties of smooth muscle cells of the rabbit superior mesenteric artery. *British Journal of Pharmacology,* 64(4), 493 – 501.

Lamb, F. S., & Webb, R. C. (1989). Regenerative electrical activity and arterial contraction in hypertensive rats. *Hypertension (Dallas, Tex.: 1979)*, *13*(1), 70–76.

Little, L. T., J., X., & R., D. B. (1995). Dye tracers define differential endothelial and smooth muscle coupling patterns within the arteriolar wall. *Circulation Research*, *76*(3), 498–504.

Lam, E., Skarsgard, P., & Laher, I. (1998). Inhibition of myogenic tone by mibefradil in rat cerebral arteries. *European Journal of Pharmacology*, 358(2), 165–168.

Lamont, C., Vainorius, E., & Wier, W. G. (2003). Purinergic and adrenergic Ca^{2+} transients during neurogenic contractions of rat mesenteric small arteries. *The Journal of Physiology*, *549*(Pt 3), 801–808.

Lands, A. M., Arnold, A., Mcauliff, J. P., Luduena, F. P., & Brown, T. G. (1967). Differentiation of receptor systems activated by sympathomimetic amines. *Nature*, *214*(5088), 597–598.

Large, W. A. (2002). Receptor-operated Ca^{2+}-permeable nonselective cation channels in vascular smooth muscle: a physiologic perspective. *Journal of Cardiovascular Electrophysiology*, *13*(5), 493–501.

Leblanc, N., Ledoux, J., Saleh, S., Sanguinetti, A., Angermann, J., O'Driscoll, K., Britton, F., Perrino, B. A., & Greenwood, I. A. (2005). Regulation of calcium-activated chloride channels in smooth muscle cells: a complex picture is emerging. *Canadian Journal of Physiology and Pharmacology*, *83*(7), 541–556.

Ledoux, J., Taylor, M. S., Bonev, A. D., Hannah, R. M., Solodushko, V., Shui, B., Tallini, Y., Kotlikoff, M. I., & Nelson, M. T. (2008). Functional architecture of inositol 1,4,5-trisphosphate signaling in restricted spaces of myoendothelial projections. *Proceedings of the National Academy of Sciences of the United States of America*, 105(28), 9627–9632.

Lee, C.-H., Poburko, D., Kuo, K.-H., Seow, C. Y., & van Breemen, C. (2002). Ca^{2+} oscillations, gradients, and homeostasis in vascular smooth muscle. *American Journal of Physiology-Heart and Circulatory Physiology*, 282(5), H1571–H1583.

Lee, C., Poburko, D., Sahota, P., Sandhu, J., Ruehlmann, D. O., & van Breemen, C. (2001). The mechanism of phenylephrine-mediated $[Ca^{2+}]_i$ oscillations underlying tonic contraction in the rabbit inferior vena cava. *The Journal of Physiology*, 534(3), 641–650.

Lee, J., Nelson, M. T., Rose, K. E., & Todorovic, S. M. (2013). Redox mechanism of S-nitrosothiol modulation of neuronal $Ca_v3.2$ T-type calcium channels. *Molecular Neurobiology*, 48(2), 274–280.

Lee, J.-H., Gomora, J. C., Cribbs, L. L., & Perez-Reyes, E. (1999). Nickel block of three cloned T-type calcium channels: low concentrations selectively block α_1H. *Biophysical Journal*, 77(6), 3034–3042.

Leone, A., Moncada, S., Vallance, P., Calver, A., & Collier, J. (1992). Accumulation of an endogenous inhibitor of nitric oxide synthesis in chronic renal failure. *The Lancet*, 339(8793), 572–575.

Li, H., & Förstermann, U. (2000). Nitric oxide in the pathogenesis of vascular disease. *The Journal of Pathology*, 190(3), 244–254.

Li, M., Hansen, J. B., Huang, L., Keyser, B. M., & Taylor, J. T. (2005). Towards selective antagonists of T-type calcium channels: design, characterization and potential applications of NNC 55-0396. *Cardiovascular Drug Reviews*, 23(2), 173–196.

Lima, B., Forrester, M. T., Hess, D. T., & Stamler, J. S. (2010). S-nitrosylation in cardiovascular signaling. *Circulation Research*, 106(4), 633–646.

Little, T. L., Beyer, E. C., & Duling, B. R. (1995). Connexin 43 and connexin 40 gap junctional proteins are present in arteriolar smooth muscle and endothelium in vivo. *American Journal of Physiology-Heart and Circulatory Physiology*, *268*(2), H729–H739.

Lin, Y.-F., Raab-Graham, K., Jan, Y. N., & Jan, L. Y. (2004). NO stimulation of ATP-sensitive potassium channels: Involvement of Ras/mitogen-activated protein kinase pathway and contribution to neuroprotection. *Proceedings of the National Academy of Sciences of the United States of America*, 101(20), 7799 LP – 7804.

Liu, M., Zhang, X., Wang, B., Wu, Q., Li, B., Li, A., Zhang, H., & Xiu, R. (2017). Functional status of microvascular vasomotion is impaired in spontaneously hypertensive rat. *Scientific Reports*, 7(1), 1–14.

Lohmann, S. M., Vaandrager, A. B., Smolenski, A., Walter, U., & De Jonge, H. R. (1997). Distinct and specific functions of cGMP-dependent protein kinases. *Trends in Biochemical Sciences*, 22(8), 307–312.

Luo, W., Liu, B., & Zhou, Y. (2016). The endothelial cyclooxygenase pathway: Insights from mouse arteries. *European Journal of Pharmacology*, 780, 148–158.

Mandalà, M., Heppner, T. J., Bonev, A. D., & Nelson, M. T. (2007). Effect of endogenous and exogenous nitric oxide on calcium sparks as targets for vasodilation in rat cerebral artery. *Nitric Oxide*, 16(1), 104–109.

McCarron, J. G., Bradley, K. N., MacMillan, D., Chalmers, S., & Muir, T. C. (2004). The sarcoplasmic reticulum, Ca^{2+} trapping, and wave mechanisms in smooth muscle. *Physiology*, 19(3), 138–147.

McCarron, J. G., MacMillan, D., Bradley, K. N., Chalmers, S., & Muir, T. C. (2004). Origin and mechanisms of Ca^{2+} waves in smooth muscle as revealed by localized

photolysis of caged inositol 1, 4, 5-trisphosphate. *Journal of Biological Chemistry*, 279(9), 8417–8427.

McNeish, A. J., Altayo, F. J., & Garland, C. J. (2010). Evidence both L-type and non-L-type voltage-dependent calcium channels contribute to cerebral artery vasospasm following loss of NO in the rat. *Vascular Pharmacology*, 53(3–4), 151–159.

Melik, Z., Zaletel, P., Virtic, T., & Cankar, K. (2017). L-arginine as dietary supplement for improving microvascular function. *Clinical Hemorheology and Microcirculation*, 65, 205–217.

Meyer, C., de Vries, G., Davidge, S. T., & Mayes, D. C. (2002). Reassessing the mathematical modeling of the contribution of vasomotion to vascular resistance. *Journal of Applied Physiology*, 92(2), 888–889.

Mishra, S. K., & Hermsmeyer, K. (1994). Selective inhibition of T-type Ca^{2+} channels by Ro 40-5967. *Circulation Research*, 75(1), 144–148.

Mistry, D. K., & Garland, C. J. (1998). Nitric oxide (NO)-induced activation of large conductance Ca^{2+}-dependent K^+ channels (BK_{Ca}) in smooth muscle cells isolated from the rat mesenteric artery. *British Journal of Pharmacology*, 124(6), 1131–1140.

Moncada, S., Gryglewski, R., Bunting, S., & Vane, J. R. (1976). An enzyme isolated from arteries transforms prostaglandin endoperoxides to an unstable substance that inhibits platelet aggregation. *Nature*, 263(5579), 663–665.

Moncada, S., Herman, A. G., Higgs, E. A., & Vane, J. R. (1977). Differential formation of prostacyclin (PGX or PGI2) by layers of the arterial wall. An explanation for the anti-thrombotic properties of vascular endothelium. *Thrombosis Research*, 11(3), 323–344.

Moncada, S., & Vane, J. R. (1979). The role of prostacyclin in vascular tissue. *Federation Proceedings*, *38*(1), 66—71.

Moosmang, S., Schulla, V., Welling, A., Feil, R., Feil, S., Wegener, J. W., Hofmann, F., & Klugbauer, N. (2003). Dominant role of smooth muscle L-type calcium channel $Ca_v1.2$ for blood pressure regulation. *The EMBO Journal*, *22*(22), 6027–6034.

Morita, H., Shi, J., Ito, Y., & Inoue, R. (2002). T-channel-like pharmacological properties of high voltage-activated, nifedipine-insensitive Ca^{2+} currents in the rat terminal mesenteric artery. *British Journal of Pharmacology*, 137(4), 467–476.

Mullins, M. E., Horowitz, B. Z., Linden, D. H. J., Smith, G. W., Norton, R. L., & Stump, J. (1998). Life-threatening interaction of mibefradil and β-Blockers with dihydropyridine calcium channel blockers. *JAMA*, 280(2), 157–158.

Mulvany, M. J., & Halpern, W. (1977). Contractile properties of small arterial resistance vessels in spontaneously hypertensive and normotensive rats. *Circulation Research*, 41(1), 19–26.

Nausch, L. W. M., Bonev, A. D., Heppner, T. J., Tallini, Y., Kotlikoff, M. I., & Nelson, M. T. (2012). Sympathetic nerve stimulation induces local endothelial Ca^{2+} signals to

oppose vasoconstriction of mouse mesenteric arteries. *American Journal of Physiology. Heart and Circulatory Physiology*, 302(3), H594–H602.

Navarro-Gonzalez, M. F., Grayson, T. H., Meaney, K. R., Cribbs, L. L., & Hill, C. E. (2009). Non-L-type voltage-dependent calcium channels control vascular tone of the rat basilar artery. *Clinical and Experimental Pharmacology and Physiology*, 36(1), 55–66.

Navedo, M. F., & Amberg, G. C. (2013). Local regulation of L-type Ca^{2+} channel sparklets in arterial smooth muscle. *Microcirculation (New York, N.Y.: 1994)*, *20*(4), 290–298.

Nelli, S., Wilson, W. S., Laidlaw, H., Llano, A., Middleton, S., Price, A. G., & Martin, W. (2003). Evaluation of potassium ion as the endothelium-derived hyperpolarizing factor (EDHF) in the bovine coronary artery. *British Journal of Pharmacology*, 139(5), 982–988.

Nelson, M. T., Cheng, H., Rubart, M., Santana, L. F., Bonev, A. D., Knot, H. J., & Lederer, W. J. (1995). Relaxation of arterial smooth muscle by calcium sparks. *Science*, 270(5236), 633–637.

Nelson, M. T., Patlak, J. B., Worley, J. F., & Standen, N. B. (1990). Calcium channels, potassium channels, and voltage dependence of arterial smooth muscle tone. *American Journal of Physiology-Cell Physiology*, 259(1), C3–C18.

Nicoll, P. A., Webb, R. L., & Lutz, B. R. (1955). Vascular Patterns and Active Vasomotion As. *Angiology*, 6(4), 291–310.

Nikitina, E., Zhang, Z., Kawashima, A., Jahromi, B. S., Bouryi, V. A., Takahashi, M., Xie, A., & Macdonald, R. L. (2007). Voltage-dependent calcium channels of dog basilar artery. *The Journal of Physiology*, 580(2), 523–541.

Nilsson, H., & Aalkjær, C. (2003). Vasomotion: mechanisms and physiological importance. *Molecular Interventions*, 3(2), 79-89.

Omote, M., Kajimoto, N., & Mizusawa, H. (1992). Phenylephrine induces endothelium-independent rhythmic contraction in rabbit mesenteric arteries treated with ryanodine. *Acta Physiologica Scandinavica*, 145(3), 295–296.

Omote, M., Kajimoto, N., & Mizusawa, H. (1993). The ionic mechanism of phenylephrine-induced rhythmic contractions in rabbit mesenteric arteries treated with ryanodine. *Acta Physiologica Scandinavica*, 147(1), 9–13.

Palmer, R. M. J., Ferrige, A. G., & Moncada, S. (1987). Nitric oxide release accounts for the biological activity of endothelium-derived relaxing factor. *Nature*, 327(6122), 524–526.

Patrick, V., & James, L. (2004). Cardiovascular biology of the asymmetric dimethylarginine: dimethylarginine dimethylaminohydrolase pathway. *Arteriosclerosis, Thrombosis, and Vascular Biology*, 24(6), 1023–1030.

Peng, H., Matchkov, V., Ivarsen, A., Aalkjær, C., & Nilsson, H. (2001). Hypothesis for the initiation of vasomotion. *Circulation Research*, 88(8), 810–815.

Perez-Reyes, E. (2006). Molecular characterization of T-type calcium channels. *Cell Calcium*, 40(2), 89–96.

Perez-Reyes, E. (2003). Molecular physiology of low-voltage-activated T-type calcium channels. *Physiological Reviews*, 83(1), 117–161.

Pérez, G. J., Bonev, A. D., & Nelson, M. T. (2001). Micromolar Ca^{2+} from sparks activates Ca^{2+}-sensitive K^{+} channels in rat cerebral artery smooth muscle. *American Journal of Physiology-Cell Physiology*, 281(6), C1769–C1775.

Perticone, F., Ceravolo, R., Pujia, A., Ventura, G., Iacopino, S., Scozzafava, A., Ferraro, A., Chello, M., Mastroroberto, P., & Verdecchia, P. (2001). Prognostic significance of endothelial dysfunction in hypertensive patients. *Circulation*, 104(2), 191–196.

Perticone, F., Sciacqua, A., Maio, R., Perticone, M., Maas, R., Boger, R. H., Tripepi, G., Sesti, G., & Zoccali, C. (2005). Asymmetric dimethylarginine, L-arginine, and endothelial dysfunction in essential hypertension. *Journal of the American College of Cardiology*, 46(3), 518–523.

Plane, F., & Garland, C. J. (1993). Differential effects of acetylcholine, nitric oxide and levcromakalim on smooth muscle membrane potential and tone in the rabbit basilar artery. *British Journal of Pharmacology*, *110*(2), 651–656.

Puri, N., Kruhlak, M. J., Whiteheart, S. W., & Roche, P. A. (2003). Mast cell degranulation requires ethylmaleimide-sensitive factor-mediated SNARE disassembly. *The Journal of Immunology*, 171(10), 5345 LP – 5352.

Quignard, J. F., Frapier, J. M., Harricane, M. C., Albat, B., Nargeot, J., & Richard, S. (1997). Voltage-gated calcium channel currents in human coronary myocytes. Regulation by cyclic GMP and nitric oxide. *The Journal of Clinical Investigation*, 99(2), 185–193.

Rahman, A., Hughes, A., Matchkov, V., Nilsson, H., & Aalkjær, C. (2007). Antiphase oscillations of endothelium and smooth muscle $[Ca^{2+}]_i$ in vasomotion of rat mesenteric small arteries. *Cell Calcium*, 42, 536–547.

Renaudin, C., Michoud, E., Lagarde, M., & Wiernsperger, N. (1999). Impaired microvascular responses to acute hyperglycemia in type I diabetic rats. *Journal of Diabetes and Its Complications*, 13(1), 39–44.

Rohit, B., M., T. R., & M., H. P. (2004). Endothelial dysfunction in pulmonary hypertension. *Circulation*, 109(2), 159–165.

Rücker, M., Strobel, O., Vollmar, B., Roesken, F., & Menger, M. D. (2000). Vasomotion in critically perfused muscle protects adjacent tissues from capillary perfusion failure. *American Journal of Physiology-Heart and Circulatory Physiology*, 279(2), H550–H558.

Russell, R. P. (1988). Side effects of calcium channel blockers. *Hypertension*, 11(32), II42.

Ryuji, I., J., J. L., Zhong, J., Juan, S., Lin, H., I., L. A., H., H. F., Max, S., Hiromitsu, M., Yasuhiro, K., Masayuki, M., Yasuo, M., & Yushi, I. (2009). Synergistic activation of vascular TRPC6 channel by receptor and mechanical stimulation via

phospholipase C/diacylglycerol and phospholipase A2/ω-hydroxylase/20-HETE pathways. *Circulation Research*, *104*(12), 1399–1409.

Sampson, L. J., Plane, F., & Garland, C. J. (2001). Involvement of cyclic GMP and potassium channels in relaxation evoked by the nitric oxide donor, diethylamine NONOate, in the rat small isolated mesenteric artery. *Naunyn-Schmiedeberg's Archives of Pharmacology*, 364(3), 220–225.

Shang-Zhong, X., & J., B. D. (2001). TRPC1 Is a membrane-spanning subunit of store-operated Ca^{2+} channels in native vascular smooth muscle cells. *Circulation Research*, *88*(1), 84–87.

Shcheglovitov, A., Vitko, I., Bidaud, I., Baumgart, J. P., Navarro-Gonzalez, M. F., Grayson, T. H., Lory, P., Hill, C. E., & Perez-Reyes, E. (2008). Alternative splicing within the I–II loop controls surface expression of T-type $Ca_v3.1$ calcium channels. *FEBS Letters*, 582(27), 3765–3770.

Shi, J., Miralles, F., Birnbaumer, L., Large, W. A., & Albert, A. P. (2017). Store-operated interactions between plasmalemmal STIM1 and TRPC1 proteins stimulate PLCβ1 to induce TRPC1 channel activation in vascular smooth muscle cells. *The Journal of Physiology*, *595*(4), 1039–1058.

Son, Y. K., Da, H. H., Li, H., Kim, D.-J., Na, S. H., Park, H., Jung, W.-K., Choi, I.-W., & Park, W. S. (2014). The Ca^{2+} channel inhibitor NNC 55-0396 inhibits voltage-dependent K^+ channels in rabbit coronary arterial smooth muscle cells. *Journal of Pharmacological Sciences*, 14054FP.

Sonkusare, S. K., Bonev, A. D., Ledoux, J., Liedtke, W., Kotlikoff, M. I., Heppner, T. J., Hill-Eubanks, D. C., & Nelson, M. T. (2012). Elementary Ca^{2+} signals through endothelial TRPV4 channels regulate vascular function. *Science*, *336*(6081), 597–601.

Spencer, N. J., & Greenwood, I. A. (2003). Characterization of properties underlying rhythmicity in mouse portal vein. *Autonomic Neuroscience*, 104(2), 73–82.

Stuehr, D. J., Cho, H. J., Kwon, N. S., Weise, M. F., & Nathan, C. F. (1991). Purification and characterization of the cytokine-induced macrophage nitric oxide synthase: an FAD- and FMN-containing flavoprotein. *Proceedings of the National Academy of Sciences*, 88(17), 7773 LP – 7777.

Szekeres, M., Nádasy, G. L., Kaley, G., & Koller, A. (2004). Nitric oxide and prostaglandins modulate pressure-induced myogenic responses of intramural coronary arterioles. *Journal of Cardiovascular Pharmacology*, 43(2), 242–249.

Takeda, Y., Nystoriak, M. A., Nieves-Cintrón, M., Santana, L. F., & Navedo, M. F. (2011). Relationship between Ca^{2+} sparklets and sarcoplasmic reticulum Ca^{2+} load and release in rat cerebral arterial smooth muscle. *American Journal of Physiology. Heart and Circulatory Physiology*, *301*(6), H2285-94.

Tsai, A. G., & Intaglietta, M. (1993). Evidence of flowmotion induced changes in local tissue oxygenation. *International Journal of Microcirculation, Clinical and Experimental*, 12(1), 75—88.

Ursino, M., Cavalcanti, S., Bertuglia, S., & Colantuoni, A. (1996). Theoretical analysis of complex oscillations in multibranched microvascular networks. *Microvascular Research*, *51*(2), 229–249.

VanBavel, E., Sorop, O., Andreasen, D., Pfaffendorf, M., & Jensen, B. L. (2002). Role of T-type calcium channels in myogenic tone of skeletal muscle resistance arteries. *American Journal of Physiology-Heart and Circulatory Physiology*, 283(6), H2239–H2243.

Vanhoutte, P. M., Shimokawa, H., Feletou, M., & Tang, E. H. C. (2017). Endothelial dysfunction and vascular disease–a 30th anniversary update. *Acta Physiologica*, 219(1), 22–96.

Waldman, S. A., & Murad, F. (1988). Biochemical mechanisms underlying vascular smooth muscle relaxation: the guanylate cyclase-cyclic GMP system. *Journal of Cardiovascular Pharmacology*, 12 Suppl 5, S115—8.

Waldron, G. J., & Garland, C. J. (1994). Contribution of both nitric oxide and a change in membrane potential to acetylcholine-induced relaxation in the rat small mesenteric artery. *British Journal of Pharmacology,* 112, 831–836.

Wever, R. M. F., van Dam, T., van Rijn, H. J. M., de Groot, F., & Rabelink, T. J. (1997). Tetrahydrobiopterin regulates superoxide and nitric oxide generation by recombinant endothelial nitric oxide synthase. *Biochemical and Biophysical Research Communications*, 237(2), 340–344.

White, R. E., Kryman, J. P., El-Mowafy, A. M., Han, G., & Carrier, G. O. (2000). cAMP-dependent vasodilators cross-activate the cGMP-dependent protein kinase to stimulate BKCa channel activity in coronary artery smooth muscle cells. *Circulation Research*, 86(8), 897–905.

Yoon, E.-J., Gerachshenko, T., Spiegelberg, B. D., Alford, S., & Hamm, H. E. (2007). Gβγ interferes with Ca^{2+}-dependent binding of synaptotagmin to the soluble N-ethylmaleimide-sensitive factor attachment protein receptor (SNARE) complex. *Molecular Pharmacology*, 72(5), 1210 LP – 1219.

Yuill, K. H., McNeish, A. J., Kansui, Y., Garland, C. J., & Dora, K. A. (2010). Nitric oxide suppresses cerebral vasomotion by sGC-independent effects on ryanodine receptors and voltage-gated calcium channels. *Journal of Vascular Research*, 47(2), 93–107.

Zhao, G., Xu, X., Ochoa, M., Shen, W., & Hintze, T. H. (1996). Interaction between prostacyclin and nitric oxide in the reflex control of the coronary circulation in conscious dogs. *Cardiovascular Research*, *32*(5), 940–948.

Zhao, Y., Vanhoutte, P. M., & Leung, S. W. S. (2015). Vascular nitric oxide: Beyond eNOS. *Journal of Pharmacological Sciences*, 129(2), 83–94.

Zygmunt, P. M., & Högestätt, E. D. (1996). Role of potassium channels in endothelium-dependent relaxation resistant to nitroarginine in the rat hepatic artery. *British Journal of Pharmacology*, 117(7), 1600–1606.

Appendix

Appendix 1: MATLAB vasomotion script

```
%% phase shift calculation

%function reads in trace, and produces a table with following values;
%Table = [amp maxFreq power cycles signal noise stnRatio no5Peaks]
%also plots detrended trace and 'perfect sine' wave, using amp and
maxFreq

%% can do a chi squared goodness of fit

%% To do
%fix for loop making sine models
%write stats analysis - goodness of fit

%need function to be rising, not just positive crossing

function PhaseShiftv4

%Y = 'Control_vasomotion';
%Y = 'LName_chaotic'; %inset label of trace
%Y = 'Control_vasomotion';
Y = '8 Aug 2016 b';
%Y = 'LName_chaotic';
Z = '.txt';
X = [Y Z];
W = 'Fourier.csv';
W2 = [Y W]; %when writing fourier outcome
a1 = dlmread(X);


%% read in, amplitude calc

%label
timeA = a1(:,1);
timeA = timeA - timeA(1); %makes graph start at edge
ta=timeA;
tensionA = a1(:,2);
[p,~,mu] = polyfit((1:numel(tensionA))',tensionA,1); %removes
ascending baseline
f_y = polyval(p,(1:numel(tensionA))',[],mu);
TA_data = tensionA - f_y;


%amplitude calc
filt = 0;
top_TA = TA_data;
top_TA(top_TA<filt) = 0; %cuts above
base_TA = TA_data;
base_TA(base_TA>filt) = 0; %cuts below
```

```
%find peaks in top and bottom halves
%pks tells us x value, locs tells y - we interested in locs

% find peaks - NB y before x in code
[locs, pks] =
findpeaks(top_TA,ta,'MinPeakProminence',0.05,'Annotate','extents');
%play around with size of interval
top_Peaks = [locs, pks]; %locs is position in time signal, pks is
height
pos_base_TA = base_TA * -1; %base needs inverting to use findpeaks
[locs, pks] =
findpeaks(pos_base_TA,ta,'MinPeakProminence',0.05,'Annotate','extents'
); %play around with size of interval
pos_base_Peaks = [locs, pks]; %locs is position in time signal, pks is
height
base_Peaks = pos_base_Peaks(:,1) * -1; %then flip back

%find average top and bottom, to calc amplitude
%sum and divide by number
basePeak = sum(base_Peaks(:,1))/(length(base_Peaks));
topPeak = sum(top_Peaks(:,1)/(length(top_Peaks)));

%put this value into matrix
amp = topPeak  - basePeak; %amplitude



%% Fourier analysis
% zero padding
nRepeats = 199;
pad = zeros((nRepeats*60000), 1);
padTA = [TA_data; pad];

%do fourier

Fs = 1000;              % Sampling frequency
T = 1/Fs;               % Sampling period
L = length(timeA);      % Length of signal
t = timeA;              % Time vector

Y = fft(padTA);

P2a = abs(Y/L);
P1a = P2a(1:L/2+1);
P1a(2:end-1) = 2*P1a(2:end-1);

fa = Fs*(0:(L/2))/L;
P1a(1)= 0; %because otherwise huge peak at zero (irregular trace)

fa2 = fa/nRepeats; %transforms axis to correct freq

h=figure;
plot(fa2, P1a)
%title('a1')
title(X)
xlabel('f (Hz)')
ylabel('|P1(f)|')
xlim([0 2.5])
ylim([0 4])
```

```
A = find(P1a == (max(P1a))); %gives row rumber of max peak
maxFreq =fa2(A);%fundamental freq in signal
power =(max(P1a));  %power of the signal
cycles = maxFreq*60; %number of cycles

padTAFou = [fa2' P1a];
%OG = [fa' P1a];
dlmwrite(W2, padTAFou);



%% STN
%find peaks in the fourier trace

[pks,locs,widths,proms] =
findpeaks(P1a,fa,'MinPeakProminence',0.005,'Annotate','extents');
%extract peaks and put into table
%2nd col = 'power', 3rd col is freq, 4th col = width, 5th col
=prominence
locs = locs/nRepeats;
widths = widths/nRepeats;
Peaks4 = [pks,locs',widths',proms]; %dont divide, so keep on larger
scale

%peak +/- half width is the integration range
%do top 3 peaks
Peaks2 = sortrows(Peaks4);
J = length(Peaks4):-1:1;
Peaks3 = [J' Peaks2];
Peaks = sortrows(Peaks3);
nPeaks = 5; %determine peaks

top3Peaks = Peaks(1:nPeaks,:); %selects top 3 - can change to five
 %calculate  x values for integration window, from width
 for s = 1:nPeaks %calc half width, and beginnging and end of peak int
window
 top3Peaks(s,6) = top3Peaks(s,4)/2; %half width value
 top3Peaks(s,7) = top3Peaks(s,3)-top3Peaks(s,6); %lower end
 top3Peaks(s,8) = top3Peaks(s,3)+top3Peaks(s,6); %upper end
 end

%produces table of fa2 values that are needed to integrate
integWindow = zeros(nPeaks, 2);
 for t = 1:nPeaks
    A = find(abs(fa2-(top3Peaks(t,7)) <0.0001));
    posA = length(A)-1;
    integWindow(t,1) = posA;
    B = find(abs(fa2-(top3Peaks(t,8)) <0.0001));
    posB = length(B)-1;
    integWindow(t,2) = posB;
 end

%sum corresponding y values
integValues = zeros(nPeaks,1);
for v = 1:nPeaks
    a = integWindow(v,1);
    b = integWindow(v,2);
    integValues(v,1) = sum(padTAFou(a:b,2));
end
```

```
signal = sum(integValues);
noise = sum(P1a);
stnRatio = signal/(noise-signal);


%% count peaks
%power is defined earlier
powerThresh = 0.05; % 5% thresh
powerThreshold = power * powerThresh;

countPeaks = [];
for w = 1:length(Peaks)
    if Peaks(w,2) > powerThreshold
       countPeaks(w) = Peaks(w,2);
    end
end

no5Peaks = length(countPeaks);

%% Table of interest
%Table = [amp freq power freq power freq power signal noise stn];

Table = [amp maxFreq power cycles signal noise stnRatio no5Peaks]

%% phase shift calc
%actual detrended - plot(timeA, TA_data);
%need to find zero crossing

n=60000;
y=TA_data;
%find zero crossings
t1=y(1:n-1);
t2=y(2:n);
tt=t1.*t2;
indx=find(tt<0); %produces list of 0 crossings

%need to check if its rising or falling?
%rising has  neg/pos then pos/neg
%fallig has pos/neg then neg/pos
%which translates to rise = neg then pos , fall = pos then neg
% use & operator

pShiftTA = zeros(1,1);
if  TA_data((indx(1))) < 0 && TA_data((indx(2))) > 0 %if neg then pos
    pShiftTA = indx(1); % the fucntions rise
elseif TA_data((indx(1))) > 0 && TA_data((indx(2))) < 0 %if falling
    pShiftTA = indx(2);
end


pShift = timeA(pShiftTA); %how much along x axis before rises across 0
timeShift = timeA-pShift;

%models - should be loooped
y = Peaks(1,2)*sin(2*pi*timeShift*(Peaks(1,3)));
y2 = Peaks(2,2)*sin(2*pi*timeShift*(Peaks(2,3)));
y3 = Peaks(3,2)*sin(2*pi*timeShift*(Peaks(3,3)));
y4= Peaks(4,2)*sin(2*pi*timeShift*(Peaks(4,3)));
y5 = Peaks(5,2)*sin(2*pi*timeShift*(Peaks(5,3)));
```

```
yb = y+y2;
yc=y+y2+y3;
yd= y+y2+y3+y4;
ye=y+y2+y3+y4+y5;


%plot models
figure;
subplot(4,1,1)
plot(timeA, TA_data);
ylim([-4 4])
title('Detrended Trace')
subplot(4,1,2)
plot(timeA, y);
ylim([-4 4])
title('model 1')
subplot(4,1,3)
plot(timeA,yb);
ylim([-4 4])
title('model 2')
subplot(4,1,4)
plot(timeA, yc);
ylim([-4 4])
title('model 3')


%% model 3 fit (can plot any model by changing yc, to yd, ye, etc
figure;
plot(timeA, TA_data);
hold on
plot(timeA, yc, 'r');
```